

---

# MEMBRANE PROCESS MODELING

---

International web conference in  
celebration of the 60th anniversary of  
Professor A.N. Filippov

**BOOK OF ABSTRACTS**

NATIONAL UNIVERSITY OF OIL AND GAS  
«GUBKIN UNIVERSITY»

## **MEMBRANE PROCESS MODELING**

International web conference in celebration of the  
60<sup>th</sup> anniversary of Professor A.N. Filippov

**BOOK OF ABSTRACTS**

LOGOS  
Stavropol  
2020

УДК 66.081.63 (063)

ББК 24.561.233

Редколлегия сборника:

В.М. Старов (председатель), Д.В. Миллионщиков, Ю.О.Королева, Д.Ю. Ханукаева.

Моделирование мембранных процессов. Международная онлайн конференция, посвященная 60-летию профессора А.Н. Филиппова. Сборник тезисов. – Ставрополь: Логос, 2020. – 88 стр.

ISBN 978-5-907258-83-9

Книга содержит тезисы докладов международной конференции «Membrane Process Modeling», посвященной 60-летию профессора А.Н. Филиппова, проходившей онлайн 3-4 декабря 2020 г. в РГУ нефти и газа (НИУ) имени И.М. Губкина  
Книга предназначена для студентов старших курсов, аспирантов и научных работников.

**УДК 66.081.63 (063)**

**ББК 24.561.233**

ISBN 978-5-907258-83-9

© Organizing Committee MPM-Filippov-60, 2020

# SCIENTIFIC COMMITTEE

**Prof. Victor M. Starov** (Loughborough University, UK) - the Chairman

**Corr. Member of RAS Andrey B. Yaroslavtsev** (Kurnakov Institute of General and Inorganic Chemistry, Russia)

**Prof. Victor V. Nikonenko** (Kuban State University, Russia)

# ORGANIZING COMMITTEE

**Prof. Dmitry V. Millionshchikov** - the Chairman

**Ass. Prof. Daria Yu. Khanukaeva** - the Secretary

**Ass. Prof. Yulia O. Koroleva**





Professor A.N. Filippov (Department of Higher Mathematics, Gubkin Russian State University of Oil and Gas), one of the leading experts in the field of membrane process modeling, celebrated his sixtieth anniversary on July 31, 2020. Friends and colleagues warmly congratulate him.

# CONTRIBUTION OF PROFESSOR ANATOLY FILIPPOV TO MODELLING OF MEMBRANE PROCESSES

Victor Starov

*Department of Chemical Engineering, Loughborough University, Loughborough, UK*

Membrane filtration is a highly demanded up to date topic. Fresh water comprises about 2.7 percent of the total water available on the Earth. About 2/3 of fresh water is in frozen condition and another 1/3 is distributed as ground water. Africa, Asia, Southern parts of the USA, Australia do not have enough potable water, therefore the water desalination is required. Some processes in pharmaceutical and food industries involve extraction of components from low concentrated water solutions or total separation of different components when both concentrate and permeate are final products. Calculations show that one requires 450 litres of water to produce 1 ton of ready mixed concentrate, 4,500 litres of water are used to produce 1 ton of steel, 30,000 litres of water is necessary to build a common car and so on. The list of the membrane separation applications in various fields of science and technology can be continued further and further. This made flows through porous media an attractive subject for investigators all over the world.

Professor A.N. Filippov is a world-wide known researcher who has contributed a lot into this area.

He graduated with honors from the Department of Mechanics and Mathematics of Lomonosov Moscow State University in 1982. After that he continued the study as a postgraduate student. During his PhD studies, Anatoly Filippov has got a Lenin scholarship, the prestigious award given to talented students. In 1985 he defended his PhD thesis "One-dimensional elastic waves in a rod and plate, taking into account the nonlinear interaction with the environment" and started his scientific career as a junior researcher in the laboratory of explosive and shock processes at the Institute of Mechanics of Lomonosov Moscow State University (1985 - 1987).

In addition to the research Anatoly Filippov teaches courses in Higher Mathematics. Starting in 1987 with Assistant Professor position in Moscow State University of Food Production, he held all possible teaching positions: Associate Professor, Full Professor, Head of Department "Pure and Applied Mathematics", Dean of the Institute of automation equipment and information technologies. Since 2010 Professor Filippov has been working in Gubkin Russian State University of Oil and Gas.

The scientific interests of Professor Filippov include Physico-Chemical Mechanics, Surface and Colloid Chemistry, Membrane Electrochemistry, Membrane Processes, Hydrodynamics of fluids under low Reynolds numbers, Nanotechnologies and Nanomaterials. The scientific projects of Professor Filippov were many times awarded by Russian and International Grants. He contributed to the following research fields:

- the asymmetry theory for diffusion permeability of charged bilayer membranes;
- the asymmetry of the retention coefficient of nano- and ultrafiltration membranes;
- the cell model of a complex-porous membrane, taking into account the influence of a uniform magnetic field on the filtration of a conductive liquid;
- the models of asymmetry of current-voltage characteristics of bilayer ion-exchange membranes and single-layer linearly charged membranes;
- the method for obtaining of a pore size distribution for the membrane based on atomic force microscopy scans of its surface;
- the theory of gradual opening of pores for a hydrophobic membrane;
- the fabrication and characterization technology of new hybrid nanocomposites for fuel cells based on the MF-4SK cation-exchange membrane with halloysite nanotubes intercalated / encapsulated with platinum and iron nanoparticles;
- the method for characterizing bilayer nanocomposite membranes taking into account the asymmetry of their transport properties;
- the cell models of micropolar flows through porous media;
- the cell model of an ion-exchange membrane which allowed to obtain the explicit expressions for its hydrodynamic permeability, electrical conductivity and electroosmotic permeability;
- the model of electrophoresis of polyelectrolyte capsules;
- the theory of an external electric field effect on the hydrodynamic permeability of a porous charged layer.

The results are presented in more than **400 publications** of Professor Filippov in Russian and international scientific journals, 4 patents of the Russian Federation for inventions and 3 monographs. Several dozens of co-authors took part in these works.

Professor Filippov participated in more than **150 scientific meetings** in different countries including USA, Germany, the Netherlands, Great Britain, Israel, Belgium, Bulgaria, Austria, Spain, Hungary, Czech Republic, Portugal, India, China.

He operated as

**Visiting Scientist** in Center for Energy and Environmental Physics, The Jacob Blaustein Institutes for Desert Research, Ben-Gurion University of the Negev, Israel (1993 and 2004);  
**Visiting Scientist** in Biochemical Engineering Group, Department of Chemical Engineering, Swansea University of Wales, Swansea, UK (1997);  
**Deputy Pro-rector** on Basic Research and International Cooperation of MSUFP (2007-2009);  
**Chairman** of the Central International Interbranch Scientific and Technical Council on Nanotechnologies and Nanomaterials in the Food Industry (2007-2010);  
**Member** of Scientific-Methodology Council of Regional Division of the Center of Metrology in Nanotechnology and Nanoindustry in the Central Federal District of Russia;  
**Deputy director** of “Membrane materials” Section of the Scientific Council “Electrochemistry” of the Russian Academy of Sciences;  
**Invited Co-editor** of the Special Issue of “Advances in Colloid and Interface Science” (Volume 139, 2008);  
Currently Professor Filippov is  
**Member** of several Dissertation Councils;  
**Member** of the Editorial Board of the journals “Membrane and Membrane Technologies”, “Membranes” (MDPI), “Colloid Journal”; Proceedings of Gubkin University;  
**Expert** of RFBR; RSF; Ministry of Science and Higher Education;  
**Member** of Russian Membrane Society, American Nanosociety and European Colloid and Interface Society;  
**Reviewer:** Journal of Membrane Science, Langmuir, Advances in Colloid and Interface Science, Colloids and Surfaces A, Colloid Journal, Separation Science and Technology, Desalination, AAM, Canadian Journal of Physics, Zeitschrift für Angewandte Mathematik und Mechanik, Meccanica, Journal of Porous Media, Membranes and Membrane Technology, Communications in Nonlinear Science and Numerical Simulation, Industrial & Engineering Chemistry Research, Chemical Engineering Research and Design, Theoretical Foundations of Chemical Engineering, Journal of Applied Electrochemistry, Russian Journal of Electrochemistry, Current Applied Physics, Mathematical Problems in Engineering, Physics of Fluids AIP, European Journal of Mechanics /B Fluids, Molecules, Surface Innovations, Colloid and Polymer Science, Mathematical Methods in the Applied Sciences, Journal of Inorganic and Organometallic Polymers and Material, Polymers, Materials, Materials and Design, International Communications in Heat and Mass Transfer, Physics Letters A, Journal of Molecular Liquids, Entropy, Membranes, MMM, ZAMP, ZAMM, Microgravity and others.

\*\*\*

The colleagues of Professor Filippov from Gubkin University decided to organize the conference Membrane Process Modeling in celebration of his 60<sup>th</sup> anniversary. This book collects the Abstracts of the conference participants and collaborators of the jubilee in the field of Membrane Theory. At the same time, scientific interests and contacts of Professor Filippov are able to compose many such conferences. This conference is just an indication of his flourishing and developing scientific career.

# KEYNOTE LECTURES

## THE ORIGIN OF OSMOSIS AND ELECTRO-OSMOSIS

Maarten Biesheuvel<sup>1</sup>, Slawomir Porada,<sup>1</sup> and Jouke Dykstra<sup>2</sup>

<sup>1</sup>Wetsus, European Centre of Excellence for Sustainable Water Technology, The Netherlands.

<sup>2</sup>Department of Environmental Technology, Wageningen University, The Netherlands.

*Summary* We present theory for osmosis and electro-osmosis in charged microporous media (ion-exchange membranes). Within the context of the two-fluid model where the solvent is described differently from the dispersed solutes, we provide a precise meaning to these terms. We obtain unprecedented accuracy in describing data for osmosis with limited fitting parameters.

### INTRODUCTION & OBJECTIVES

Osmosis and electro-osmosis are mechanisms by which solvent (water in most cases) transports across a selective layer driven by a concentration difference or current. The origin and explanation of both contributions to water flow is quite ambivalent in the literature, with many explanations and different meanings of words.

We use the two-fluid approach to the description of ion and water flow. In this approach ions (and other solutes) are dispersed particles with the hydration shell part of the solute particle, and with the ('free') water filling up all space between these dispersed particles. The theory for the solvent is different from that for the solutes. We do not favor or put forward certain simplistic models that extrapolate Maxwell-Stefan theories (valid for gases) to solutions.

'Why' water flows to a solution of higher salt concentration is a topic of almost philosophical interest, and multiple conflicting theories are put forward. But we do know that a macroscopic thermodynamic approach is valid (increase of total ion entropy in the system), while we put forward a microscopic approach that explains the actual mechanism, namely that a hydrostatic pressure gradient inside the membrane that is due to the mechanical equilibrium in the EDLs on the outsides of the membrane, pushes the water across the membrane.

Electro-osmosis is a term with many different meanings. But the problem is, why would water flow because of electrical fields, because it is not charged of itself. Only the ions are charged. We show how electro-osmosis is a logical consequence of ion-water friction, i.e., the ('free') water is dragged along by the ions (besides the volume flow of the hydrated ions themselves). We show how the classical modified Navier-Stokes equation is congruent with a force balance on the water that includes osmotic forces, and we show the extension of this equation when ions have friction with the membrane matrix.

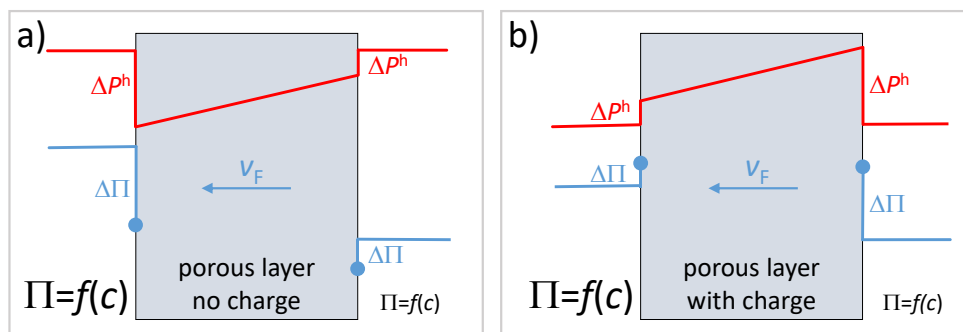


Figure 1. The origin of osmosis for non-charged and charged layers, explained as being the consequence of mechanical equilibrium in the Donnan EDL structures on the outsides of the membrane.

## RESULTS & CONCLUSIONS

We present results of osmosis experiments with a homemade Fumatech membrane of 200  $\mu\text{m}$  thickness where we start with a diluate NaCl concentration of 4 mM which during 35 hour increases to 130 mM. During that time the concentration on the concentrate side drops from 800 mM to 525 mM. There is volumetric transport to the concentrated side. Based on this one experiment, where we follow concentrations and volume continuously, the data in Figure 2 are derived from very accurate analysis of volume flow (volumes on the two sides of the membrane) and concentration changes. As far as we know, there are no data in literature that based on measurement of concentrations and volume changes calculate simultaneously the water flow through a membrane and the salt flux leakage.

Very interestingly, the two fluxes are in opposite direction which means the water flow is not large enough to drag the salt ions (that diffuse to the low-salt side) along with it. Thus inside the membrane we have water flowing in one direction, and both ions in the other direction.

Because of these counter-directed fluxes, to then get a theory to fit data accurately, we find that that is actually very challenging. And we do not know of successful examples in literature. But our two-fluid model works well. We need to include one non-ideality, either a small partitioning coefficient for ions other than due to their charge, or a small ion-membrane friction coefficient.

This good fit of theory to data corroborates the usefulness and accuracy of the two-fluid approach to describe ion transport, osmosis and –by extension– electro-osmosis.

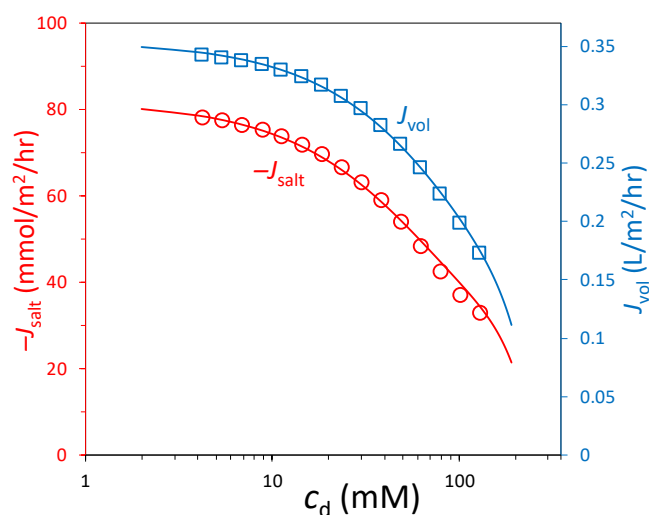


Figure 2. Osmosis across Fumatech cation-exchange membrane. Data and theory for salt leakage (red, left axis) and water flow (blue, right axis). Note that water flows in opposite direction to the salt flux. Results as function of concentration of NaCl on diluate side.

## References

- [1] P.M. Biesheuvel, Two-fluid model for the simultaneous flow of colloids and fluids in porous media, *J. Colloid Interface Sci.* 355, 389-395 (2011).
- [2] M. Tedesco, H.V.M. Hamelers, and P.M. Biesheuvel, Nernst-Planck transport theory for (reverse) electrodialysis: II. Effect of water transport through ion-exchange membranes, *J. Membrane Sci.* 531, 172-182 (2017).
- [3] Biesheuvel, P.M., Dykstra, J.E., *Physics of Electrochemical Processes*. www.physicsofelectrochemicalprocesses.com. ISBN 978-90-9033258-1 (2020).

## SIMULATION OF SOLUTE TRANSPORT IN A CROSS-FLOW PAST A ROW OF HOLLOW-FIBER MEMBRANES

Vasily Kirsch<sup>1,2</sup>

<sup>1</sup>A.V. Topchiev Institute of Petrochemical Synthesis, Russian Academy of Sciences, Moscow, Russia

<sup>2</sup>A.N. Frumkin Institute of Physical Chemistry and Electrochemistry, Russian Academy of Sciences, Moscow, Russia

A coupled simulation of the transverse flow of a viscous incompressible liquid (gas) and convection-diffusion mass transfer of a solute in a single row of parallel absorbing fibers (hollow-fiber membranes), was performed in the stationary approximation for fiber Reynolds numbers up to  $Re = 100$ , in a wide range of Schmidt numbers  $Sc = 1 - 1000$ . The Navier-Stokes and convection-diffusion equations were solved numerically and the fiber average Sherwood number was calculated as a function of  $Re$ ,  $Sc$ , and fiber packing density, for constant concentration and diffusion flux conditions set at the outer fiber surface. Best-fit approximations for the fiber drag force and fiber Sherwood number were suggested. The results of simulations are consistent with existing asymptotical solutions derived analytically for low and high Peclet numbers,  $Pe = Re Sc$ .

Fundamental studies in hydrodynamics and convective mass transfer in fibrous media are important for optimization of the separation and purification processes that use hollow-fiber membrane contactors, sorption filters, and fibrous filters for removing suspended particles in gases and liquids. In this work, we consider the process of the transport with the removal of a substance dissolved in a gas or a liquid flow past a model fibrous medium with a regular arrangement of fibers. A row of parallel fibers, placed normally to the direction of the flow, is considered as a model.

2D laminar viscous incompressible transverse (cross) flow and concentration fields in model fibrous media were simulated for a single row of parallel fibers (Figure 1). The dimensionless Navier-Stokes equations were solved numerically together with the equation of convection-diffusion in the stationary approximation. The no-slip condition was set at the streamlined fiber surface (4). The conditions of an unperturbed flow and uniform inlet concentration were set at the inlet boundary of the cell (1), while the conditions of the absence of viscous stresses and lowering of concentration were set at the outlet (3). On the side faces of the cell (2), symmetry conditions were set for the velocity components and concentration. The governing equations were solved with the help of the finite-difference schemes on the composite grids of a high-dimension. The technique of solution is partly described in [1–3]. Dirichlet and Neumann boundary conditions for concentration were employed at the outer fiber surface, i.e. the condition of the constant concentration,  $C = 0$ , and the flux boundary condition,  $\partial C/\partial r = kC$ , which accounts for the transport in the membrane.

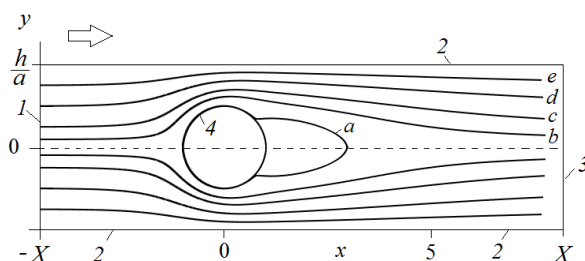


Figure 1. Sketch of the simulation cell: laminar transverse 2D flow past a row of parallel fibers: the streamlines and the hydrodynamic wake with the stagnant zone, the values of the streamlines (the inlet ordinates):  $10^{-4}$  (a), 0.2 (b), 0.5 (c), 1 (d), 1.5 (e);  $Re = 20$ , the row blockage parameter  $b = 0.5$ ; the arrow indicates the direction of the flow.

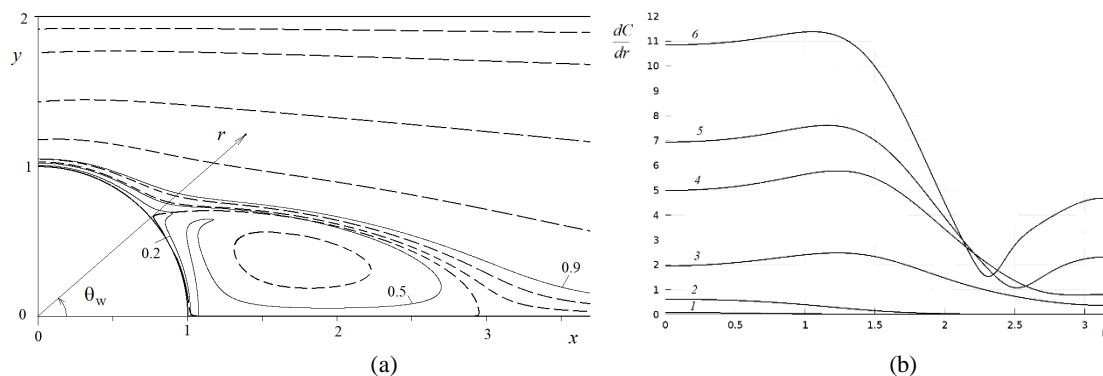


Figure 2. (a) Hydrodynamic and diffusion wakes behind the fiber: streamlines (dotted lines) and concentration isolines (solid, figures denote dimensionless concentration values) in the wake zone:  $b = 0.5$ ,  $Sc = 1000$ ,  $Re = 20$ ;

(b) concentration derivative with respect to the radius on the fiber surface (local Sherwood number) vs. the polar angle at  $Re = 0.01$  (1), 0.1 (2), 1 (3), 10 (4), 20 (5), 50 (6); the condition of zero concentration was used at the fiber surface; blockage parameter  $b = 2/3$ ,  $Sc = 1000$ .

Figure 2 illustrates the hydrodynamic and diffusion wakes, where the angle  $\theta_w$  determines the boundary of the diffusion wake. The recirculation zone and the diffusion wake are formed with a delay with increasing Reynolds number. In the

general case, the hydrodynamic and diffusion wakes do not coincide. The boundary of the diffusion wake coincides with the boundary of the recirculation zone (separated flow region) only in the limit of high Peclet numbers.

The dimensionless fiber collection efficiency (mean Sherwood number  $Sh$  of a fiber), defined as an integral density of the diffusion flux on the fiber surface (per unit fiber length),

$$\eta = 2Pe^{-1} \int_0^\pi \left. \frac{\partial C(r, \theta)}{\partial r} \right|_{r=1} d\theta,$$

was calculated as a function of the Reynolds ( $Re = 2aU/\nu$ ) and Schmidt ( $Sc = \nu D^{-1}$ ) numbers, Peclet number  $Pe = Re Sc$ , and the row blockage ratio  $b = h/a$ . Here  $D$  is the solute diffusion coefficient,  $a$  the fiber radius,  $\nu$  the kinematic viscosity,  $U$  the inlet flow velocity,  $2h$  the distance between the fiber axes. A wide range of Schmidt numbers  $Sc$  relating to gas and liquid flows,  $Sc = 1 - 1000$ , was considered. At low and high Peclet numbers, the results of simulations agree with existing asymptotical solutions derived analytically in [5, 6]. The fiber drag force also coincides with known analytical formulas derived for loose and dense fiber rows.

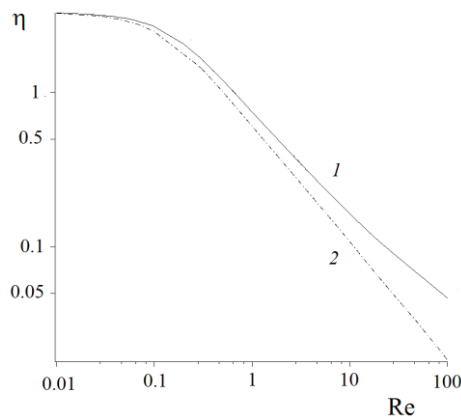


Figure 3. The fiber collection efficiency (mean Sherwood number) versus the Reynolds number for  $Sc = 10$ , found with the boundary condition for total absorption  $C = 0$  (curve 1) and with the diffusion flux condition with  $k = 5$  (curve 2); row blockage parameter  $b = 0.3$ .

The results of simulations reveal the complex multi-parametric dependencies of the fiber collection (retention) efficiency in conditions of the confined flow (which is strongly influenced by the neighbor fibers). It was shown that the use of the full absorption condition  $C = 0$  gives an upper estimate for the collection efficiency. At the same time, the calculations with the two boundary conditions give significantly different results for high and intermediate Peclet numbers, namely, different power dependences of the mean Sherwood number against  $Pe$ . This behavior is illustrated in Figure 3. It can be seen from this Figure, that at low Peclet numbers in the diffusion dominant region, the fiber retention efficiency calculated with both boundary conditions tends to a constant value inversely proportional to the row blockage parameter. The obtained results will be used to design and optimize hollow fiber membrane contactors, fiber filters, heat exchangers, thermal insulation, and catalytic fibrous materials.

This work was carried out in A.V. Topchiev Institute of Petrochemical Synthesis (Russian Academy of Sciences) and was funded by the Russian Science Foundation, Project number 19-19-00647.

## References

- [1] Launder B.E., Massey T.H. The Numerical Prediction of Viscous Flow and Heat Transfer in Tube Banks, *ASME J. Heat Transf.* 100, 565–571, 1978.
- [2] Berkovskii B.M., Polevikov V.K. Effect of the Prandtl number on the convection field and the heat transfer during natural convection (English transl.), *J. Eng. Phys.* 24, 598–603, 1973
- [3] Kirsh V.A., Deposition of aerosol nanoparticles in fibrous filters, *Colloid J.* 65, 795–801, 2003.
- [4] Kirsh V.A., Bazhenov S.D., Numerical simulation of solute removal from a cross-flow past a row of parallel hollow-fiber membranes, *Separation and Purification Technology*, 242, 116834, 2020
- [5] Natanson G.L., Diffusional precipitation of aerosols on a streamlined cylinder with a small capture coefficient (English transl., Dokl. Akad. Nauk SSSR), *Proc. Acad. Sci. USSR Phys. Chem. Sec.* 112, 21–25, 1957.
- [6] Chernyakov A.L., Kirsh A.A., Roldugin V.I., Stechkina I.B. Diffusion deposition of aerosol particles on fibrous filters at small Peclet numbers, *Colloid J.* 62, 490–494, 2000.

## STRUCTURE OF SURFACTANT ADSORPTION LAYERS AT THE WATER/ALKANE INTERFACE – COMPETITIVE AND COOPERATIVE EFFECTS

Reinhard Miller<sup>1</sup>, Valentin B. Fainerman<sup>2</sup>, Nenad Mucic<sup>3</sup>, Aliyar Javadi<sup>4</sup>, Libero Liggieri<sup>5</sup>, Francesca Ravera<sup>5</sup>, Giuseppe Loglio<sup>5</sup>, Alexander V. Makievski<sup>2</sup> and Emanuel Schneck<sup>1</sup>

*1 Department of Physics, Technische Universität Darmstadt, 64289 Darmstadt, Germany*

*2 SINTERFACE Technologies, 12489 Berlin, Germany*

*3 Faculty of Technology, University of Novi Sad, 21000 Novi Sad, Serbia*

*4 Helmholtz-Zentrum Dresden-Rossendorf (HZDR), Institute of Fluid Dynamics, 01328 Dresden, Germany*

*5 Institute of Condensed Matter Chemistry and Technologies for Energy, 16149 Genoa, Italy*

**Summary** Until recently, the adsorption of surfactants at water/oil interfaces was described by models derived for water/air surfaces, and most of the observed peculiarities were interpreted by a penetration into or squeezing out of oil molecules of the adsorbed layer of the surfactant's alkyl chains. To improve the theoretical description of surfactant adsorption layers at water/oil interfaces, we proposed a new approach which assumes a simultaneous adsorption of oil and surfactant molecules. At low surfactant bulk concentrations, the oil molecules in the interfacial layer act in a cooperative way and enhance the surfactant adsorption. In contrast, with increasing surfactant bulk concentrations, the adsorption of surfactants increases and gradually and replace the oil molecules from the interface due to competition. The presentation provides a brief description of the thermodynamic model and then presents experimental data mainly for the homologous cationic surfactants C<sub>n</sub>TAB at the water/hexane interface.

In the past, most investigations on the properties of surfactants were performed at the water/air (W/A) surface. Until recently, without significant changes, the gained physical interpretations were used also for the characterization of surfactant adsorption at water/oil (W/O) interfaces. There are, however, several significant differences for surfactants adsorbed at the W/A and W/O interfaces, respectively. For example, the molar area for adsorbed surfactant molecules at the water/oil interface is larger and was explained by a penetration of oil molecules into the alkyl chain layer of the adsorbed surfactant molecules. Moreover, the adsorption of surfactants at W/O interfaces becomes measurable at much lower bulk concentration (two orders of magnitude and more) as compared to the W/A surface.

In their work published in 2000, Medrzycka and Zwierzykowski [1] applied a Frumkin adsorption model to interpret the adsorption behavior of three alkyl trimethyl ammonium bromides C<sub>n</sub>TAB with n = 12, 14 and 16 adsorbed at different water/alkane interfaces. The summary of their results are as follows:

1. at the W/A interface the C<sub>n</sub>TAB adsorption is lower at low and higher at high bulk concentrations, as compared to all studied W/O interfaces;
2. at the W/A interface, the change in surface tension is observed at C<sub>n</sub>TAB concentrations of about two orders of magnitude below the corresponding CMC while at W/O interfaces, the interfacial tension starts decreasing at concentrations of about four orders of magnitude below the respective CMC;
3. the surface concentration of a certain C<sub>n</sub>TAB is the lowest when the chain length of the alkane matches that of the surfactant.

A new thermodynamic model which was derived recently [2], considers a co-adsorption of alkane and surfactant molecules and form a mixed interfacial layer. In this model it is assume that the alkane (index a) adsorbs from the oil drop, while the surfactant (index s) adsorbs from the aqueous solution surrounding the oil drop. When we assume further that for both components the Frumkin model applies, we obtain a set of equations to describe the composition of a mixed interfacial layer. The adsorption isotherms for alkane and surfactant molecules, respectively, have then the form:

$$b_a c_a = \frac{\theta_a}{1 - \theta_a - \theta_s} \exp[-2a_a \theta_a - 2a_{as} \theta_s] \quad \text{and} \quad b_s c_s = \frac{\theta_s}{1 - \theta_a - \theta_s} \exp[-2a_s \theta_s - 2a_{sa} \theta_a].$$

Note, b<sub>a</sub> and b<sub>s</sub> are the surface activities of alkane and surfactant, respectively, c<sub>a</sub> and c<sub>s</sub> are the corresponding bulk concentrations, θ<sub>a</sub> and θ<sub>s</sub> are the surface coverages, a<sub>a</sub>, a<sub>s</sub> and a<sub>as</sub> are the respective interfacial interaction constants. We proposed in [1] a further improvement of this thermodynamic model by introducing a cooperativity of the adsorption of the two compounds. For this, it was assumed that the surface activity of alkane depends on the adsorbed amount of the surfactant via b<sub>a</sub> = b<sub>a0</sub> · θ<sub>s</sub> [2], limited by a maximum value b<sub>a,max</sub>.

In Figures 1 and 2 present the interfacial tension isotherms for four C<sub>n</sub>TABs at the W/A (Figure 1) and water/hexane (W/H) (Figure 2) interfaces. It is easily seen that the concentration range over which each isotherm spans, and the total change in interfacial tension are significantly larger at the W/H as compared to the W/A interface.

There are still several open questions in the general understanding, for example about the adsorption dynamics of surfactants, which happen in cooperation/competition in the mixed oil/surfactant adsorption layers. The presence of oil (alkane) molecules at the interface should have impact on the adsorption kinetics. The exchange of matter during interfacial area perturbations should also be enhanced/decelerated accordingly. At low interfacial coverage, a cooperativity between the two compounds at the interface acts. For medium and high interfacial layer coverage, however, additional relaxation mechanisms could exist connected with the competition between the two compounds (Figure 3). The answer of these open questions do not only require new experiments but also new theories and molecular simulations.

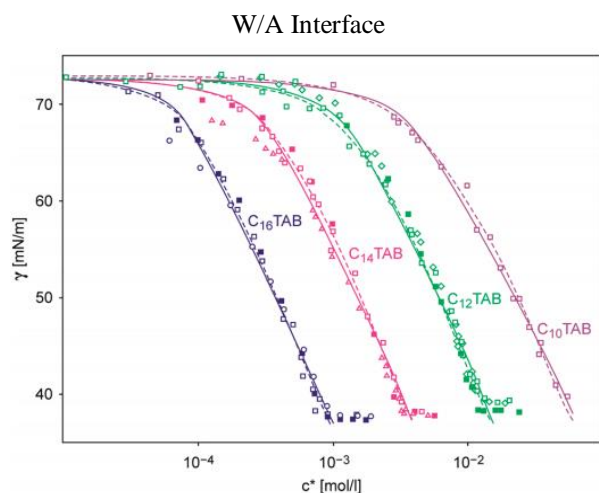


Figure 1 Equilibrium interfacial tension isotherms for  $C_n$ TAB solutions at the W/A interface; different symbols refer to data from different sources; solid curves are calculated from a modified Frumkin adsorption model [4]

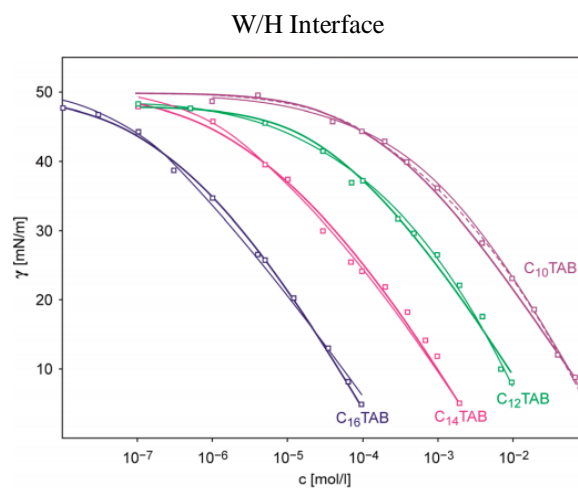


Figure 2 Equilibrium interfacial tension isotherms for  $C_n$ TAB at the W/H interface; symbols – experimental data taken from [5], solid lines are calculated from the new proposed thermodynamic model [3]

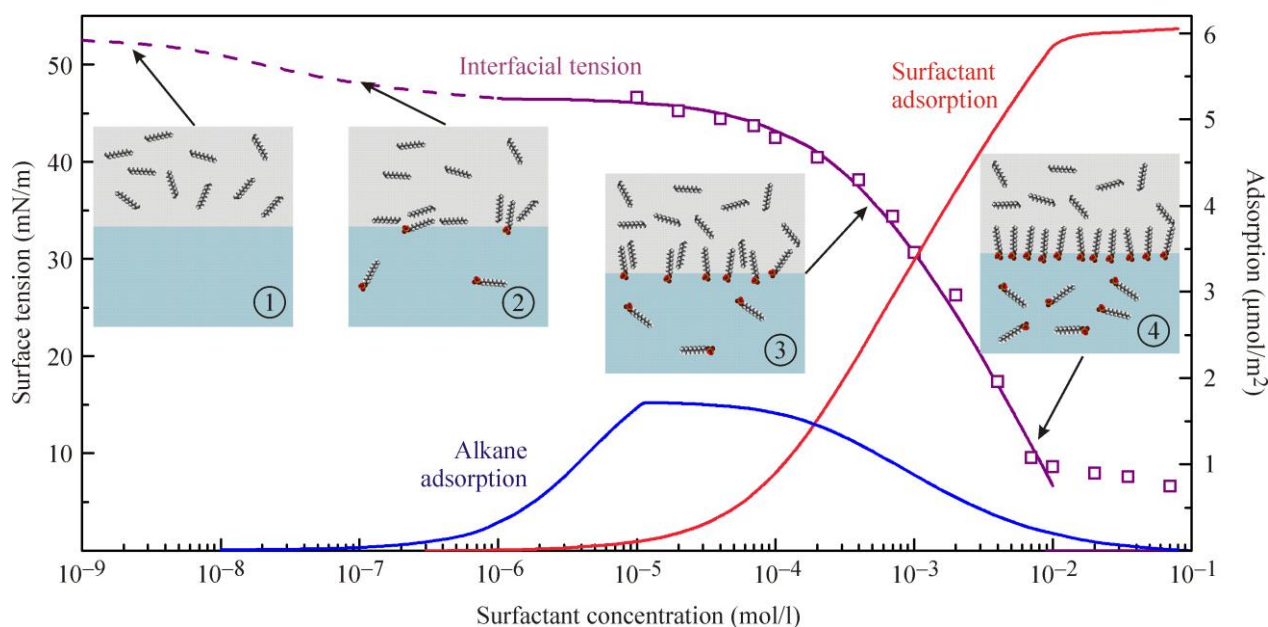


Figure 3 Schematic of the adsorption layer situation at the surfactant solution/alkane interface:

- 1 – no adsorption due to extremely low (zero) surfactant concentration;
- 2 – first adsorbed surfactant molecules attract alkane molecules and vice versa (cooperativity effects);
- 3 – increased surfactant adsorption leads to step by step replacement of adsorbed alkane (competition);
- 4 – at sufficiently high surfactant concentration, the alkane disappears from the adsorption layer; taken from [2].

## References

- [1] Mędrzycka K, Zwierzykowski W. Adsorption of alkyltrimethyl ammonium bromides at the various interfaces. *J Colloid Interface Sci.*, 230 (2000) 67–72.
- [2] V.B. Fainerman, E.V. Aksenenko, A.V. Makievski, M.V. Nikolenko, A. Javadi, E. Schneck and R. Miller, Particular behavior of interfacial tension at the interface between aqueous surfactant solutions and alkane, *Langmuir*, 35 (2019) 15214-15220.
- [3] V.B. Fainerman, E.V. Aksenenko, V.I. Kovalchuk, N. Mucic, A. Javadi, L. Liggieri, F. Ravera, G. Loglio, E. Schneck and R. Miller, New view of the adsorption of surfactants at the water/alkane interface – competitive and cooperative effects of surfactant and alkane molecules, *Adv. Colloid Interface Sci.*, 279 (2020) 102143.
- [4] V.B. Fainerman, R. Miller and H. Möhwald, General Relationships of the Adsorption Behaviour of Surfactants at the Water/Air Interface, *J. Phys. Chem.*, 106 (2002) 809–819.
- [5] V. Pradines, V.B. Fainerman, E. V. Aksenenko, J. Krägel, N. Mucic and R. Miller, Alkyltrimethyl ammonium bromides adsorption at liquid/liquid interfaces in the presence of neutral phosphate buffer, *Colloids Surf. A*, 371 (2010) 22–28.

# HIGHLY SELECTIVE SEPARATION OF CATIONS WITH THE SAME CHARGE BY A NEW MEMBRANE METHOD USING SIMULTANEOUSLY APPLIED ELECTRIC AND PRESSURE FIELDS

Victor Nikonenko<sup>\*1</sup>, Dmitrii Butylskii<sup>1</sup>, Semyon Mareev<sup>1</sup>, Andrey Kislyi<sup>1</sup>,  
Natalia Pismenskaya<sup>1</sup>, and Pavel Apel<sup>2</sup>

<sup>1</sup>Membrane Institute, Kuban State University, Krasnodar, Russia

<sup>2</sup>Joint Institute for Nuclear Research, Dubna, Russia

**Summary** High specific membrane permselectivity allowing removal/isolation of certain ions (such as Li<sup>+</sup>) from mixed natural or industrial solutions is a great issue nowadays. A new approach is proposed, where an electric potential gradient and a pressure gradient are applied simultaneously across a nanoporous membrane. We show that the application of this method allows obtaining a high specific permselectivity along with a high flux of the preferably permeable ion.

## INTRODUCTION

When developing highly selective membranes, the researchers face a problem known as the trade-off between permeability and selectivity [1-4]: the nature of membrane material is so that either high ion fluxes or high selectivity can be achieved, but not both simultaneously. Another problem is the concentration polarization of the external solution, which “kills” the permselectivity when the current density approaches its limiting value [4, 5]. Actually, the latter is one of the causes resulting in the trade-off relationship. We propose a new approach, where an electric potential gradient and a pressure gradient are applied simultaneously across a membrane.

## PRINCIPLE OF THE METHOD

When a potential gradient is applied across a membrane, the ions with the same charge move through a pore with a velocity proportional to their mobility, e.g., the K<sup>+</sup> ion moves faster than the Li<sup>+</sup> ion. The pressure gradient reduces their electromigration velocity,  $v_k^{el}$ , by the same value,  $v_k^{conv}$ . It is possible to select a pressure gradient so that the resulting velocity of Li<sup>+</sup> becomes zero, but K<sup>+</sup> continues to move across the membrane (Figure 1).

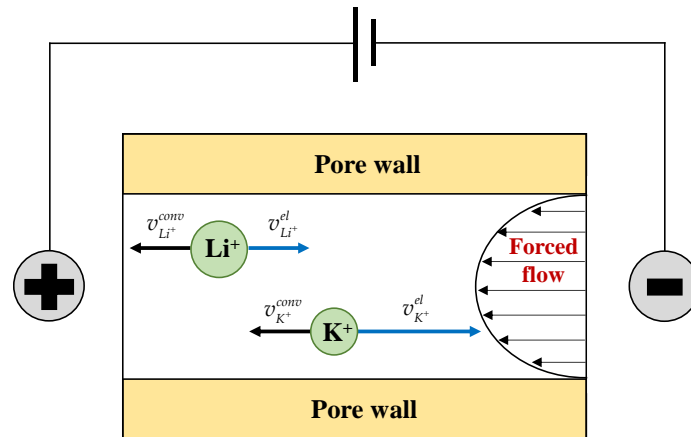


Figure 1. Scheme of K<sup>+</sup>/Li<sup>+</sup> separation by electro-baromembrane method. The electromigration and convective drift velocities of ion  $k$  ( $v_k^{el}$  and  $v_k^{conv}$ , respectively) are presented by blue and black arrows, respectively

## THEORY

The flux densities of competing ions 1 and 2 [in mol/(m<sup>2</sup> membrane surface)×s] can be written as follows:

$$j_k = \frac{iT_k}{z_k F} + c_k v^{conv} \gamma, k = 1, 2 \quad (1)$$

where  $i$  is the current density,  $j_k$ ,  $T_k$ ,  $c_k$  and  $z_k$  are the flux density, effective transport number, concentration and charge number of ion  $k$ ,  $\gamma$  is the fraction of the membrane surface occupied by the pore openings.

Along with this simplified description, a 1D model based on the Nernst-Planck equations is developed taking into account the effect of diffusion boundary layers.

\*Corresponding author. E-mail: v\_nikonenko@mail.ru.

## EXPERIMENT

The case of two cations with very different mobilities,  $K^+$  and Rhodamine 6G ( $R6G^+$ ), and a practically important case of  $K^+/Li^+$  were studied. A polyethylene terephthalate track-etched membrane (TM) was used. The membrane thickness is 10  $\mu m$ ; the uniform cylindrical pores with a diameter of 50 nm are randomly distributed over the surface ( $3.0 \times 10^9$  pores/cm<sup>2</sup>). A four compartment ED cell was used. A MK-40 cation-exchange membrane (Shchekinoazot, Russia) separated the TM from the cathode, and a MA-41 anion-exchange membrane separated it from the anode. Two mixed solutions, 0.1M KCl+ $10^{-4}$  M R6GCl, and 0.13M KCl+0.07M LiCl, were used. In each case, such a mixed solution flowed through the compartment to the left of the track-etched membrane, and a 0.1 M KCl solution, through the compartment to the right. The solution in the right-hand compartment was under a pressure exceeding the pressure in the left-hand compartment by  $\Delta p = 0 - 0.12$  bar.

Selective permeability of the membrane towards  $K^+$  compared to  $R6G^+$  is quantified using the characteristic called permselectivity:  $P_{K^+/R6G^+} = (j_{K^+}/j_{R6G^+}) \times (c_{R6G^+}/c_{K^+})$ . When a constant voltage  $U=1V$  is applied across the TM at  $\Delta p = 0$ , the  $j_{K^+}/j_{R6G^+}$  ratio is close to  $10^4$  (Figure 2), so that  $P_{K^+/R6G^+}$  is about 10, in accordance with the ratio of  $K^+$  and  $R6G^+$  mobilities, which is equal to 8.8. With increasing  $\Delta p$ , both  $K^+$  and  $R6G^+$  fluxes decrease, however, that of  $R6G^+$  approaches zero at  $\Delta p = 0.125$  bar, while that of  $K^+$  remains far from zero, it is about 0.3 mmol/cm<sup>2</sup>h (3 mol/m<sup>2</sup>h). The latter is close to that, which could be obtained at the limiting current density in conventional electrodialysis (ED). The obtained result exceeds the upper limit of the ionic flux vs. permselectivity trade-off diagram for monovalent/bivalent cations [6].

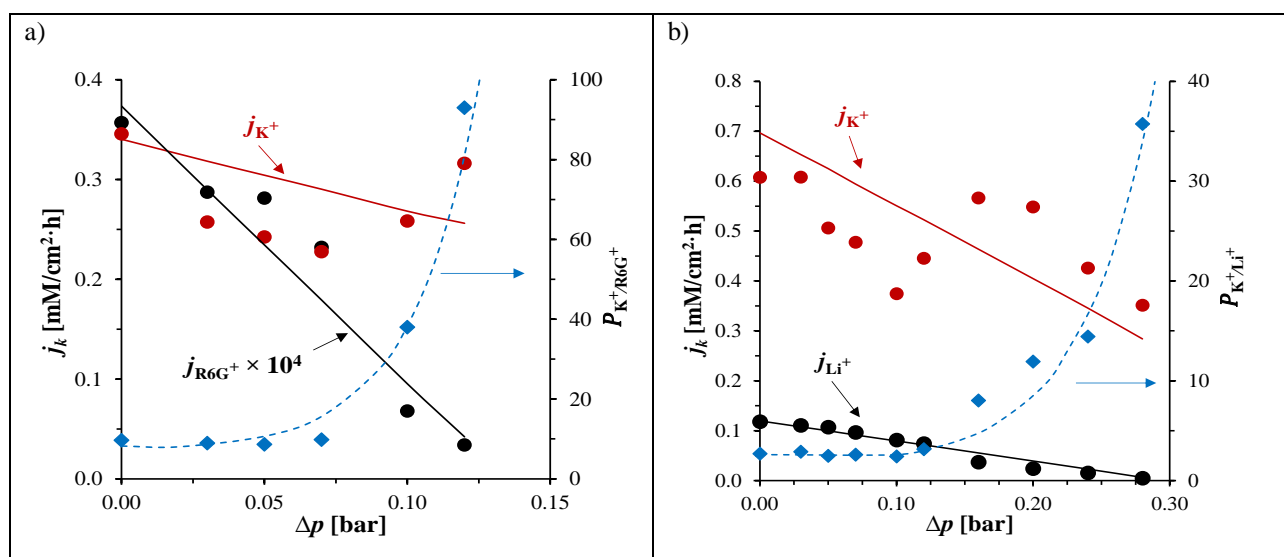


Figure 2. Results of  $K^+/R6G^+$  (a) and  $K^+/Li^+$  (b) separation by electro-baromembrane method at different applied pressure drops  $\Delta p$  at a transmembrane voltage of 1.0 and 0.5 V, respectively. Experimental data are shown by symbols, solid lines show theoretical calculations

## CONCLUSIONS

It is possible to achieve a nearly zero flux of one of the competing ions, while the flux of its competitor is close to that obtained at the limiting current density in electrodialysis. The uniqueness of the proposed method is that it allows separation of ions with the same charge, which is almost impossible when using ED or NF.

The work is supported by the Russian Science Foundation, project #19-19-00381.

## References

- [1] Robeson L.M., The upper bound revisited. *J. Membr. Sci.* 320, 390–400, 2008.
- [2] Park H.B., Kamcev J., Robeson L.M., Elimelech M., Freeman B.D., Maximizing the right stuff: The trade-off between membrane permeability and selectivity, *Science* 356, 6343, 2017.
- [3] Golubenko D.V., Pourcelly G., Yaroslavtsev A.B., Permselectivity and ion-conductivity of grafted cation-exchange membranes based on UV-oxidized polymethylpenten and sulfonated polystyrene. *Sep. Purif. Technol.* 207, 329–335, 2018.
- [4] Stenina I., Golubenko D., Nikonenko V., Yaroslavtsev A., *Int. J. Mol. Sci.* 2020, 21, 5517.
- [5] Rubinstein I., Theory of concentration polarization effects in electrodialysis on counter-ion selectivity of ion-exchange membranes with differing counter-ion distribution coefficients, *J. Chem. Soc. Faraday Trans.* 86, 1857–1861, 1990.
- [6] Ge L., Wu B., Yu D., Mondal A.N., Hou L., Afsar N.U., Li Q., Xu T., Miao J., Xu T., Monovalent cation perm-selective membranes (MCPMs): New developments and perspectives, *Chinese J. Chem. Eng.* 25, 1606-1615, 2017.

## MECHANISMS OF HYDRODYNAMIC INSTABILITY IN CONCENTRATION POLARIZATION

Isaak Rubinstein, Boris Zaltzman\*

*Blaustein Institutes for Desert Research, Ben-Gurion University of the Negev, Sede-Boqer, Israel*

**Summary** The passage of the electric current from a binary electrolyte solution into a charge selective solid, such as a metal electrode, an ion exchange membrane or a junction of micro-nano-channels, is hydro-dynamically unstable: above a certain current threshold, a microvortical flow spontaneously emerges near the interface. This instability is caused by one of the two distinct mechanisms. Distinguishing between these two mechanisms for different systems is a fundamental challenge. In this experimental and theoretical study, we resolve this ambiguity for one important membrane system. Our approach may be useful for identifying the instability mechanism in other systems as well.

One-dimensional steady state passage of direct electric current from a binary electrolyte solution into a charge selective solid such as a metal electrode or an ion exchange membrane is hydrodynamically unstable. Instability is preceded by concentration polarization, i.e. depletion of the electrolyte in the interface diffusion layer and yields a microvortical flow in this layer. An ambiguity persists regarding the mechanism of this instability. The buoyant mechanisms are disregarded because instability also occurs in a gravitationally stable position and in diffusion layers too thin for buoyancy to mediate the flow. Therefore, instability is attributed to the electric forces acting in or near the interface electric double layer. These forces cause a slip-like flow known as electro-osmosis which comes in two varieties. One is the classical equilibrium electro-osmosis related to the space charge of the electric double layer. The other is the non-equilibrium electro-osmosis related to the extended space charge which forms near the interface at high depletion.

Both types of electroosmosis may yield instability. The question is which one is at work in each particular system. The non-equilibrium electro-osmotic instability, unlike the equilibrium one, is of the short-wave type. This implies that its induced vortices are small compared to the width of the diffusion layer. Therefore, this width, which has not been clearly defined in most experiments so far, is crucial for the identification of the instability mechanism. In this talk, we report the results of our combined experimental and theoretical study of concentration polarization in a custom-designed experimental cell with a particular cation exchange membrane.

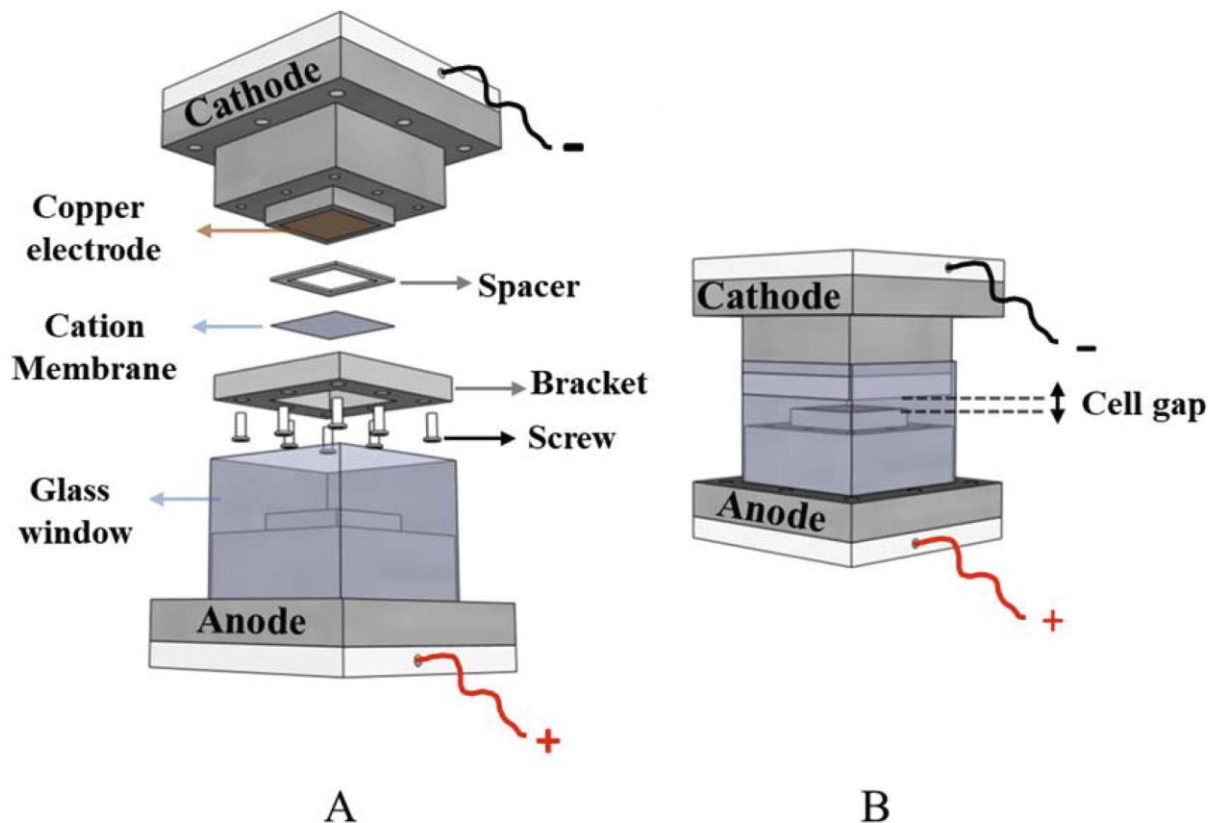


Figure 1. Schematic three-dimensional drawing of the experimental electrolyte cell.

\*Corresponding author. E-mail: boris@bgu.ac.il

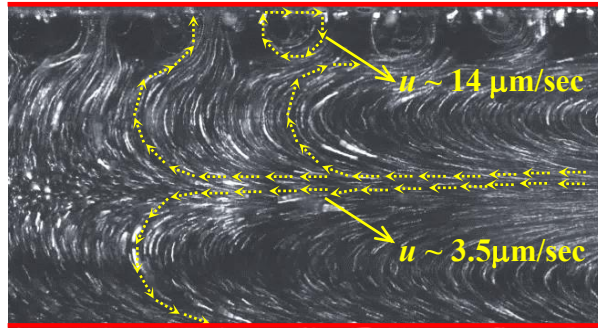


Figure 2. Time-lapse snapshots of the flow in the cell. Large scale convective flow and small convective vortices seen near the membrane surface (cathode)

As a part of our study we investigate the recently predicted thermo-convective instability. This instability is of the long-wave type and its related flow involves a pair of wide vortices spanning the diffusion layer. We experimentally retrieve this flow which clearly marks the width of the diffusion layer. We observe that for high voltages this thermo-convection is accompanied by electro-osmotic instability.

Upon the background set by thermo-convection we are able to conclude that the observed electro-osmotic instability is of the short-wave type and is thus due to the non-equilibrium electro-osmosis. We suggest that a similar approach might be useful for identifying the instability mechanism in other charge selective systems as well.

## THEORY OF ION TRANSPORT AND SELECTIVITY IN MEMBRANES WITH ELECTRICALLY CONDUCTIVE SURFACE

Ilya Ryzhkov<sup>1</sup>, Atrur Krom<sup>1</sup>, Mikhail Simunin<sup>2</sup>

<sup>1</sup>*Institute of Computational Modelling SB RAS, Krasnoyarsk, Russia*

<sup>2</sup>*Siberian Federal University, Krasnoyarsk, Russia*

**Summary.** The theoretical framework for describing ion transport in nanoporous membranes with electrically conductive surface is developed. Comparison between the 2D Space-charge and 1D Uniform potential models on the basis of Navier-Stokes, Nernst-Planck, and Poisson equations is performed. The models are successfully applied to the description of experimental data on switchable ionic selectivity of conductive membranes.

Over the last two decades, a lot of research has been focused on the development of nanochannel systems and nanoporous membranes, which can change their transport properties in ionic solutions in response to the applied electric field [1]. When the channel dimension becomes comparable with the Debye length, the overlap of electric double layers leads to the accumulation of counter-ions and exclusion of co-ions [2]. In this case, the direct manipulation of ion transport through the nanochannel can be performed by applying a transmembrane potential difference and/or varying the surface charge. If membrane material is electrically conductive, then the surface charge can be altered by applying a prescribed potential to the membrane, i.e. by injecting or withdrawing electrons to or from the membrane surface. It provides a powerful tool for changing and adjusting such membrane characteristics as ionic selectivity, ionic conductivity, and ion rejection (in filtration applications).

In this work, we have developed the theoretical framework for describing ion transport in nanoporous membranes with electrically conductive surface [3–7]. A membrane is modelled as an array of cylindrical pores separating two reservoirs with specified values of potential, ion concentration, and pressure. The pore interior is divided into the diffuse layer and the Stern layer with inner and outer parts bounded by the inner and outer Helmholtz planes (iHp and oHp), respectively (Figure 1). The chemical charge arising from specifically adsorbed ions or reactive surface groups is located at the iHp and assumed to be constant.

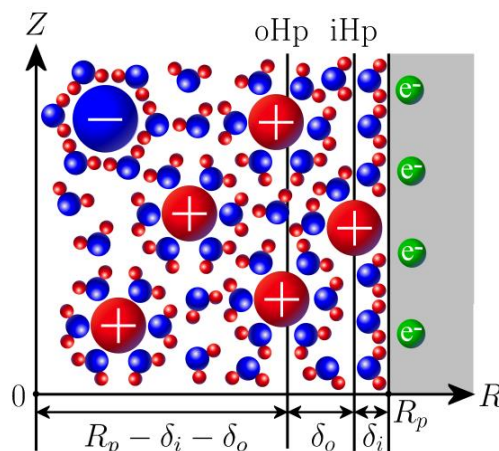


Figure 1. The scheme of electric double layer in a nanopore with conductive wall.

The electrical potential in the Stern layer satisfies the Poisson equation, while the potential, ion concentrations, and pressure in the diffuse layer are described by the two-dimensional Space charge (SC) or one-dimensional Uniform potential (UP) models. We have first generalized these models to the case of constant surface potential in the presence of Stern layer and chemical charge. A new algorithm for solving the SC model equations is proposed. An extensive comparison between the two models is performed by analyzing the impact of surface potential on the ionic selectivity. The latter is evidenced by the sign and magnitude of membrane potential at zero current.

It is shown that the ionic selectivity can be continuously switched from cation to anion by the variation of surface potential. The ideally selective state corresponds to minimum of ion fluxes and maximum of osmotic velocity, while in the non-selective state, the ion fluxes are at maximum and osmotic flow is absent. The decrease of Stern layer permittivities leads to higher potential drop in this layer and lower diffuse layer potential. It reduces the ionic selectivity and makes the transition between selective states more smooth. A similar effect is produced by the increase of pore radius when it exceeds the Debye length. The SC and UP models provide close results for membrane potential and average surface and diffuse layer charge densities even when the pore radius significantly exceeds the Debye length. An overestimation (underestimation) of average osmotic velocity by the UP model is observed at low (high) applied potentials. At the same time, the UP model underestimates the magnitudes of ion fluxes as well as iHp and oHp potentials.

The proposed models provide a qualitative and quantitative description of experimental results on switchable ionic selectivity of track-etched membranes modified by the gold coating [8] as well as C-Nafen membranes prepared from conductive carbon coating [3]. These models can be employed for prediction of ion transport in conductive membranes with application to nano- and ultrafiltration, (reverse) electrodialysis, electrochemical sensors, and nanofluidic devices.

The reported study was funded by Russian Foundation for Basic Research, Government of Krasnoyarsk Territory, Krasnoyarsk Regional Fund of Science, to the research project 18-48-242011 "Mathematical modelling of synthesis and ionic transport properties of conductive nanoporous membranes".

## References

- [1] Siwy Z.S., Howorka S. Engineered voltage-responsive nanopores, *Chem. Soc. Rev.* 39, 1115–1132, 2010.
- [2] Schoch R.B., Han J., Renaud P. Transport phenomena in nanofluidics. *Rev. Modern Phys.* 80, 839–883, 2008.
- [3] Ryzhkov I.I., Lebedev D.V., Solodovnichenko V.S., Minakov A.V., Simunin M.M. On the origin of membrane potential in membranes with polarizable nanopores. *J. Membr. Sci.* 549 (2018) 616–630.
- [4] Ryzhkov I.I., Vyatkin A.S., Minakov A.V. Theoretical study of electrolyte diffusion through polarizable nanopores. *J. Siber. Fed. Univer.: Mathematics & Physics* 11 (4) (2018) 494–504.
- [5] Ryzhkov I.I., Vyatkin A.S., Medvedeva M.I. Modelling of electrochemically switchable ion transport in nanoporous membranes with conductive surface. *J. Siber. Fed. Univ.: Mathematics & Physics* 12 (5) (2019) 579–589.
- [6] I.I. Ryzhkov, A.S. Vyatkin, E.V. Mikhlina. Modelling of conductive nanoporous membranes with switchable ionic selectivity. *Membranes and Membrane Technologies* 2 (1) (2020) 10–19.
- [7] L. Zhang, P.M. Biesheuvel, I.I. Ryzhkov. Theory of ion and water transport in electron--conducting membrane pores with pH--dependent chemical charge. *Phys. Rev. Appl.* 12 (2019) 014039.
- [8] C.R. Martin, M. Nishizawa, K. Jirage, M. Kang, S.B. Lee. Controlling ion-transport selectivity in gold nanotubule membranes. *Adv. Mater.* 2001, V. 13, 1351.

## MATHEMATICAL SIMULATION OF GAS TRANSPORT THROUGH COMPOSITE MEMBRANES

Valery Ugrozov

*Department of Mathematics, Financial University under the Government of the Russian Federation,  
Moscow, Russia*

### INTRODUCTION

Intensive development and experimental studies of new high-performance gas-separation composite membranes with thin active (selective) layers applied to a porous support (Figure 1) indicate the need to clarify the traditional theoretical concepts about of transport gas through the composite membrane (CM), taking into account a number of factors whose influence on gas transmission through the CM was previously neglected or not considered.

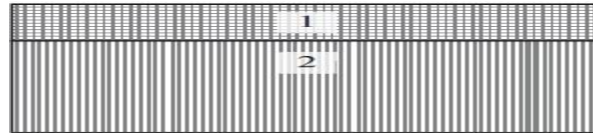


Figure 1. Representation of a composite membrane. (1) the selective layer and (2) the support.

### INFLUENCE OF POROUS SUPPORT STRUCTURE

Since the permeability of a porous CM support is usually noticeably higher than that of the active layer, it was assumed until recently that its porous structure does not have a noticeable effect on gas transmission through the CM. However, experimental studies on the transport of various gases through CMs with thin active layers ( $< 1 \mu\text{m}$ ) conducted in recent years have shown that their gas permeability coefficients depend on the thickness of the active layer [1-2]. Such dependence cannot be predicted by the traditional one-dimensional model of resistances [3], which satisfactorily describes many experiments on gas transmission through various CMs with active layer thickness  $> 1 \mu\text{m}$ .

In [4-5], it was assumed that the observed dependence is due to the influence of the porous support on the gas transfer, since gas molecules are forced to diffuse in the active layer at different distances in order to get into the pores of the support (the transfer through the non-porous support matrix is neglected). A three-dimensional diffusion model should be used to model such a gas transport mechanism. It is shown that this model can numerically describe the dependence of the permeability coefficient on the thickness of the active layer.

To model the observed dependence of gas permeability through CM, we proposed another approach [6], which follows from the assumption that it is necessary to take into account the process of gas adsorption on the surface of the active layer, since the diffusion rate decreases, when the thickness of the active layer decreases and can become comparable to the adsorption rate, the influence of which on gas transport is usually neglected, assuming that sorption occurs much faster than diffusion. In the framework of this approach, a one-dimensional CM gas transfer equation has been obtained and it has been shown that it adequately predicts the experimentally observed dependences of gas permeance of composite membrane -  $Q_c$  on the active layer thickness -  $l_s$ .

### INFLUENCE OF PENETRATION OF THE ACTIVE LAYER INTO PORES SUPPORT

A noticeable effect on gas transfer through the CM may have the effect of penetration of the active layer into the pores of the CM support. The analysis of experimental data on gas permeability of a number of gases through CMs with the active layer of PTMSP and UVFK and MFFC-1 supports [8] has shown that in the process of CM formation by applying the active layer the permeability of the support can significantly decrease due to the active layer penetration into the pores of the polymer. It was also found that dependence of the permeability from the active layer thickness of all investigated gases is described by a simple linear equation of the species.

The penetration of the active layer into the support pores, as shown by our estimates within the resistance model [9], can significantly reduce the gas permeability of CM (Figure 3).

It should be noted that at present, there are no gas transfer models that allow for more detailed consideration of the process of penetration into the support pores, because it depends on the methods and conditions of obtaining CMs and the porous structure of supports, many of which are strongly disordered.

### GAS TRANSFER ASYMMETRY EFFECT IN MULTILAYER MEMBRANES

At present, there are active scientific studies of the mechanisms of asymmetry of transport (dependence of the flow value on the transport direction) of gases and liquids through various membranes. In a number of our works [10-12], the possible mechanisms of the effect of asymmetry of gas transport (EAGT) through CM and multilayer non-porous membranes have been investigated by method mathematical modeling. In [10], it was shown that EAGT through the CM can occur when the contribution of a viscous current to the gas transfer in the pores of the support is comparable to the

Knudsen flow. In [11] it was shown for the first time that EAGT can occur when desorption velocities differ on the outer surfaces of single-layer polymer membrane. In [12] it is shown that when transferred through a two-layer non-porous polymer membrane, EAGT may occur in the membrane layers if sorption in the layers is described by nonlinear absorption isotherms. Analytical expression for estimation of EAGT intensity is obtained. It is established that the adsorption rate significantly affects the EAGT intensity in the two-layer membrane. It was found that if rate of adsorption is a limiting stage of transfer, the membrane can function as a gas "diode". Modeling of atomic hydrogen transport through a palladium membrane applied to a porous support [13] has established the possibility of EAGT formation. It is shown that its intensity reaches the highest value when the transfer of hydrogen in palladium is determined by diffusion and gas permeability of hydrogen in both layers is close. Modelling the diffusion transport of atomic hydrogen through a three-layer vanadium membrane coated with palladium layers has shown that EAGT can occur at final pressures of molecular hydrogen if the palladium layers have different thicknesses. It was shown that gas permeability of hydrogen reaches the highest value at the contact of a thin layer of palladium with the penetrating layer [14].

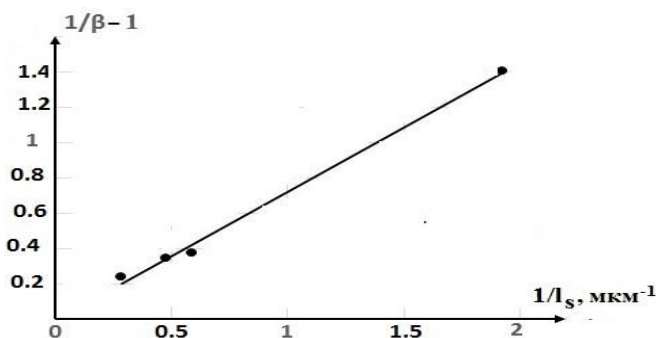


Figure 2. Dependence  $(1/\beta - 1)$  on  $1/l_s$  in case of gas transfer of CO<sub>2</sub> through PEI/Pebax composite membrane [7].  $\beta = Q_c/Q_v$ ,  $Q_v$  is the permeance of the polymer with the thickness  $l_s$  forming the active CM layer.

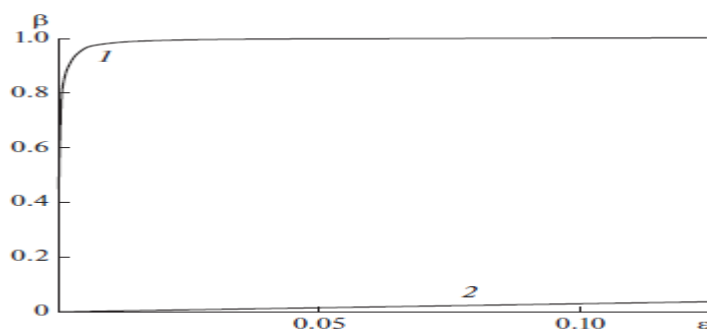


Figure 3. Dependence of the relative permeability of CO<sub>2</sub> through CM on the surface density of the support skin layer -  $\varepsilon$  when the polymer of the active layer does not penetrate into the pores of the support (1) and penetrates into the pores to the depth of the skin layer (2).

## References

- [1] Ramon G. Z., Wong M.C.Y., Hoek E.M.V. // *J. Membr. Sci.* 2012. V.415-416. P.298.
- [2] Wijmans J. G., Hao P.J.// *J. Membr. Sci.* 2015, V.494. P. 78.
- [3] Henis J.M.S., Tripody M.K.// *J.Membr.Sci.*1981, V.8, P.233.
- [4] Zhu L., YavariM., Jia W., Furlani E.P., Lin H. // *Ind. Eng. Chem. Res.* 2017.V.56. N.1. P.351.
- [5] Zhu L., Jia W., Kattula M., Ponnuru K., Furlani E. P., Lin H. // *J. Membr. Sci.* 2016, V.514.P. 684.
- [6] Ugrozov V.V., Filippov A.N. *Colloid. J.* in print.
- [7] Afshoun H.R., Chenar M.P., Ismail A.F., Matsuura T.// *Korean J. Chem. Eng.* 2017.V.34.P.3178.,
- [8] Ugrozov V.V., Bakhtin D.S., Balynin A.V., Polevaya V.G., Volkov A.V. // *Membrane and Membrane Technology.*2019. V.1, N.6, P.347.
- [9] Ugrozov V.V., Volkov A.V.// *Colloid Journal*, 2020, Vol. 82, No. 4, P. 1.
- [10] Ugrozov V.V., Volkov A.V.// *Colloid Journal*, 2020, Vol. 82, No. 2, P. 194.
- [11] Ugrozov V.V., Filippov A.N.// *Colloid Journal*, 2012, Vol. 74, No. 6, P. 777.
- [12] Ugrozov V.V.// *Colloid Journal*, 2018, Vol. 80, No. 2, P. 1.
- [13] Ugrozov V.V. // *Colloid Journal*, 2018, V. 80, No. 3, P. 344.
- [14] Ugrozov V.V. // *Colloid Journal*, 2017, V. 79, No. 1, P. 90.

## THE PHENOMENON OF SPACE CHARGE BREAKDOWN IN ELECTRO-MEMBRANE SYSTEMS

Anna Kovalenko<sup>1</sup>, Matthias Vessling<sup>2</sup>, Victor Nikonenko<sup>3</sup>, Elizaveta Evdochenko<sup>2</sup>, Machamet Urtenov<sup>\*4</sup>,

<sup>1</sup>*Department of Intelligent Information Systems, Kuban State University, Krasnodar, Russia*

<sup>2</sup>*Chemical Process Engineering AVT.CVT, RWTH Aachen University, Aachen, Germany*

<sup>3</sup>*Membrane Institute, Kuban State University, Krasnodar, Russia*

<sup>4</sup>*Department of Applied Mathematics, Kuban State University, Krasnodar, Russia*

**Summary** This article is the first to study the breakdown of space charge in electromembrane systems, namely, in the desalination channel of an electro dialysis apparatus formed by anion-exchange (AEM) and cation-exchange (CEM) membranes. First, we study the desalination channel in the absence of forced convection using a one-dimensional mathematical model of salt ion transport in the cross-section of the desalination channel. Then, in the presence of forced convection and electroconvection using a two-dimensional mathematical model. The main patterns of breakdown are established.

Breakdown is loss of electrical strength under the influence of an electric field can occur in all electrical systems and devices, from microchips to any household appliance. The main consequence of the breakdown is the formation of a channel of increased conductivity. The theory of breakdown in liquid dielectrics is currently sufficiently investigated. Electromembrane systems, in contrast to liquid dielectrics, have interesting features related to the formation and development of space charge regions in each of the ion-exchange membranes. The effect of space charge on the structure of the diffusion layer in an ion exchange membrane was first studied in the article [1]. It was shown in the article [2] that the value of the space charge must have a local maximum, and when the potential jump increases, the local maximum shifts to the depth of the diffusion layer. In the cross-section of the desalination channel, the situation is completely different. First, the AEM, the space charge has a negative value. Second, the space charge waves of different signs begin to interact, which leads to a new effect, namely, the space charge breakdown effect [3]. Thus, the breakdown of the space charge occurs even before the classical breakdown occurs in dielectrics.

At the next stage, a breakdown in the desalination channel of the electro dialysis apparatus formed by the AEM was investigated (Figure1 left) and CEM (in Figure1 on the right) with membranes taking into account forced (the solution flows from the bottom up), as well as electric convections.

Figure 1 shows how the breakdown is formed. First, rather isolated, sometimes narrow regions of the greatest conductivity are formed (Figure 1b). The space charge wave moves along these regions, and the space wave moves from the space charge region (SCR) at the CEM to the SCR at the AEM (Figure 1a). This is due to the fact that the overlimiting state of the CEM is reached earlier (for a solution of sodium chloride). At the time of the breakdown and sometime after the breakdown, the size and number of electroconvective vortices significantly decreases (Figure 1b). Thus, the breakdown of the space charge has a stabilizing effect.

Numerical analysis shows that over time, with an increase in the potential jump, there are more breakdowns and they are more noticeable and powerful.

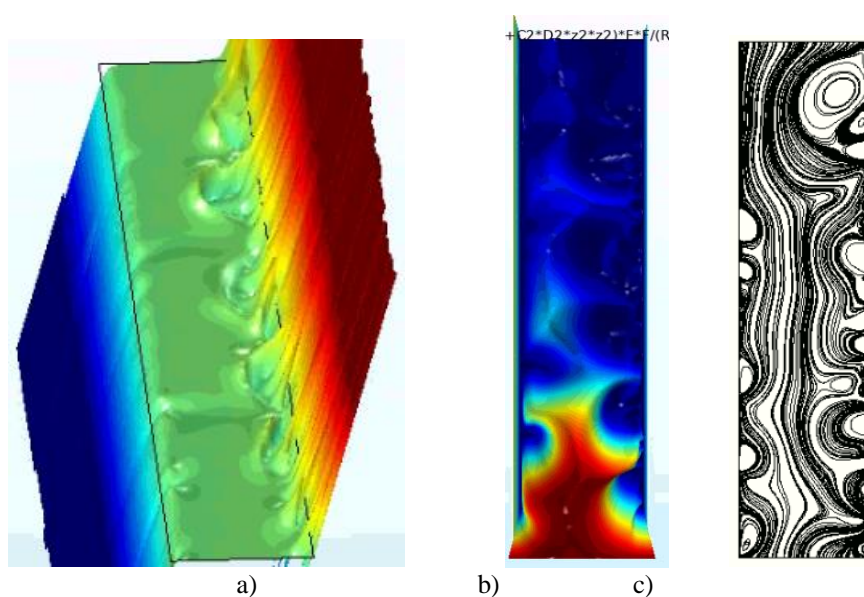


Figure 1. Comparison of the space charge density (a) with the conductivity (b) and the solution current lines (c) at the moment of breakdown.

\*Corresponding author. E-mail: [urtenovmax@mail.ru](mailto:urtenovmax@mail.ru).

## CONCLUSIONS

It is shown that the initial breakdown occurs at a certain jump along the line of least resistance of the solution. The breakdown directly has little effect on the conduction current, and very significantly on the bias current. The effect of breakdown on the hydrodynamic and diffusion instability of the salt ion transport process is investigated.

This work was supported by the Russian Foundation for Basic Research, project No. 20-58-12018 NNIO\_a: The influence of electroconvection, water dissociation, and geometry of spacers on electro dialysis desalination in intensive current regimes.

## References

- [1] Rubinshtein, I.; Zaltzman, B.; Prez, J.; Linder C. Experimental verification of the electroosmotic mechanism for the formation of overlimiting current in a system with a cation-exchange electro dialysis membrane. *Electrochemistry*. 38, № 8, 956-967, 2002.
- [2] Urtenov M.H. Boundary value problems for the system of Nernst-Planck-Poisson equations. Krasnodar. 126 p, 1998.
- [3] Urtenov, M.; Chubyr, N.; Gudza, V. Reasons for the Formation and Properties of Soliton-Like Charge Waves in Membrane Systems When Using Overlimiting Current Modes. *Membranes*. 10, 189, 2020.

# ORAL PRESENTATIONS

## INFLUENCE OF MAGNETIC FIELD ON HYDRODYNAMIC PERMEABILITY OF BIPOROUS MEMBRANE

Satya Deo<sup>\*1</sup>, Deepak Kumar Maurya<sup>1,2</sup>, and Anatoly Filippov<sup>3</sup>

<sup>1</sup>Department of Mathematics, University of Allahabad, Prayagraj, India

<sup>2</sup>Department of Mathematics, Prof. Rajendra Singh (Rajju Bhaiya) Institute of Physical Sciences for Study and Research, V. B. S. Purvanchal University, Jaunpur, India

<sup>3</sup>Department of Higher Mathematics, Gubkin Russian State University of Oil and Gas, Moscow, Russia

**Summary** This work is concerned with the effect of magnetic field on hydrodynamic permeability of biporous membrane of micropolar liquid using four well known cell models. The governing equations of micropolar liquid are expressed in modified form using Nowacki's approach. Fluid velocity, microrotation vectors, shear stresses and couple stresses are investigated which are combinations of modified Bessel functions of first and second kinds. Arbitrary parameters are determined by applying analyticity condition at origin, continuity of velocities (both linear and micro-rotational), continuity of stresses (both shear and couple) at the porous interfaces along with an equivalent condition to Happel, Kuwabara, Kvashnin and Mehta-Morse models at the cell surface. Expressions of volumetric flow rate, superficial/filtration velocity and hydrodynamic permeability are reported. The graphical behaviours of hydrodynamic permeability, fluid velocity and microrotation are plotted under the effect of micropolar parameter, Hartmann number, permeability parameters and conductivity ratio parameters, and discussed for different values of these parameters.

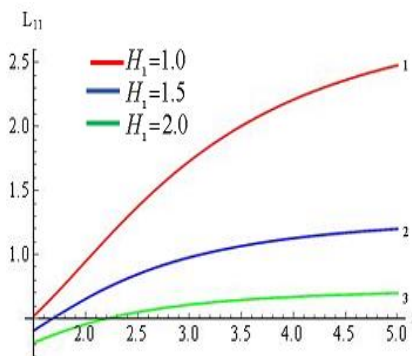


Figure 1. Variation of the hydrodynamic permeability on particle volume fraction parameter  $m$ : (1)  $H_1 = 1$ ; (2)  $H_1 = 1.5$ ; (3)  $H_1 = 2$

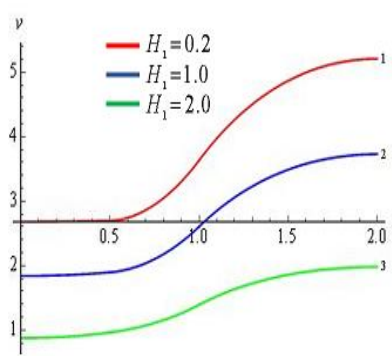


Figure 2. Variation of the fluid velocity on radial coordinate  $r$ : (1)  $H_1 = 0.2$ ; (2)  $H_1 = 1$ ; (3)  $H_1 = 2$ .

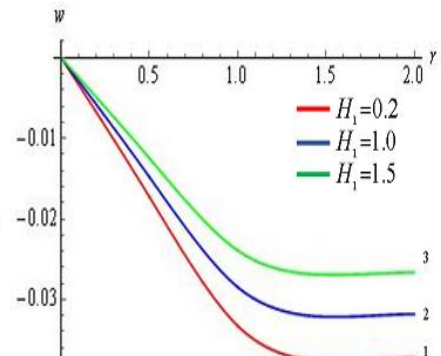


Figure 3. Variation of the microrotation on radial coordinate  $r$ : (1)  $H_1 = 0.2$ ; (2)  $H_1 = 1$ ; (3)  $H_1 = 1.5$ .

### HIGHLIGHTS

- The hydrodynamic permeability of biporous membrane of micropolar liquid in the presence of a magnetic field has been investigated, using four well known cell models when direction of the magnetic field is perpendicular to the direction of fluid flow (*i.e.*, axis of cylinders).
- Micropolar fluid velocities, microrotations, stresses (shear and couple) and Hydrodynamic permeability are obtained analytically using different cell models.
- No-slip condition, continuity of velocity, continuity of microrotation and continuity of stresses (shear and couple) along with equivalent condition of Happel /Kuwabara / Kvashnin / Mehta-Morse cell models are used in boundary conditions.
- Hydrodynamic permeability, fluid velocity and microrotation have been plotted graphically under the effect of micropolar parameter, Hartmann number, permeability parameters and conductivity ratio parameters, for different values of these parameters.

### CONCLUSIONS

The present analysis has some non-trivial physical background and mechanical applications of the micropolar liquid flow which is applicable to describe the motion of blood through human veins/ arteries, flow of droplet of heavy syrups

\*Corresponding author. E-mail: sd\_mathau@yahoo.co.in.

through a swarm of porous aggregates, extraction of crude oil through the porous pipes, etc.. Following conclusions are made:

- Hydrodynamic permeability decreases whenever either micropolar parameter or Hartmann number or permeability parameter increases while it increases as the conductivity ratio parameters increases.
- Micropolar fluid velocity decreases whenever either micropolar parameter or Hartmann number or permeability parameter increases while it increases as the electrical conductivity ratio parameter increases.
- The microrotation decreases as micropolar parameter ( $M$ ), or permeability parameter ( $\eta_1$ ) or conductivity ratio parameter ( $\Lambda_3$ ) increases and it increases whenever Hartmann number ( $H_1$ ) increases.
- On the variation of radial coordinate  $r$ , the curve of fluid velocity expands in the cases of either micropolar parameter ( $M$ ) or Hartman number ( $H_1$ ) or conductivity ratio parameter ( $\Lambda_3$ ) increases while coincides in the case of permeability parameter ( $\eta_1$ ).

## References

- [1] Eringen, A.C. Theory of micropolar fluids. *J. Math. Mech.* 16, 1-18, 1966.
- [2] Nowacki, W. Theory of micropolar elasticity. Springer, New York 1970.
- [3] Happel, H. Viscous flow relative to arrays of cylinders. *A.I.Ch.E.* 5, 174-179, 1959.
- [4] Kuwabara, S. The forces experienced by randomly distributed parallel circular cylinders or spheres in a viscous flow at small Reynolds numbers. *J. Phys. Soc. Jpn.* 14, 527-532, 1959.
- [5] Mehta, G. D, Morse, T. F. Flow through charged membranes. *J. Chem. Phys.* 63, 1878-1889, 1975.
- [6] Kvashnin, A. G. Cell model of suspension of spherical particles. *Fluid Dyn.* 14, 598-602, 1979.
- [7] Stokes, V. K. Theories of fluids with microstructure. Springer, New York 1984.
- [8] Lukaszewicz, G. Micropolar Fluids : Theory and Applications. Springer, New York 1999.
- [9] Deo, S. Stokes flow past a swarm of porous circular cylinders with Happel and Kuwabara boundary conditions. *Sadhana* 29, 381-387, 2004.
- [10] Deo, S., Filippov, A., Tiwari, A., Vasin, S., Starov, V. Hydrodynamic permeability of aggregates of porous particles with an impermeable core. *Adv. Colloid Interface Sci.* 164, 21-37, 2011.
- [11] Yadav, P. K., Tiwari, A., Deo, S., Yadav, M. K., Filippov, A., Vasin, S., Erysheva, E. Sh. Hydrodynamic permeability of biporous membrane. *Colloid J.* 75, 473-482, 2013.
- [12] Khanukaeva D. Yu., Filippov, A. N. Isothermal Flows of micropolar liquids: formulation of problems and analytical solutions. *Colloid J.* 80, 14-36, 2018.
- [13] Khanukaeva, D. Yu., Filippov, A. N., Yadav, P. K., Tiwari, A. Creeping flow of micropolar fluid parallel to the axis of cylindrical cells with porous layer. *Eur. J. Mech. B Fluids* 76, 73-80, 2019.
- [14] Yadav, P. K., Jaiswal, S., Puchakarla, J. Y. Micropolar fluid flow through the membrane composed of impermeable cylindrical particles coated by porous layer under the effect of magnetic field. *Math. Method Appl. Sci.* 1-13, 2019.
- [15] Sherief, H. H., Faltas, M.S., Ashmawy, E. A., Hameid, A. M. A. Parallel and perpendicular flows of a micropolar fluid between slip cylinder and coaxial fictitious cylindrical shell in cell models. *Eur. Phys. J. Plus* 129: 217, 2014.
- [16] Madasu, K. P., Bucha, T. Impact of magnetic field on flow past cylindrical shell using cell model. *J. Braz. Soc. Mech. Sci. Eng.* 41, 2019.
- [17] Yadav, P. K. Motion through a non-homogeneous porous medium: hydrodynamic permeability of a membrane composed of cylindrical particles. *Eur. Phys. J. Plus* 133: 1, 2018.
- [18] Srivastava, B. G., Yadav, P. K., Deo, S., Singh, P. K., Filippov, A. Hydrodynamic permeability of a membrane composed of porous spherical particles in the presence of uniform magnetic field. *Colloid J.* 76, 725-738, 2014.
- [19] Deo, S., Maurya, D. K., Filippov, A. N. Influence of magnetic field on micropolar fluid flow in a cylindrical tube enclosing an impermeable core coated with porous layer. *Colloid J.* 2020 (Accepted).

## PROTON TRANSPORT ACROSS ANION EXCHANGE MEMBRANES IN ELECTROCHEMICAL SYSTEMS

Jouke Dykstra<sup>1</sup>, and Maarten Biesheuvel<sup>2</sup>

<sup>1</sup>*Department of Environmental Technology, Wageningen University, Wageningen, The Netherlands*

<sup>2</sup>*Wetsus, European Centre of Excellence for Sustainable Water Technology, Leeuwarden, The Netherlands*

### Summary

In many electrochemical systems amphoteric ions are present, which undergo acid-base reactions. We present a system-level theory for an electrochemical cell that includes electrochemical reactions and ion transport across an ion exchange membrane (in this case either an anion exchange membrane or a bipolar membrane). We find that, when amphoteric ions are present, protons can be easily transferred across an anion exchange membrane. Furthermore, based on our analysis for a BPM, we conclude that a commonly made assumption that, in BPMs, the current is carried by  $H^+$  and  $OH^-$ , and that these species are produced at the interface between AEM and CEM, is not correct. We conclude that, in order to describe and explain ion transport in BPMs, all ionic species have to be considered, especially the amphoteric ions.

### INTRODUCTION

In many electrochemical systems amphoteric ions are present, which undergo acid-base reactions. In these systems the transport rate is dependent on, amongst others, the local pH. In present work, we discuss several theoretical approaches to describe the transport of amphoteric ions because of an electrical field. We show that some of these approaches result in many difficulties, and require to make assumptions when it comes to which ionic species within a group of amphoteric ions exactly participates in a certain reaction (e.g.  $HCO_3^-$  or  $CO_2$ ). We show that, by grouping amphoteric ions, one can derive an elegant description of ion transport and electrochemical reactions by assuming infinitely fast acid-base reactions. This assumption makes numerical analysis much easier compared to other models that include finite rates of the acid-base reactions.

We present a system-level theory for an electrochemical cell that includes electrochemical reactions at the electrodes and ion transport across the membranes to study the transport of the most prominent anions and cations, in combination with acid-base reactions. This theory builds on previous work in which one dimensional steady-state theory was presented that described ion transport as a function of concentration and potential gradients in electrochemical systems [1,2].

### RESULTS

We analyze the transport of several amphoteric ions in two frequently used membranes in an electrochemical system: an anion exchange membrane (AEM) and a bipolar membrane (BPM). We show results for a system in which acetate ( $Ac^-$ ), acetic acid (HAc), bisulphate ( $HSO_4^-$ ) and sulphate ( $SO_4^{2-}$ ) ions are present.

We find that, across the membrane, the ionic current is mainly carried by the group of ionic species with the pK-value closest to the local pH. Thus, when the pH is close to the pK of the  $Ac^-$ -HAc equilibrium (pK=4.8), the current is mainly carried by these species, but when the pH is close to pK of the  $SO_4^{2-}$ - $HSO_4^-$  equilibrium (pK=1.9), these ions carry the current.

In case an AEM is used in the system we study, several ions contribute to charge transport. As the compositions of the solution on both sides of the membrane are completely different, the contribution of ions to charge transport is also different at both sides of the membrane. In the studied case, at the anode side, charge is mainly carried by  $HSO_4^-$  and  $SO_4^{2-}$  ions, with  $SO_4^{2-}$  being transported from cathode to anode, and  $HSO_4^-$  from anode to cathode. At the cathode side, the charge is carried by  $Ac^-$  and HAc ions, with  $Ac^-$  being transported from cathode to anode, and HAc from anode to cathode.

Interestingly, for the case we study, we observe a net transport of protons across the AEM from the anode to the cathode, which are shuttled by the  $SO_4^{2-}$ - $HSO_4^-$  group and the  $Ac^-$ -HAc group. To quantify this phenomenon, we can define a ‘proton shuttle number’ (PSN), which is the contribution of each of these groups to proton transport. Figure 1 shows the PSN of sulphate and acetate as function of the position inside the membrane. Furthermore, Figure 1 shows the proton transfer rate, which is (in this case) the rate with which protons are transferred from  $HSO_4^-$  to  $Ac^-$ , resulting in  $SO_4^{2-}$  and HAc.

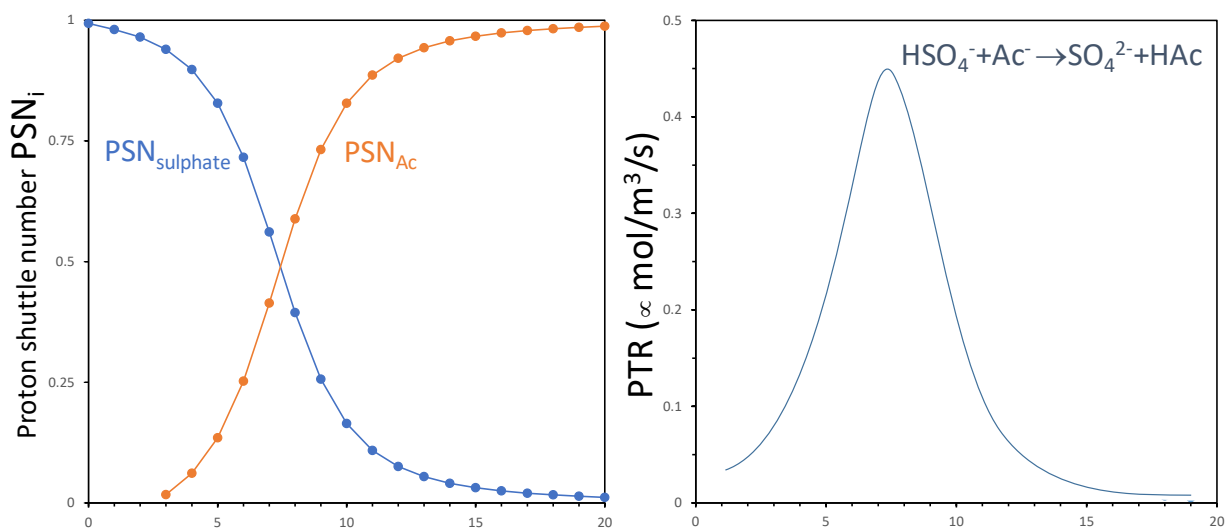


Figure 1. Ion transport across an anion exchange membrane. The composition of the electrolyte is different on each side of the membrane. The proton shuttle number quantifies the contribution of the respective group, in this case either sulphate ( $\text{HSO}_4^-$  and  $\text{SO}_4^{2-}$ ) or acetate ( $\text{HAc}$  and  $\text{Ac}^-$ ), to the transport of protons across the membrane from the anode (left side, position 0) to the cathode (right side, position 20).

Lastly, we analyzed ion transport across BPMs. In the cation exchange layer of the BPM, we find that the current is carried by protons. In the anion exchange layer, we find that  $\text{SO}_4^{2-}$  is transported from the anode through the anion exchange layer of the BPM to the interface with the cation exchange layer, and  $\text{HSO}_4^-$  is transported in the opposite direction. Therefore, also in this case we observe a net transport of protons from the anode, across the anion exchange layer of the BPM, to the interface with the cation exchange layer of the BPM.

## CONCLUSIONS

In conclusion, the results show that a commonly made assumption that, in BPMs, the current is carried by  $\text{H}^+$  and  $\text{OH}^-$ , and that these species are produced at the interface between AEM and CEM, is not correct. We find that, in order to describe and explain ion transport in BPMs, all ionic species have to be considered, especially the amphoteric ions. These amphoteric ions, for example  $\text{HSO}_4^-$ , can carry a proton across the anion exchange layer of the BPM to interface with the cation exchange layer, and is thereafter transported in the reversed direction in the unprotonated form,  $\text{SO}_4^{2-}$ .

## References

- [1] Lichtervelde A.C.L., Ter Heijne A., Hamelers H.V.M., Biesheuvel P.M., Dykstra J.E. Theory of Ion and Electron Transport Coupled with Biochemical Conversions in an Electroactive Biofilm. *Phys. Rev. Appl.* 12, 014018, 2019.
- [2] Dykstra J.E., Biesheuvel P.M., Bruning H., Ter Heijne A. Theory of ion transport with fast acid-base equilibrations in bioelectrochemical systems. *Phys. Rev. E.* 90, 013302, 2014.
- [3] Biesheuvel, P.M., Dykstra, J.E., Physics of Electrochemical Processes. [www.physicsofelectrochemicalprocesses.com](http://www.physicsofelectrochemicalprocesses.com). ISBN 978-90-9033258-1 (2020).

## CAPILLARY MODEL OF ELECTROOSMOTIC TRANSFER IN ION-EXCHANGE MEMBRANES

Irina Falina\*, Olga Demina, and Victor Zabolotsky

Department of Physical Chemistry, Kuban State University, Krasnodar, Russia

**Summary** The work presents the results of estimation of free water transport numbers through the ion-exchange membrane using the Stern double electric layer theory and physicochemical and structural characteristics of the membrane, if the ion-exchange membrane is presented as a capillary system. A good agreement between the experimental data and the results of calculations in frames of the model for alkaline metals chlorides solutions with concentration  $\geq 1$  mol/L was observed, that is practically important for electro dialysis concentrating of salt solutions. A significant influence of the polymer matrix and counter ion nature on the fraction of the through mesopores has been revealed.

### INTRODUCTION

Water transport in the membrane plays a key role in the efficiency of the electromembrane processes, such as electrolyte concentrating by electro dialysis or generating electricity in proton exchange membrane fuel cell (water management). The purposeful creation of a membrane material with appropriate electroosmotic transfer needs the information on the relationship between the electroosmotic permeability of the membrane with its structural, physicochemical and transport characteristics. This problem could be successfully resolved by modelling the water transport in membranes. Present work is devoted to experimental examination of capillary model of free solvent electroosmotic transport for ion-exchange membranes with different matrixes and fixed groups in solutions of alkali metals chlorides.

### THEORY

The membranes structure is traditionally represented as a beam of thin isoporous capillaries with uniformly distributed fixed ions (Figure 1). In the mesopores ( $1.5 < \text{pore radius} < 50$  nm), where the electroosmotic transport of the free solvent occurs, and in concentrated solutions ( $C > 1$  mol/L) the thickness of the electric double layer is much smaller than its radius. We also assumed that fixed groups are uniformly distributed on the pore wall.

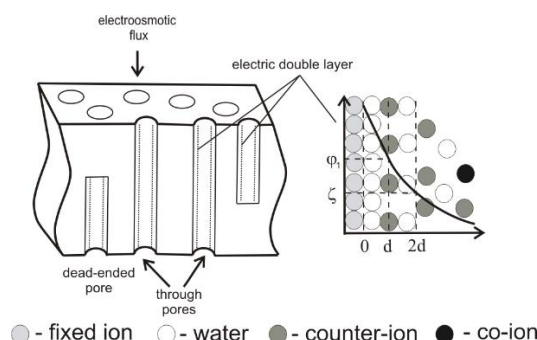


Figure 1. Schematic presentation of the membrane as the isoporous capillary system and structure of the electric double layer.

The electrostatic potential in the Helmholtz plane in such system is determined by the equation of the Stern theory for the planar electric double layer without adsorption [1]. The Gouy-Chapman theory describes the variation in potential with distance for a diffuse double layer [1]. Accounting the Helmholtz-Smoluchowski equation for linear electroosmotic velocity of the solvent in a capillary one can obtain the formulae for calculating the transport number of a free solvent ( $\beta_w$ , mol H<sub>2</sub>O/F) in membrane [2]

$$\beta_w = FC_w \frac{\varepsilon \varepsilon_0}{\eta} \frac{\theta \Delta V \rho_m}{\kappa_m} \zeta$$

where  $\kappa_m$  is specific conductivity of the membrane;  $\Delta V$  is volume of water located in mesopores;  $\zeta$  is the electrokinetic potential calculated by Gouy-Chapman equation;  $\theta$  is the portion of transverse pores directed along the transport axis;  $\rho_m$  is density of swollen membrane;  $\eta$  is the dynamic viscosity of the solution;  $\varepsilon$  is the relative dielectric constant of the solution;  $\varepsilon_0$  is the dielectric constant of vacuum;  $C_w$  is water concentration in solution. The free solvent transport number could be calculated as difference in water transport number and first hydration number of counter-ions.

\*Corresponding author. E-mail: falina@chem.kubsu.ru.

## RESULTS

For model verification of the proposed model we used the set of commercial and experimental membranes with different polymer matrixes, fixed groups, ion-exchange capacity and water content: heterogeneous membranes were MK-40, MK-40×4; MK-41, MK-41×4; MA-41 (JSC “Shekinoazot”, Shekino, Russia); and homogeneous was MF-4SC (JSC “Plastpolymer”, St.-Petersburg, Russia). The specific surface area and volume of water located in mesopores was determined from the experimental standard contact porosimetry data. Figure 2 shows the concentration dependencies of the free water transport numbers  $\beta_w$  in NaCl solutions estimated on the base of experimental data (dots and dashed lines) and calculated in frames of capillary model (solid lines). One can see that in diluted solutions, the calculation results significantly exceed the experimental data. At the same time in concentrated solutions ( $C \geq 1$  mol/L), the good agreement between experimental and calculated values is observed. It is consistent with the fact that in diluted solutions ( $C < 1$  mol/L) the condition  $r / L_D \gg 1$  (where  $r$  is the pore radius and  $L_D$  is the Debye length) is not satisfied and the Helmholtz-Smoluchowski equation could not be used. Similar results were obtained for heterogeneous membranes.

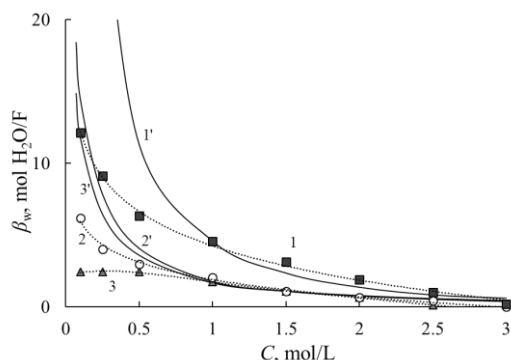


Figure 2. Experimental (dashed lines and dots 1-3) and calculated in frames of capillary model accounting  $\theta$  value (solid lines 1'-3') concentration dependencies of free solvent transport numbers through MF-4SK membranes with different specific water in NaCl solutions: 1 – 11.3 mol H<sub>2</sub>O/mol SO<sub>3</sub><sup>-</sup>; 2 – 22.2 mol H<sub>2</sub>O/mol SO<sub>3</sub><sup>-</sup>; 3 – 36.3 mol H<sub>2</sub>O/mol SO<sub>3</sub><sup>-</sup>.

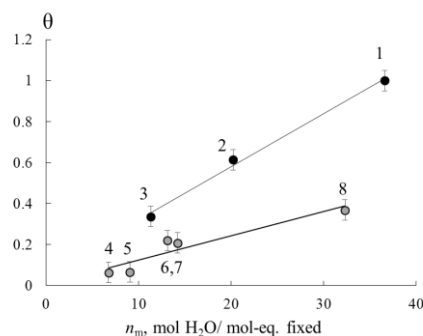


Figure 3. Dependencies of  $\theta$  values on specific water content of the membranes in NaCl solutions: 1 – MF-4SK-1; 2 – MF-4SK-2; 3 – MF-4SK-3; 4 – MK-41; 5 – MK-41×4; 6 – MK-40; 7 – MA-41; 8 – MK-40×4

The dependencies of  $\theta$  on the specific water content of the samples are shown on Figure 3. One can see that  $\theta$  values form two linear dependencies for homogeneous and heterogeneous membranes. This result corresponds to the difference in structure of the membranes under investigation. We should note that the  $\theta$  value is independent on the nature of fixed groups in heterogeneous membrane. Therefore, the received dependencies permit to estimate the  $\theta$  value on the base of specific water content of the membrane.

The free water transport numbers for MK-40 membrane in Li<sup>+</sup>, Na<sup>+</sup> and K<sup>+</sup>-forms were calculated. Decrease in  $\theta$  value with increasing specific water content was observed. This effect is probably caused by the steric limitations to transport of the hydrated ions. In series of the investigated cations K<sup>+</sup>-ion has the smallest size in hydrated form, so the greater quantity of through mesopores with radii 5-50 nm are available for transport. This effect should more pronounced for H<sup>+</sup>-form of the membrane. This information could be used for prediction the water transport in membrane under the restricted humidity conditions that is realized in proton exchange membrane fuel cell.

## CONCLUSIONS

It is shown the possibility to use the capillary model of electroosmotic transfer to estimate the free water transport numbers through ion-exchange membranes of different structural types. Experimental data on conductivity concentration dependencies, curves of effective pore radii distribution, ion exchange capacity and specific surface area were used for the calculations. The comparison of the calculation results and independent electroosmotic experiments shown the agreement of calculated values with the experimental ones when the solutions concentrations exceed 1M. Investigation of the influence of membranes nature on fraction of through mesopores has shown that its magnitude is considerably greater for non-crosslinked homogeneous membranes then for the heterogeneous ones since they are non-crosslinked materials and transport channels form in cluster area near fixed groups.

The work is supported by Russian Foundation for Basic Research (project No 20-08-00637).

## References

- [1] Newman J., Thomas-Alyea K.E., Electrochemical systems, 3rd ed. John Wiley & Sons, New Jersey 2004.
- [2] Falina I.V., Zabolotsky V.I., Demina O.A., Sheldeshov N.V. Capillary model of free solvent electroosmotic transfer in ion-exchange membranes: verification and application *J. Membr. Sci.* 573, 520-527, 2019.

## ANALYSIS OF THE CURRENT VOLTAGE CURVE OF ELECTROMEMBRANE SYSTEMS

Anna Kovalenko<sup>\*1</sup>, Makhamet Urtenov<sup>2</sup>

<sup>1</sup>*Department of Intelligent Information Systems, Kuban State University, Krasnodar, Russia*

<sup>2</sup>*Department of Applied Mathematics, Kuban State University, Krasnodar, Russia*

**Summary** In a number of recent studies, the authors derived and substantiated a formula for calculating the theoretical current-voltage curve (CVC) of electromembrane systems (EMS). This formula was created for the flow cell of desalination of the electrodiagnosis apparatus formed by an anion exchange (AEM) and a cation exchange membranes (CEM) in the potentiodynamic mode based on the charge conservation law. In this paper, the formula for the CVC (I – V characteristic) is investigated, its physical meaning, and the contribution of various factors to the CVC are revealed. A new simplified formula is proposed for calculating CVC, stable with respect to rounding errors. The critical values of the current density were determined and the current voltage curve was divided into separate sections. In the article, we showed that for characteristic values of the average flow rate of the electrolyte solution, the initial concentration in all sections of the CVC, the contribution of the convective current is small. The main role belongs to the electromigration (ohmic) current, especially in the overlimiting sections of the current – voltage curve. The contribution of the diffusion current in limiting and underlimiting sections is quite significant, although less than the ohmic current.

The current-voltage curve (CVC) is the most important integral characteristic of ion transport in electromembrane systems (EMS). The role of the CVC is especially important in the study of the overlimiting current density flows. A research of the experimental CVC in the overlimiting current mode, carried out by the methods of Fourier analysis [1], wavelet analysis [2], and dynamic chaos methods [3], shows a complex, unsteady and unstable behavior of the CVC. However, a theoretical study of the CVC has not yet been carried out. This is due to the lack of a formula for calculating the CVC, which, on the one hand, adequately reflects the non-stationary and unstable behavior of the I – V characteristics in time, and, on the other hand, it is stable with respect to rounding errors in spatial variables. For the first time, a formula was derived in [4, 5] that allows one to calculate the theoretical CVC on the basis of a new mathematical model of processes occurring in an electromembrane system.

Consider the flow cell of the desalination of the electrodiagnosis apparatus. The Oy axis passes through the AEM, and the Ox axis perpendicular to it is directed toward the CEM. Let the cell width be equal  $H$  and the length -  $L$ . The current density at a random point in the cell at some point in time is denoted  $\vec{I}(t, x, y)$ . In [5–8], a 2D mathematical model of the main processes occurring in the desalination channel, namely, diffusion, electromigration, forced convection, and electroconvection, was formulated and researched in the form of a connected system of Nernst-Planck-Poisson and Navier-Stokes (NPPNS) equations with the corresponding boundary conditions, and the adequacy of these models was showed. To analysed the CVC formula, it is necessary to construct a basic electrical diagram of the desalination cell.

When analyzing the results of physical and numerical experiments [3-16], we found some data remain relatively unchanged, however, some of the data vary from experiment to experiment. If we restrict ourselves to experiments with a NaCl solution, then the diffusion coefficients of the cation and anion can be considered unchanged. The density of the solution and the kinematic viscosity coefficient, as well as the universal constants are considered to remain constant: the Faraday number  $F$ , the universal gas constant  $R$ , the absolute temperature  $T$ , and the dielectric constant of the medium  $\varepsilon$ .

In the analysis of CVC, the Leveck limit diffusion current [11] is used.

Let us consider the point  $x=0$ . We show that, the total current is solenoidal, the bias current is potential (in principle, the current  $\vec{I}_c(t, x, y)$  is not solenoidal or potential).

$$\text{From equations (1): } \frac{\partial(z_1 C_1 + z_2 C_2)}{\partial t} = -\text{div}(z_1 \vec{J}_1 + z_2 \vec{J}_2), \quad \frac{\partial \rho}{\partial t} = -\text{div} \vec{I}_c.$$

$$\text{From (3) it follows } \varepsilon_a \text{div} \vec{E} = F(z_1 C_1 + z_2 C_2) = \rho.$$

$$\text{Then } \varepsilon_a \frac{\partial}{\partial t} \text{div} \vec{E} = -\text{div} \vec{I}_c \text{ or } \text{div} \vec{I}_c = -\varepsilon_a \frac{\partial}{\partial t} \text{div} \vec{E}, \quad \text{div} \vec{I}_c = -\varepsilon_a \frac{\partial}{\partial t} \text{div} \vec{E} = -\frac{\partial}{\partial t} \rho(t, x, y), \text{ where } \text{div}(\vec{I}_c + \varepsilon_r \frac{\partial}{\partial t} \vec{E}) = 0,$$

$$\text{given } \vec{I}_{d,1} = \varepsilon_r \frac{\partial}{\partial t} \vec{E}, \quad \vec{I}_{g,1} = \vec{I}_c + \vec{I}_{d,1}.$$

We get  $\text{div} \vec{I}_{g,1} = 0$ , i.e.,  $\vec{I}_{g,1}(t, x, y)$  - the solenoidal vector. On the other hand,  $\vec{I}_{d,1} = \varepsilon_r \frac{\partial}{\partial t} \vec{E} = -\varepsilon_r \frac{\partial}{\partial t} \nabla \varphi = -\varepsilon_r \nabla(\frac{\partial}{\partial t} \varphi) = -\varepsilon_r \nabla \psi$ , where  $\psi = \frac{\partial}{\partial t} \varphi$ . Thus,  $\vec{I}_{d,1} = -\varepsilon_r \nabla \psi$  i.e.  $\vec{I}_{d,1}$  potential vector. The corresponding relations for a point  $x=H$  are proved in a similar way.

---

<sup>\*</sup>Corresponding author. E-mail: savanna-05@mail.ru.

Given the fact that the vectors  $\vec{I}_{g,1}$  and  $\vec{I}_{g,2}$  are solenoidal, from the formulas  $\vec{I}_{g,1} = \vec{I}_c + \vec{I}_{d,1}$ ,  $\vec{I}_{g,2} = \vec{I}_c - \vec{I}_{d,2}$  follows that  $\text{div}\vec{I}_c = -\text{div}\vec{I}_{d,1} = \text{div}\vec{I}_{d,2}$ .

$$\text{Hence, } \frac{1}{2HL} \int_0^L \int_0^H (H-2x) \text{div}\vec{I} dx dy = -\frac{1}{2HL} \int_0^L \int_0^H (H-2x) \text{div}\vec{I}_{d,1} dx dy = \frac{1}{2HL} \int_0^L \int_0^H (H-2x) \text{div}\vec{I}_{d,2} dx dy$$

$$\text{or } \frac{1}{2HL} \int_0^L \int_0^H (H-2x) \text{div}\vec{I}_{d,1} dx dy = -\frac{\partial}{\partial t} \frac{1}{2HL} \int_0^L \int_0^H (H-2x) \rho(t, x, y) dx dy = -\frac{\partial}{\partial t} \hat{\rho}_{av}(t),$$

when  $\hat{\rho}_{av}(t) = \frac{F}{2HL} \int_0^L \int_0^H (H-2x) \rho(t, x, y) dx dy = \frac{F}{2HL} \int_0^L \int_0^H (H-2x) (z_1 C_1 + z_2 C_2) dx dy$  is a reduced average space charge density.

Thus, the first term  $i_{av}(t)$  in formula (3) is the averaged ohmic current carried by ions, and the value of the second term  $i_d(t)$  is the averaged divergence of the bias current or the rate of change of the reduced average space charge density.

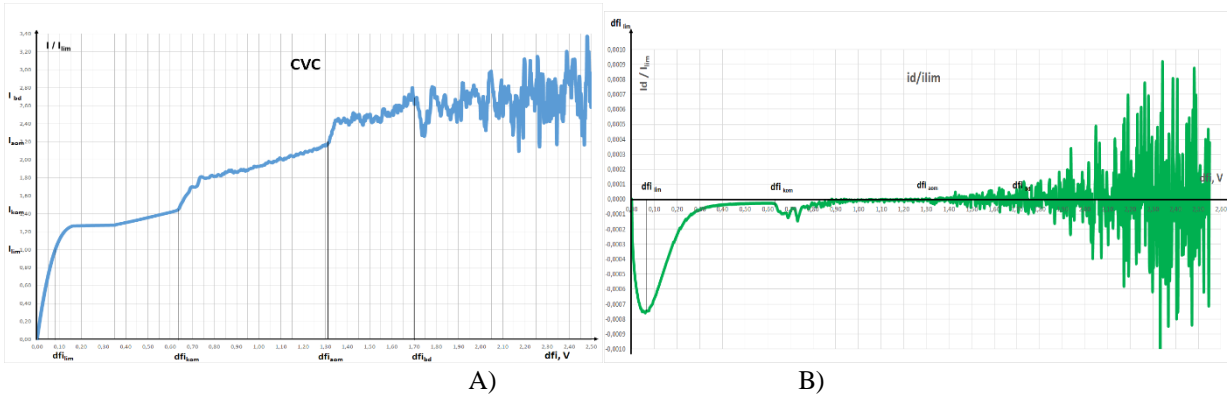


Figure 1. Graphs of currents  $i_{av}(t)$  and  $i_d(t)$

Although the total current in the calculation of the CVC is not constant in time, its change can be considered to be slow. In this case, capacitors practically do not pass the electric current. Therefore, when calculating the CVC of the salt ion transport process, it is not necessary to take into account the bias current. In addition, the bias current does not need to be considered if the current-voltage curve of the conduction current  $\vec{I}_c$  is investigated. In these cases, the CVC must be calculated via the formula:

$$i_{av}(t) = \frac{1}{HL} \int_0^H \int_0^L I_x(t, s, y) dy ds.$$

The reported study was funded by RFBR according to the research project № 19-08-00252 A.

## References

- [1] Budnikov E.Yu., Kukoev I.Yu., Gulyaev A.M., Miroshnikova I.N., Maksimych A.V., Timashev S.F. Wavelet and Fourier analysis of electrical fluctuations in semiconductor and electrochemical systems. *Measuring Technique*. 11, 40-44, 1999.
- [2] Budnikov E.Yu. Analysis of fluctuation phenomena in the field of transcendental currents in an electro-membrane system. *Diss. Cand. Phys.-Math.* 115 p., 2000.
- [3] Kovalenko A.V., Evdochenko E.N. and Urtenov M.H. Calculation and analysis of time behavior of electroconvection in membrane systems. *Scientific journal KubSAU*. 05, 109, 1-13, 2015.
- [4] Urtenov M.Kh., Kovalenko A.V., Sukhinov A.I., Chubyr N.O., Gudza V.A. Model and numerical experiment for calculating the theoretical current-voltage characteristic in electro-membrane systems. *IOP Conference Series: Materials Science and Engineering Collection of materials of the XV International Scientific - Technical Conference. Don State Technical University*. 012030. 2019.
- [5] Urtenov MK, Uzdénova AM, Kovalenko AV, Nikonenko VV, Pismenskaya ND, Vasil'eva VI, Sistat P., Pourcelly G. Basic mathematical model of overlimiting transfer enhanced by electroconvection in flow-through electro dialysis membrane cells. *Journal of Membrane Science*. 447, 190-202, 2013.
- [6] Pham V. S., Li Z., Lim K. M., White J. K., and Han J. Direct numerical simulation of electroconvective instability and hysteretic current-voltage response of a permselective membrane. *Phys Rev*. 86, 046310, 2012.
- [7] Kwak R., Pham V. S., Lim K. M., and Han J., Shear Flow of an Electrically Charged Fluid by Ion Concentration Polarization: Scaling Laws for Electroconvective Vortices. *Phys. Rev. Lett.* 110, 114501, 2013.
- [8] Druzgalski, C. L., Andersen, M. B., Mani, A. Direct numerical simulation of electroconvective instability and hydrodynamic chaos near an ion-selective surface. *Phys. Fluids*, 25, 11, 110804. 2013.
- [9] Randles J.E.B. Kinetics of rapid electrode reactions. *Discussions of the Faraday Society*. 1, 11, 1947.

- [10] Macdonald D.D., Reflections on the history of electrochemical impedance spectroscopy. *Electrochim. Acta.* 51, 1376, 2006.
- [11] Nikonenko V.V., Kozmai A.E. Electrical equivalent circuit of an ion-exchange membrane system. *Electrochimica Acta.* 56, 1262–1269, 2011.
- [12] Zabolotsky V.I., Nikonenko V.V. Ion transfer in membranes. *Nauka.* 392, 1996.
- [13] Nikonenko V. V., Mareev S. A., Pis'menskaya N. D., Uzdenova A. M., Kovalenko A. V., Urtenov M. Kh., Pourcelly G. Effect of electroconvection and its use in intensifying the mass transfer in electro dialysis (Review). *Russian Journal of Electrochemistry* 53, 1122–1144, 2017.
- [14] Nikonenko V.V., Kovalenko A.V., Urtenov M.K., Pismenskaya N.D., Han J., Sistas P., Pourcelly G. Desalination at overlimiting currents: State-of-the-art and perspectives. *Desalination.* 342, 85–106, 2014.
- [15] Urtenov M.K., Uzdenova A.M., Kovalenko A.V., Nikonenko V.V., Pismenskaya N.D., Vasil'eva V.I., Sistas P., Pourcelly G. Basic mathematical model of overlimiting transfer enhanced by electroconvection in flow-through electro dialysis membrane cells. *Journal of Membrane Science.* 447, 190-202, 2013.
- [16] Nikonenko V.V., Pismenskaya N.D., Urtenov M.K., Uzdenova A.M., Kovalenko A.V., Mareev S.A., Pourcelly G. Effect of electroconvection and its use in intensifying the mass transfer in electro dialysis (Review). *Russian Journal of Electrochemistry.* 53(10), 1122-1144, 2017.

## CHRONOPOTENTIOMETRY OF MONOPOLAR ION-EXCHANGE MEMBRANES: MODELING AND EXPERIMENT

Semyon Mareev, Victor Nikonenko, and Natalia Pismenskaya

*Department of Physical Chemistry, Membrane Institute, Kuban State University, Krasnodar, Russia*

**Summary** The influence of ion-exchange membranes (IEMs) properties on the shape of chronopotentiogram (ChP) has been investigated via experiment and numerical simulations. Using a 1D model, we find that the coion transport can cause the formation of local maximum of potential drop on ChP and the consequent new possibility of quantifying the ion transport numbers based on ChP analysis. The conditions for the occurrence of the phenomenon of two chronopotentiometric transition times in a weak electrolyte solution are specified. It is shown that the values of each transition time depend on the nature of the weak electrolyte, the pH of the solution, and the diffusion coefficients of coions in the membrane. 2D simulation and experiments using IEMs with tailored surface showed that in dilute solutions of strong electrolytes, the membrane surface inhomogeneity leads to the phenomenon of two transition times due to the curvature of electric current lines and formation of electroconvective vortices in diffusion boundary layer in proximity to the IEM/solution interface.

### INTRODUCTION

Chronopotentiometry is a powerful method for characterizing IEMs. However, the theory in this area has been developed only for homogeneous IEMs at underlimiting current modes. One-dimensional rather than two-dimensional approaches prevail and there are no models applicable at over-limiting currents. At the same time, experimental studies are carried out mainly at current densities above the limiting value, at which the concentration polarization effects coupled with the flow of electric current are developing: electroconvection, intense dissociation of water and weak electrolytes, sorption of products of chemical reactions in the membrane bulk, etc.

Thus, the development of theoretical concepts of non-stationary processes of ion transfer in electrodialysis systems with IEMs, taking into account the electrical inhomogeneity of the membrane surface, forced and electroconvection, dissociation of ions of weak electrolytes and other effects in conditions of chronopotentiometry, as well as the experimental study of such systems are urgent problems of membrane electrochemistry.

### RESULTS AND DISCUSSIONS

A simple method [1] for simulation of chronopotentiograms at overlimiting current densities was developed. The model takes into account the concentration dependence of diffusion coefficient, the influence of electroconvection and chemical reactions. It is shown that the model describes well experimental chronopotentiograms of homogeneous IEMs at all applied current densities in strong and weak electrolyte solutions. We show that in the case where the bathing solution contains  $\text{Ca}^{2+}$  or  $\text{Mg}^{2+}$  ions, the ChPs of the homogeneous CMX cation-exchange membrane at overlimiting current densities have a local maximum (Figure 1), which appears a few seconds after the transition time. The cause of the maximum is the increase in coion transfer caused by the current-induced concentration polarization of the bathing solution. This increase in coion transfer results in increasing the limiting current density, which at constant current leads to a reduction in the resistance of the depleted diffusion layer over time and the appearance of a maximum on the ChP. Fitting the calculation to the experimental ChP allows determination of the coion transport number in the IEM.

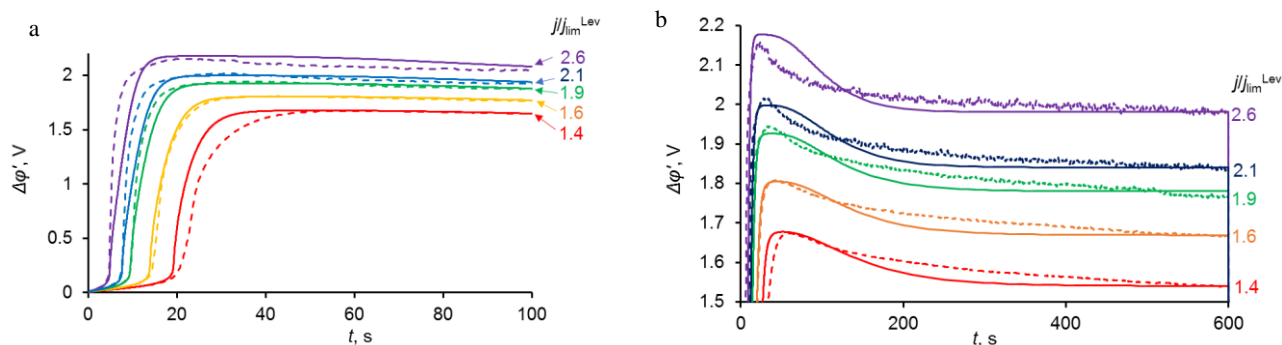


Figure 1. Theoretical (solid lines) and experimental (dashed lines) chronopotentiograms of a CMX membrane in 0.02 N  $\text{CaCl}_2$  solution; (a) shows the initial part of ChPs and (b) shows the upper part of ChPs with local maximums.

The chronopotentiograms of the homogeneous anion-exchange Neosepta AX membrane were measured in 0.02 M  $\text{NaH}_2\text{PO}_4$  solution. In intense current modes, two transition times are observed on the chronopotentiograms. The numerical simulation results showed that the first transition time corresponds to the classical Sand transition time, caused by the diffusion constraints on the transport of  $\text{H}_2\text{PO}_4^-$  counterions through the depleted diffusion layer. A decrease in the concentration of  $\text{NaH}_2\text{PO}_4$  in a depleted diffusion layer with time leads to a decrease in the concentration of co-ions ( $\text{H}^+$  in particular) and an increase in pH in the internal solution of the membrane, consequently the equilibrium of phosphate anion forms shifts towards the multiply charged ions  $\text{HPO}_4^{2-}$  and  $\text{PO}_4^{3-}$ , while their effective transport number increases.

When singly charged  $\text{H}_2\text{PO}_4^-$  ions enter the membrane, some of these ions dissociate and the generated  $\text{H}^+$  ions become additional charge carriers in a depleted diffusion layer, which provides an increase in the current density with an increase in the potential drop across the membrane. After the first transition time, the concentration of singly charged  $\text{H}_2\text{PO}_4^-$  ions in the membrane volume rapidly decreases from the side of the depleted diffusion layer, and the concentration of doubly charged  $\text{HPO}_4^{2-}$  in the membrane increases. After reaching the  $\text{HPO}_4^{2-}$  flux limit, a decrease in its concentration in the membrane at the depleted diffusion layer/IEM interface to a value corresponding to the stationary value at the limiting current density, the number of charge carriers in the depleted diffusion layer becomes insufficient to provide the required amount charge carriers. As a result, the potential drop in the system increases significantly, which corresponds to the second transition time. Overcoming the limitations that determine the second transition time is possible only if the rate of delivery of charge carriers in the depleted diffusion layer is increased, which is ensured by electroconvective mixing of the solution.

We report an approach for 2D modelling of transient ion transfer across a surface composed of conductive and nonconductive areas [2, 3]. In the model formulation and solution, we use the electrical current stream function. For the first time, chronopotentiograms of a system with heterogeneous IEM are calculated. It is shown that the presence of electrical inhomogeneity leads to the phenomenon of two transition times. It is shown that the first transition time corresponds to the classical concepts associated with the diffusion delivery of charge carriers to the conductive regions of the membrane surface, and corresponds to a moment when the concentration of the solution near these regions reaches a critically small value. At such a concentration value, electroconvection is "triggered", the intensity of which has a significant effect on the rate of mass transfer. Local vortices develop, which are much smaller than the thickness of the diffusion layer, but are capable of mixing the solution in the vicinity of the boundary between the conducting and non-conducting regions of the surface. The second transition time corresponds to convective limitations caused by an increase in the diameter of electroconvective vortices and their achievement of the characteristic size of the electrical inhomogeneity of the membrane surface. The concentration reaches a critical value over the entire membrane surface. This critical value determines the beginning of a more powerful stage of electroconvection, at which the size of the vortices becomes comparable with the thickness of the diffusion layer.

## CONCLUSIONS

In this work, using the experiments and numerical simulations, we have investigated the influence of electrical inhomogeneity of the membrane surface, electroconvection, coion transfer and dissociation of weak electrolyte ions on the shape of chronopotentiograms. All the mentioned effects should be taken into account during the interpretation of experimental data. Using the developed models, it is possible to find out the impact of each phenomenon on transition time(s), the parameters of the local maximum or the trends of potential drop when approaching the stationary state, as well as other characteristics of chronopotentiometric curve.

## ACKNOWLEDGMENTS

The work was carried out within the framework of joint Russian-French laboratory "Ion-Exchange Membranes and Related Processes". The authors are grateful to the RFBR (grant No. 18-08-00397a).

## References

- [1] Mareev S.A., Butylskii D.Yu., Pismenskaya N.D., Nikonenko V.V. Chronopotentiometry of ion-exchange membranes in the overlimiting current range. Transition time for a finite-length diffusion layer: modeling and experiment. *J. Membr. Sci.* 500, 171-179, 2016.
- [2] Butylskii D.Y., Mareev S.A., Pismenskaya N.D., Apel P.Y., Polezhaeva O.A., Nikonenko V.V. Phenomenon of two transition times in chronopotentiometry of electrically inhomogeneous ion exchange membranes. *Electrochim. Acta.* 273, 289-299, 2018.
- [3] Mareev S.A., Nebavskiy A.V., Nichka V.S., Urtenov M.K., Nikonenko V.V. The nature of two transition times on chronopotentiograms of heterogeneous ion exchange membranes: 2D modelling. *J. Membr. Sci.* 575, 179-190, 2019.

## MODELING OF ALCOHOLS RECOVERY FROM DILUTED WATER SOLUTIONS WITH MEMBRANE VAPOR SEPARATION

Maxim Shalygin\*, Alina Kozlova, and Vladimir Teplyakov

*A.V.Topchiev Institute of Petrochemical Synthesis, Russian Academy of Sciences, Moscow, Russia*

**Summary** Membrane separation of gas mixtures is widely used nowadays and modelling of such processes is well developed. Membrane separation of vapor and gas-vapor streams is another area with promising potential for further development. Transport of vapors in dense membranes often follows dissolution-diffusion mechanism similarly to gases that provides possibility to apply existing models. Nevertheless, modelling of processes with membrane vapor separation have own particularities in comparison with gas separation due to the possibility of some components condensation, which allows to consider more opportunities for process design and optimization. Modelling of ethanol recovery and concentration from diluted aqueous solutions with application of membrane vapor separation is considered and comparison of different process design is carried out in this work.

Currently, there is a significant increase in the production and use of various types of biofuels: biomethane, hydrogen, biodiesel and bio-alcohols. Bio-alcohols are a convenient alternative fuel because they can be used directly or as additives to gasoline. The production of bio-alcohols formed diluted water-alcohol mixture with typical ethanol concentration of about 10 wt.% (after ethanol fermentation) and butanol concentration of about 1.5 wt.% (after ABE fermentation). In the case of subsequent alcohols use as renewable energy carriers the recovery and concentration steps should be highly effective in order to provide maximum further utilization of energy.

The combination of gas stripping and membrane vapor separation is suggested as promising technology for continuous recovery of bioalcohols from fermentation broth. Among other advantages membrane vapor-phase separation method allows to apply water-selective membranes for recovery and concentration of alcohols from dilute aqueous solutions without the need of evaporation of bulk water instead of pervaporation and possibility of achieving of high alcohol concentration in product stream in one stage.

The schemes of processes for ethanol recovery and concentration from fermentation broth with vapor membrane separation by water-selective membranes were suggested (Figure 1) and mathematical modelling of the processes was carried out for the comparison of its characteristics and each design benefits and limitations.

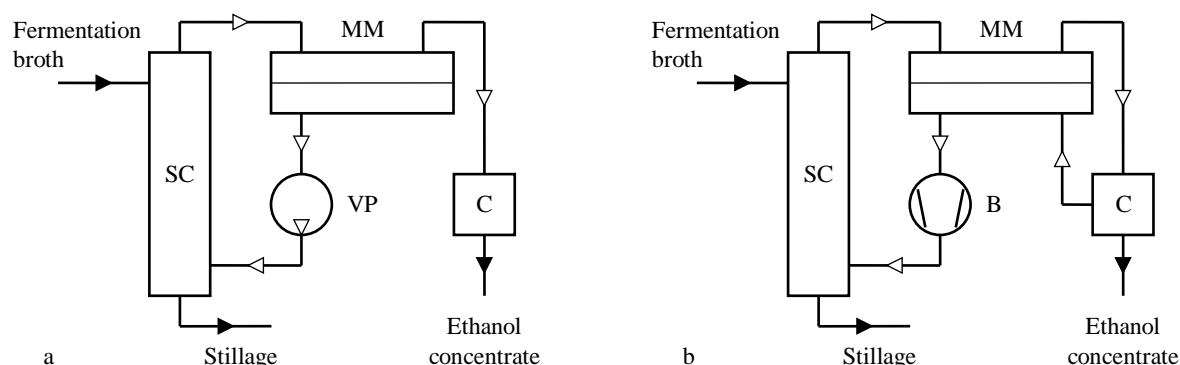


Figure 1. Process design for ethanol recovery and concentration from fermentation broth with vapor membrane separation: a – evacuation of permeate; b – stripping of permeate with gas. Names: B – blower, C – condenser, MM – membrane module, SC – stripping column, VP – vacuum pump.

The transfer of vapors in dense polymeric membrane materials often following the dissolution-diffusion mechanism similarly to gases. There is a few data on the permeability coefficient and its components (diffusion and solubility coefficients) for vapors compared to the available data for gases. Nevertheless, the knowledge about diffusion and solubility coefficients undoubtedly is necessary for fundamental studies, understanding of complex and unusual mass transfer effects, study and modelling of kinetic (unsteady) separation processes. Another important area of study is estimation of transport characteristics of vapor in polymers by application of correlation approach, which demands determination of molecules parameters. The diffusion coefficients of water and methanol in PVTMS were determined and effective diffusion diameters of molecules and Lennard-Jones potentials were calculated that allows estimation of transport characteristics of these vapors in different polymers using correlation approach.

\*Corresponding author. E-mail: mshalygin@ips.ac.ru.

## UNDERSTANDING THE ROLE OF MEMBRANE THICKNESS IN ELECTRO-MEMBRANE PROCESSES VIA NERNST-PLANCK APPROACH

Michele Tedesco

*Wetsus, European Centre of Excellence for Sustainable Water Technology, Leeuwarden, The Netherlands*

**Summary** The effect of the thickness of ion exchange membranes has been investigated for electro dialysis (ED) and reverse electro dialysis (RED), both experimentally and through theoretical modeling. By developing a two-dimensional model based on Nernst-Planck theory, we theoretically find that reducing the membrane thickness benefits process performance only until a certain value, below which performance drops due to the effects of coion leakage. Model calculations compare well with experimental data collected with a series of homogeneous membranes with the same chemical composition and a thickness in the range of 10–100  $\mu\text{m}$ . Our results show that the classical picture that membranes should be as thin as possible is insufficient, and must be replaced by a more accurate theoretical framework.

### INTRODUCTION

Ion exchange membranes (IEMs) are used for a variety of applications, and are typically selected based on a small number of key features (i.e., selectivity and resistance), according to the type of process. The thickness of IEMs is usually not identified as a key determining parameter, since its effect cannot be separated from other membrane properties. Ideally, reducing the IEM thickness gives a linear reduction of the electrical resistance, without affecting other properties. However, reducing the thickness also affects the transport properties of the membrane (i.e., mass transfer rates for co- and counter-ions). Therefore, predicting the actual performance of an electro-membrane process using ultra-thin membranes is still difficult.

The aim of this work is to investigate the effect of the thickness of ion exchange membranes in electro dialysis (ED) and reverse electro dialysis (RED), in order to describe the process when very thin membranes are used. By using a model based on the Nernst-Planck theory [1–3], we theoretically discover that an optimum value for the IEM thickness can be identified [4]. To validate the model, experiments are performed using a series of homogeneous IEMs with the same chemical composition, and with a thickness in the range of 10–75  $\mu\text{m}$ . We aim to understand the relation between IEM thickness and other relevant membrane properties, in order to identify the optimal range for the membrane thickness, given certain process conditions.

### MATERIALS AND METHODS

A series of homogeneous IEMs (Fumatech GmbH, Germany) was tested. All the membranes have the same chemical composition and homogeneous structure, and differ only for the customized thickness, which is in the range of 10–75  $\mu\text{m}$ . A lab-scale stack (10x10  $\text{cm}^2$  electrode area, N=5 cell pairs) was used for all the measurements. We performed experiments with a salt concentration of 30 g/L NaCl (i.e., mimicking seawater) for the ED test, and 30 g/L vs. 1 g/L NaCl for the RED tests (i.e. mimicking seawater-fresh water conditions).

### RESULTS AND DISCUSSION

The mass transport theory adopted in this work relies on the two-dimensional model for (R)ED used in Refs. [2,3], which is based on the Sonin-Probstein framework [1]. In these earlier works [2,3], we considered “symmetrical” behavior of cation and anion exchange membranes (AEMs and CEMs), i.e., assuming that the two membranes have the same thickness and transport properties (diffusion coefficient for counter-/coions, and water permeability), and the same fixed charge density,  $X$ , except for the difference in sign (i.e.,  $\omega X > 0$  for an AEM, and  $\omega X < 0$  for a CEM). Instead, in the present work, all of these symmetry assumptions are dropped, and we include a possible difference in diffusion coefficients between anion and cation both in the membranes and in the spacer channel. In this way, it is possible to investigate the use of unequal thickness, porosity and fixed charge density for AEM and CEM.

We investigate both experimentally and theoretically the influence of membrane thickness on a number of process variables, e.g., on the average current efficiency in ED (Figure 1A), and on the maximum power density in RED (Figure 1B). For ED, Figure 1A shows that the average current efficiency is relatively constant for membranes with thickness  $\delta_m > 30 \mu\text{m}$ , while it decreases with thickness for  $\delta_m < 30 \mu\text{m}$ . For RED, the maximum power density decreases significantly for membrane thicknesses  $\delta_m < 20 \mu\text{m}$  (Figure 1B). The effect of reducing thickness on process performance can be related to the high coion leakage, in the case of very thin membranes.

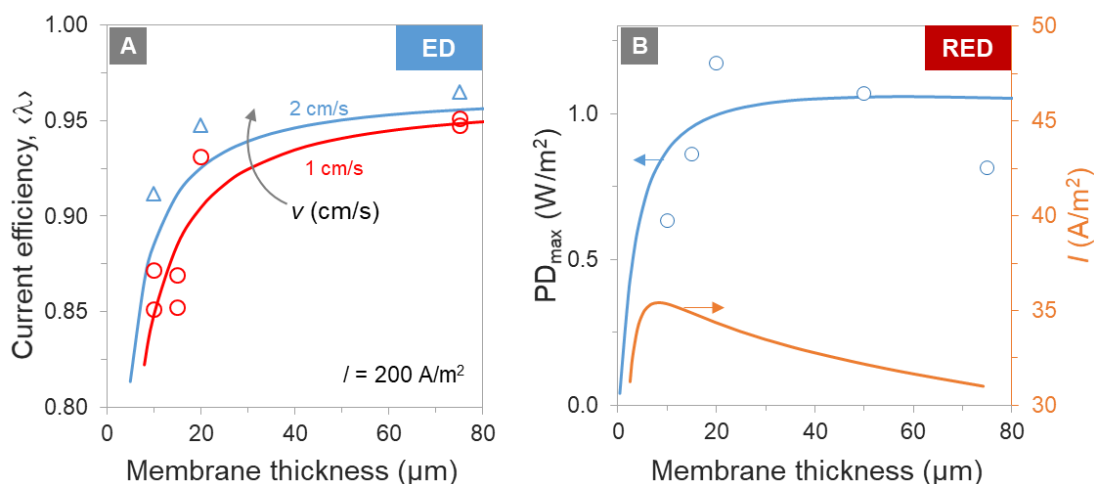


Figure 1. Influence of membrane thickness on A) average current efficiency in ED, and on B) maximum power density and corresponding current density in RED. Comparison between experimental data (symbols) and model predictions (lines). [4]

## CONCLUSIONS

The aim of this work has been to investigate the behavior of ion exchange membranes as function of membrane thickness, focusing on thicknesses below 100  $\mu\text{m}$ . We showed both theoretically and experimentally that reducing the membrane thickness to  $\sim 20 \mu\text{m}$  is beneficial for ED, mainly as a result of the reduced electrical resistance. A further reduction of the thickness leads to a decrease of performance because of higher coion leakage. For RED, as long as the membrane thickness is larger than  $\delta_m = 20 \mu\text{m}$ , the influence of thickness on selectivity and on electrical resistance almost cancel out, resulting in a weak dependence of the maximum power density on thickness.

Thus, our work shows that, in the case of membranes thinner than 100  $\mu\text{m}$ , the effect on process performance of reducing the thickness is not trivial, and a careful analysis is necessary. Ultra-thin membranes, i.e., with thickness  $\delta_m < 20 \mu\text{m}$ , can suffer from high coion leakage under actual process conditions. It is important to note that our calculation results are limited to the case of a 1:1 salt solution, while the presence of other ions in solution also affects process performance. Therefore, future studies should include the effect of ion mixtures on the performance of ED and RED.

## ACKNOWLEDGMENTS

This work was performed in the cooperation framework of *Wetsus, European Centre of Excellence for Sustainable Water Technology* ([www.wetsus.eu](http://www.wetsus.eu)). Wetsus is co-funded by the Dutch Ministry of Economic Affairs and Ministry of Infrastructure and Environment, the Province of Fryslân, and the Northern Netherlands Provinces. The authors would like to thank the participants of the research theme “Blue Energy” for fruitful discussions and financial support.

## References

- [1] A.A. Sonin, R.F. Probstein, A hydrodynamic theory of desalination by electrodialysis, *Desalination*. 5 (1968) 293–329. doi:10.1016/S0011-9164(00)80105-8.
- [2] M. Tedesco, H.V.M.M. Hamelers, P.M. Biesheuvel, Nernst-Planck transport theory for (reverse) electrodialysis: I. Effect of co-ion transport through the membranes, *J. Memb. Sci.* 510 (2016) 370–381. doi:10.1016/j.memsci.2016.03.012.
- [3] M. Tedesco, H.V.M. Hamelers, P.M. Biesheuvel, Nernst-Planck transport theory for (reverse) electrodialysis: II. Effect of water transport through ion-exchange membranes, *J. Memb. Sci.* 531 (2017) 172–182. doi:10.1016/j.memsci.2017.02.031.
- [4] M. Tedesco, H.V.M. Hamelers, P.M. Biesheuvel, Nernst-Planck transport theory for (reverse) electrodialysis: III. Optimal membrane thickness for enhanced process performance, *J. Memb. Sci.* (2018). doi:10.1016/j.memsci.2018.07.090.

## CREEPING FLOW OF VISCOELASTIC FLUID THROUGH A SWARM OF POROUS CYLINDRICAL PARTICLES: BRINKMAN-FORCHHEIMER MODEL

Amit Kumar Saini, Satyendra Singh Chauhan, and Ashish Tiwari\*

*Department of Mathematics, Birla Institute of Technology and Science Pilani, Rajasthan- 333031, India*

**Summary** The present work is a theoretical attempt to investigate the impact of temperature-dependent viscosity on the creeping flow of viscoelastic fluid through membrane consisting the aggregates of the porous cylindrical particles. The flow pattern of the Jeffrey fluid is taken along the axial direction of the cylindrical particles and the cell model approach is utilized to formulate the governing equations driven by a constant pressure gradient. The flow regime is divided into two-layer form, one is inside the porous cylindrical particle enclosing a solid core, which is governed by the Brinkman-Forchheimer equation, and another one is outside of the porous cylindrical particle, which is governed by the Stokes equation. Being a nonlinear equation, an analytical solution of the Brinkman-Forchheimer equation is intractable. To overcome this difficulty, the regular and singular perturbation method are employed to solve the Brinkman-Forchheimer equation for small and large permeability of the porous medium, respectively under the assumption of temperature-dependent viscosity; however, an analytical approach is utilized to solve the Stokes equation. The analytical expressions for velocity in different regions, hydrodynamic permeability of the membrane, and Kozeny constant are derived. The impact of various control parameters such as viscosity parameter, Forchheimer number, permeability of the porous medium, and viscoelastic parameter on the above quantities are discussed and validated with previously published works on the Newtonian fluid in the limiting cases. The present work is in good agreement with the previously published work on Newtonian fluid under constant viscosity assumptions where the porous media flow was governed by the Brinkman equation. The remarkable observation of the present study is that higher viscosity and viscoelastic parameters lead to enhanced velocity profile and hence the hydrodynamical permeability of the membranes. The coating of porous layer can be attributed to adsorption of polymers on the solid particles and further makes the present model to be more relevant in understanding the membrane filtration process.

**Keywords:** Jeffrey fluid; Cell model; Variable viscosity; Perturbation technique; Brinkman-Forchheimer equation.

### INTRODUCTION

The flow of liquids through membranes comprising a swarm of particles has been a topic of immense interest for researchers to get an insight of the flow of fluid through porous media owing to its prominent applications in diverse areas like physical and biological science such as flow through smooth muscle cells, petroleum reservoirs and the sand beds. The mathematical conceptualization of the flow of liquid through membranes modeled as a swarm of porous particles is a complex phenomenon in terms of mathematical formulation for flow visualization as it is difficult to simultaneously observe the flow field past several particles as well as its dependence on particle interactions. To address this issue, the cell model technique or particle-in-cell method was introduced. The cell model technique is employed to analyze the flow of liquid a periodic array of particles by considering a particle confined within a hypothetical cell and the appropriate boundary conditions are imposed on the hypothetical cell to formulate the impact of neighboring particles on the particle concerned. The modeling of filtration process through membranes composed of aggregates of particles can be done by applying the traditional particle-in-cell approach to analyze the flow of fluid through a randomly oriented swarm of particles. The advantage of the cell model technique is to select a single particle inside a fluid envelop among large numbers of cells and analyze the behavior of neighboring particles through imposed boundary conditions on the cell surface.

### PROBLEM FORMULATION AND MODEL DESCRIPTION

The flow is assumed to be along the axis of the solid cylindrical particle with a porous layer confined within a cell of the same geometry as demonstrated in Figure 1 which is an axially symmetric, laminar, incompressible, steady and fully developed flow. The viscoelastic nature of Jeffrey fluid with temperature-dependent viscosity regulates the flow through a swarm of porous cylindrical particles. The flow regime is divided into two regions: Region-I delineates the flow of fluid inside the porous cylindrical particle and Region-II replicates the flow of clear fluid outside the porous cylindrical particle. The Brinkman-Forchheimer equation governs the flow of fluid through porous media inside the porous cylindrical particle; however, the Stokes equation governs the flow of clear fluid outside the porous cylindrical particle.

### BOUNDARY CONDITIONS

The dimensionless boundary conditions are described as (i) No slip condition and zero temperature gradient on the surface of the solid cylinder are considered. (ii) The continuity of velocities at fluid-porous interface is considered. (iii) The discontinuity of shear stresses at the fluid-porous interface is considered. (iv) The conditions on the hypothetical cell surface are defined for velocity and temperature distributions.

---

\*Corresponding author. E-mail: ast79.ashish@gmail.com

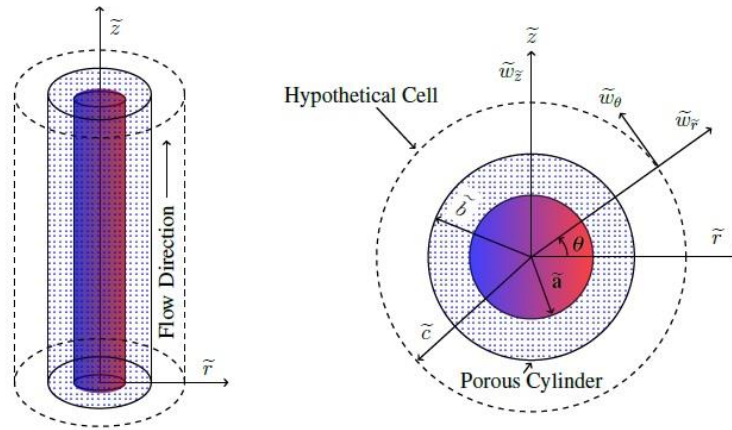


Figure 1. The physical sketch of an identical cylindrical particle coated over a porous layer with solid core

### SOLUTION OF THE PROBLEM

The solutions of the energy and clear fluid region equations solved analytically. Due to presence of nonlinear Forchheimer term in the porous region equation, the analytical solution is intractable. In order to overcome this difficulty, we propose here the perturbation approach in case of small and large permeability of the porous medium. First, we are going to tackle the problem for large permeability and later on for small permeability of the porous medium. The regular perturbation method is utilized to solve the governing equations for large permeability however, singular perturbation with matched asymptotic expansion is utilized to solve the porous medium equation for small permeability.

### RESULTS AND DISCUSSION

A rising particle volume fraction leads to decay in the hydrodynamic permeability of the swarm for both the formulations (small and large permeability of the porous medium) owing to the enhanced resistance which can be accredited to the relatively larger space of porous region in comparison to clear fluid region. That is the envelope occupies lesser region containing clear fluid offering less resistance in comparison to porous region offering more resistance to fluid flow. It is further observed that the decay rate is relatively higher for higher varying viscosity parameters. A novel observation is that a growth in Kozeny constant with porosity parameter is observed for Newtonian ( $\lambda_1 = 0$ ) and Jeffrey ( $\lambda_1 \neq 0$ ) fluids. It is also observed that a rising Jeffrey fluid parameter contributes to decay in growth rate of Kozeny constant with porosity parameter for both the formulations (low as well as high permeability of the porous medium).

### CONCLUSIONS

From the discussion of the aforementioned results, the main findings are concluded as follows: (i) It is observed that a decay in viscosity leads to growth in velocity profile, and hydrodynamic permeability of the membranes, however a decay in Kozeny constant is observed with increasing viscosity parameter. (ii) For porous cylinder in cell and solid cylinder in cell (both are the limiting cases of our present model), the membrane permeability decays with particle volume fraction but grows with viscosity and Jeffrey fluid parameters. (iii) A noteworthy observation is that the rising viscosity parameter and the shear-thinning behavior of the fluid ( $\lambda_1 \neq 0$ ) contribute to decay in growth rate of the Kozeny constant with porosity parameter.

## CURRENT PROBLEMS IN KINETICS OF WETTING AND SPREADING

Anna Trybala\* and Victor Starov

Department of Chemical Engineering, Loughborough University, Loughborough, UK

**Summary** There has been a substantial increase in the number of publications in the field of wetting and spreading since 2010 [1]. This increase in the rate of publications can be attributed to the broader application of wetting phenomena in new areas. Some topics in the field of wetting and spreading are selected to be presented, with the emphasis given to the kinetics of wetting and spreading of non-Newtonian liquid (blood) over porous substrates [2, 3].

These topics are as follows: (i) Contact angle hysteresis on smooth homogeneous solid surfaces via disjoining/conjoining pressure. It is shown that the hysteresis contact angles can be calculated via disjoining/conjoining pressure. The theory indicates that the equilibrium contact angle is closer to a static receding contact angle than to a static advancing contact angle. (ii) The wetting of deformable substrates, which is caused by surface forces action in the vicinity of the apparent three-phase contact line, leading to a deformation on the substrate. (iii) The kinetics of wetting and spreading of non-Newtonian liquid (blood) over porous substrates. We showed that in spite of the enormous complexity of blood, the spreading over porous substrate can be described using a relatively simple model: a power low-shear-thinning non-Newtonian liquid. (iv) The kinetics of spreading of surfactant solutions. In this part, new results related to various surfactant solution mixtures (synergy and crystallization) are discussed, which shows some possible direction for the future revealing of superspreading phenomena. (v) The kinetics of spreading of surfactant solutions over hair. Fundamental problems to be solved are identified.

The wetting and spreading of pure Newtonian liquids over solid surfaces has been well documented in the literature from both theoretical and experimental points of view. However, most commonly found liquids in our everyday life such as blood, shampoos, hair colorants, and paints are colloidal suspensions or polymeric solutions that exhibit non-Newtonian behavior. Frequently, the surfaces where these solutions are applied, such as skin, hair tresses, and textile materials, are porous.

The spreading/imbibition process of a droplet over a porous surface can be subdivided into three subsequent stages in a partial wetting case (Figure 1a): stage (1), fast spreading of the droplet until its base radius expands and the contact angle decreases to the static advancing contact angle; stage (2), constant radius of the contact line (at its maximum value) while the contact angle decreases from the value of a static advancing to static receding contact angle; stage (3), a shrinkage of the droplet base at the fixed static receding contact angle until complete disappearance. The main characteristic of partial wetting is the contact angle hysteresis: this results in the existence of stage 2, when the droplet edge is pinned. However, there is no hysteresis in complete wetting; therefore, stage 2 in partial wetting is absent in complete wetting behavior (Figure 1b), and there are only two stages of spreading.

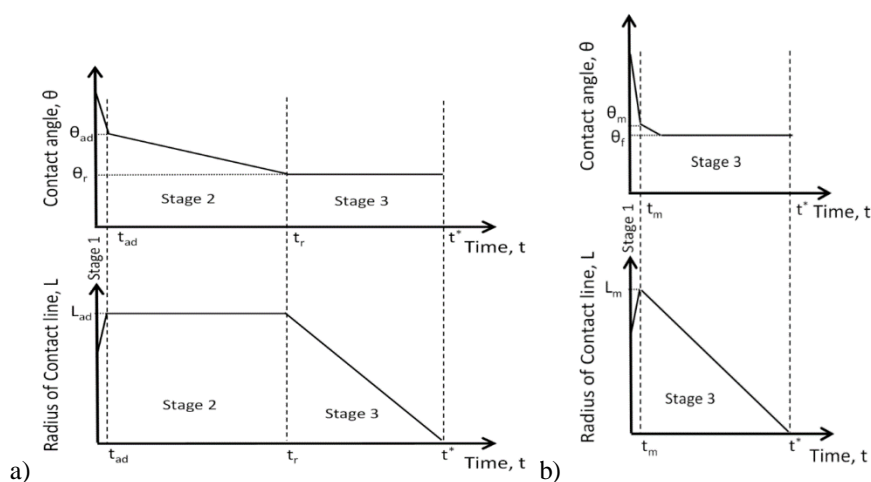


Figure 1. Droplet spreading/imbibition over porous substrate a) partial wetting case: three stages.  $L_{ad}$  is the maximum radius of droplet base,  $\theta_{ad}$  is the advancing contact angle,  $t_{ad}$  is the time when  $\theta_{ad}$  is reached,  $\theta_r$  is the receding contact angle,  $t_r$  is the time when  $\theta_r$  is reached and  $t^*$  is the time when imbibition is finished; b) Complete wetting case: only two stages.  $L_m$  is the maximum radius of droplet base,  $t_m$  is the time when  $L_m$  is reached,  $\theta_m$  is the contact angle at  $t_m$ ,  $t^*$  is the time when complete imbibition is finished and  $\theta_r$  is the final contact angle at  $t^*$ . Note, in the case of complete wetting the stage 2 is absent

\*Corresponding author. E-mail: [A.Trybala@lboro.ac.uk](mailto:A.Trybala@lboro.ac.uk)

The work is supported by European Science Foundation Marie Curie ITN grants MULTIFLOW, CoWet and NanoPaint; the European Space Agency under grants FASES, PASTA, and MAP EVAPORATION.

## References

- [1] O. Arjmandi-Tash, N. M. Kovalchuk, A. Trybala, I. V. Kuchin, V. Starov, *Langmuir*, 2017, 33, 4367–4385.
- [2] Chao, T. C.; Arjmandi-Tash, O.; Das, D. B.; Starov, V. M. Simultaneous Spreading and Imbibition of Blood Droplets over Porous Substrates in the Case of Partial Wetting. *Colloids Surf., A* 2015, 505, 9–17.
- [3] Chao, T. C.; Trybala, A.; Starov, V.; Das, D. B. Influence of Haematocrit Level on the Kinetics of Blood Spreading on Thin Porous Medium during Dried Blood Spot Sampling. *Colloids Surf., A* 2014, 451, 38–47.

## OSCILLATORY MEMBRANE MICROFILTRATION FOR THE SEPARATION OF CRUDE OIL DROPS FROM PRODUCED WATER

Asmat Ullah<sup>\*1</sup>, and Victor Starov<sup>2</sup>

<sup>1</sup>*Department of Chemical Engineering, University of Engineering & Technology Peshawar, Pakistan*

<sup>2</sup>*Department of Chemical Engineering, Loughborough University, UK*

A new method of purification of produced water has been evaluated. Recently membrane oscillation for separating solid particles and liquids drops has attracted researchers globally. Metallic slotted pore membranes were used in the experiments. Membrane oscillation generates a shear rate that drives particles, oil drops away from the membrane surface and, hence, fouling is reduced. It is shown that reduction of the fouling is directly related to the intensity of the membrane oscillation. It is shown that membrane oscillation results in decreasing pore blocking and it was found that pore blocking was also reduced with increase of the membrane oscillation frequency. The latter conclusion was confirmed both experimentally and theoretically. The applied shear rate has a strong influence on the larger particles as compared to the smaller ones and therefore, cut-off of separating particles increases with the membrane oscillation. The method was suggested to predict concentration of particles in the permeate. The experiments reviewed were mainly on separation of drops of both vegetable oil and crude oil from aqueous produced water.

**Keywords:** oil/water separation; membrane oscillation; microfiltration; slotted pore membrane

---

\*Corresponding author. E-mail: [a.ullah@uetpeshawar.edu.pk](mailto:a.ullah@uetpeshawar.edu.pk)

# MATHEMATICAL MODELING OF ELECTROCONVECTION IN FLOW-THROUGH ELECTRODIALYSIS MEMBRANE CELLS: INFLUENCE OF THE INLET BOUNDARY CONDITION FOR THE ION CONCENTRATION

Aminat Uzdenova\*

*Department of Computer Science and Computational Mathematics, Umar Aliev Karachai-Cherkess State University, Karachaevsk, Russia*

**Summary** Flow-through flow membrane systems are widely used. Mathematical modeling of the mass transfer process in membrane systems is performed on the basis of the Navier-Stokes, Nernst-Planck and Poisson equations. In 2D modeling, the forced fluid flow is determined by the boundary conditions at the channel inlet. This article focuses on variations in the determination of the boundary condition for the concentration of ions at the channel inlet.

## INTRODUCTION

The process of mass transfer in electro dialysis (ED) systems, as a rule, is mathematically described by the Navier-Stokes, Nernst-Planck, and Poisson equations, as well as by a system of corresponding boundary conditions. In 2D modeling, the forced fluid flow is determined by the boundary conditions at the channel inlet. A constant uniform distribution of ion concentrations is assumed [1-4], that is, an ideal mixing of the electrolyte solution is prescribed. Nevertheless, it is clear that at overlimiting currents with depletion of the ion concentration in the region near the membrane surface, the concentration at the inlet boundary cannot remain uniform. Consider a variant of the inlet boundary condition, when the ion concentrations are not fixed, but the ion fluxes are given, that is, the Dankwert's condition is determined [5].

## MATHEMATICAL MODEL

The system under consideration is a binary electrolyte in half of a flow-through ED desalination channel at the cation-exchange membrane (CEM). Let  $x$  and  $y$  be the transverse and longitudinal coordinates, respectively;  $x = 0$  relates to the middle of the ED channel,  $x = h$  is the electrolyte solution/CEM interface;  $y = 0$  corresponds to the inlet and  $y = l$  to the outlet of the channel.

The Navier-Stokes equations, Eqs. (1), describe the velocity field under the action of the forced flow and the electric body force. The equations of Nernst-Planck, Eqs. (2), and Poisson, Eq. (3), describe the ion concentrations and potential fields.

$$\frac{\partial \vec{V}}{\partial t} + (\vec{V}\nabla)\vec{V} = -\frac{1}{\rho_0} \nabla P + \nu \Delta \vec{V} - \frac{1}{\rho_0} F(z_1 c_1 + z_2 c_2) \nabla \varphi, \quad \text{div} \vec{V} = 0, \quad (1)$$

$$\frac{\partial c_i}{\partial t} = -\text{div} \left( -\frac{F}{RT} z_i D_i c_i \nabla \varphi - D_i \nabla c_i + c_i \vec{V} \right), \quad i = 1, 2, \quad (2)$$

$$\Delta \varphi = -\frac{F}{\varepsilon} (z_1 c_1 + z_2 c_2), \quad (3)$$

Here  $\vec{V}$  is the velocity;  $D_i$ ,  $z_i$  and  $c_i$  are individual ion diffusion coefficients, charge number and concentration of the  $i$ -th ion;  $P$  is pressure;  $t$  is time;  $F$  is the Faraday constant;  $R$  is the gas constant;  $T$  is the absolute temperature;  $\varphi$  is electric potential;  $\varepsilon_0$  is the dielectric constant;  $\varepsilon_r$  is the solution relative permittivity;  $\rho_0$  is the solution density,  $\nu$  is the kinematic viscosity.  $\vec{V}$ ,  $p$ ,  $c_1$ ,  $c_2$ ,  $\varphi$  are unknown functions of  $x$ ,  $y$  and  $t$ .

At the channel inlet, a parabolic Poiseuille flow is accepted for the velocity:

$$V_x(x, 0, t) = 0, \quad V_y(x, 0, t) = 1.5V_0(1 - (x/h)^2) \quad (4)$$

for the potential of the electric field, the condition is specifying zero tangential current density:

$$\frac{\partial \varphi}{\partial y}(x, 0, t) = -\frac{RT}{F(z_1^2 D_1 + z_2^2 D_2)c_0} \left( z_1 D_1 \frac{\partial c_1}{\partial y} + z_2 D_2 \frac{\partial c_2}{\partial y} \right) \quad (5)$$

For the ion concentration, a uniform distribution, Eqs. (6), or conditions for ion fluxes, Eqs. (7), are taken:

$$c_i(x, 0, t) = c_0 \quad (6)$$

$$\left( -\frac{F}{RT} z_i D_i c_i \frac{\partial \varphi}{\partial y} - D_i \frac{\partial c_i}{\partial y} + c_i V_y \right)(x, 0, t) = c' V_y, \quad i = 1, 2, \quad (7)$$

where  $c' = c_0$  is the input electrolyte concentration. Conditions (7), by analogy with the Dankwert's condition [5], describe the fact that arrival rate of ions into the channel is equal to the rate with which they cross the plane  $y = 0$  by the combination of flow, electromigration, and diffusion. Boundary conditions at other boundaries are described in [1].

---

\*Corresponding author. E-mail uzd\_am@mail.ru.

## RESULTS AND DISCUSSION

Figure 1 shows the concentration profiles in the longitudinal ( $x/h = 0.994$ ) and transverse ( $y = 0$ ) sections of the channel in the region near the membrane surface at the channel inlet. The results of calculations with the condition of uniform distribution of the ion concentrations, Eqs. (6), and with the Dankwert's condition, Eqs. (7), at the potential drop  $\Delta\phi = 0.5$  V are presented. Comparison of the graphs shows a significantly greater longitudinal gradient in the case of conditions (6) than for conditions (7). As a result, in the calculation with conditions (6), a stationary vortex is formed at the channel inlet when the potential drop below the threshold value of the electroconvection development in the rest of the channel. In the calculation with conditions (7), the first vortices appear at a larger value of the potential drop ( $\Delta\phi \approx 0.6$  V) at the outlet of the channel.

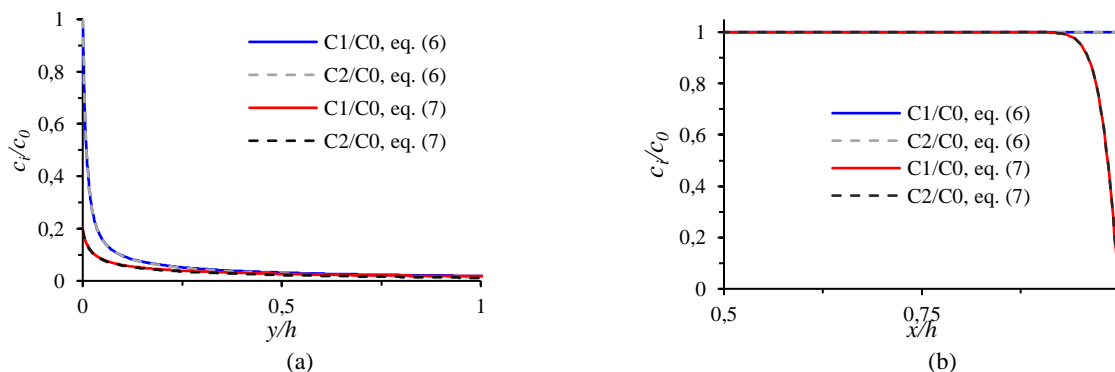


Figure 1. Concentration profiles of cations ( $c_1$ , solid lines) and anions ( $c_2$ , dashed lines) in sections  $x/h = 0.994$  (a) and  $y = 0$  (b). Calculation at  $\Delta\phi = 0.5$  V with conditions (6) (blue and gray lines) and with Danckwerts' conditions (7) (red and black lines).

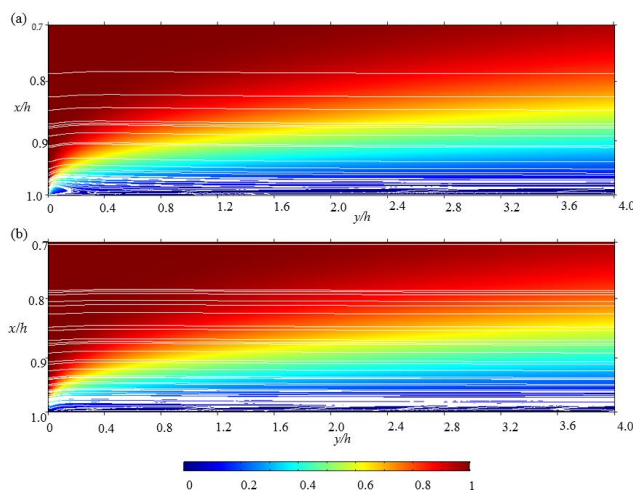


Figure 2. Distribution of cation concentration (the magnitude is shown by different colors), solution streamlines (white lines) in the area at the membrane surface. Calculation for  $\Delta\phi = 0.5$  V with conditions (6) (a) and with Danckwerts' conditions (7) (b).

## CONCLUSIONS

Thus, the method for setting the ion concentration at the inlet boundary affects the structure of the electroconvective flow.

The work is supported by RFBR according to the research project №18-38-00572.

## References

- [1] Urtenov M.K., Uzdenova A.M., Kovalenko A.V., Nikonenko V.V., Pismenskaya N.D., Vasil'eva V.I., Sizat P., Pourcelly G. Basic mathematical model of overlimiting transfer enhanced by electroconvection in flow-through electro dialysis membrane cells. *J. Membr. Sci.* 447, 190-202, 2013.
- [2] Pham S.V.; Kwon H.; Kim B.; White J.K.; Lim G.; Han J. Helical vortex formation in three-dimensional electrochemical systems with ion-selective membranes. *Phys. Rev. E* 93, 033114, 2016.
- [3] Magnico P. Electro-Kinetic Instability in a Laminar Boundary Layer Next to an Ion Exchange Membrane. *Int. J. Mol. Sci.* 20, 2393, 2019.
- [4] Liu W., Zhou Y., Shi P. Shear electroconvective instability in electro dialysis channel under extreme depletion and its scaling laws. *Phys. Rev. E* 101, 043105, 2020.
- [5] Danckwerts P.V. Continuous flow systems. Distribution of residence times. *Chem. Eng. Sci.* 2, 1-13, 1953.

## NUMERICAL STUDY OF STOKES-BRINKMAN SYSTEMS WITH VARYING LIQUID VISCOSITY

Anatoly Filippov<sup>1</sup>, Yulia Koroleva<sup>1</sup>, Amit Verma<sup>2</sup>

<sup>1</sup>Department of Higher Mathematics, Gubkin Russian State University of Oil and Gas, Moscow, Russia

<sup>2</sup>Department of Mathematics, Indian Institute of Technology Patna, Bihta, Patna-801103, India.

**Summary** In this work we study Stokes-Brinkman system with varying liquid viscosity which demonstrates the fluid flow along an ensemble of partially porous cylindrical particles using the cell modeling [1]. Figure given below gives schematic representation of a viscous flow through and around partly porous fiber.

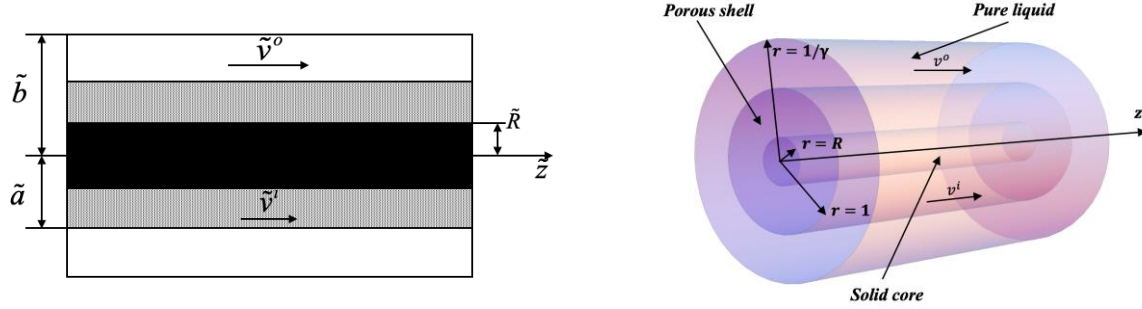


Figure 1. Schematic representation of a viscous flow through and around partly porous fiber: (left) – in dimensional coordinates, (right) – in dimensionless coordinates.

We consider the steady, incompressible viscous fluid flowing with uniform velocity  $\tilde{U}$  through an assemblage of composite cylindrical particles of radius  $\tilde{a}$ , along their parallel axes ( $z$ -axis). This assemblage of partly porous cylindrical particles having impermeable cores and radially varying viscosity  $\tilde{\mu}^i(\tilde{r})$  in porous shells is hydrodynamically equivalent to a fibrous membrane. We assume that each non-homogeneous porous cylindrical particle is enveloped by a hypothetical liquid concentric cell of radius  $\tilde{b}$ . The radius of the hypothetical cell  $\tilde{b}$  is such that the particle volume fraction  $\gamma^2$  of the swarm is equal to the particle volume fraction of the cell, i.e.,  $\gamma^2 = \frac{\pi \tilde{a}^2}{\pi \tilde{b}^2}$ .

Due to axisymmetric pattern of the flow, let  $\tilde{v}^{(k)} = (0, 0, \tilde{v}^{(k)}(\tilde{r}))$ , ( $k = i, o$ ) be the fluid axial velocities and

$$\frac{d\tilde{p}^{(i)}}{d\tilde{z}} = \frac{d\tilde{p}^{(o)}}{d\tilde{z}} \equiv \tilde{\omega} = \text{const} < 0$$

be the constant pressure gradients inside the non-homogeneous porous and outside regions, respectively. The flow inside the non-homogenous porous region ( $\tilde{R} \leq \tilde{r} \leq \tilde{a}$ ) in the cylindrical polar coordinates is governed by the Brinkman's equation:

$$\frac{1}{\tilde{r}} \frac{d}{d\tilde{r}} \left( \tilde{\mu}^i(\tilde{r}) \left( \tilde{r} \frac{d\tilde{v}^{(i)}}{d\tilde{r}} \right) \right) - \frac{\tilde{\mu}^o}{\tilde{k}} \tilde{v}^{(i)} = \tilde{\omega},$$

where,  $\tilde{k} = \text{const}$  is the specific permeability coefficient of non-homogenous porous region. Effective viscosity  $\tilde{\mu}^i(\tilde{r})$  of the Brinkman fluid is taken to be varying radially and depends on the nature of porous media,  $\tilde{\mu}^o = \text{const}$  is the value of the pure liquid viscosity.

The flow outside the non-homogeneous porous region ( $\tilde{a} \leq \tilde{r} \leq \tilde{b}$ ) is governed by the Stokes equation given as follows:

$$\tilde{\mu}^o \frac{1}{\tilde{r}} \frac{d}{d\tilde{r}} \left( \tilde{r} \frac{d\tilde{v}^{(o)}}{d\tilde{r}} \right) = \tilde{\omega}.$$

Let us introduce the following dimensionless variables and parameters:

$$v^{(k)} = \frac{\tilde{v}^{(k)}}{\tilde{U}}, (k = i, o), p = \frac{\tilde{p} \tilde{a}}{\tilde{\mu}^o \tilde{U}}, r = \frac{\tilde{r}}{\tilde{a}}, z = \frac{\tilde{z}}{\tilde{a}}, k = \frac{\tilde{k}}{\tilde{a}^2}, \gamma = \frac{\tilde{a}}{\tilde{b}}, \mu^i = \frac{\tilde{\mu}^i}{\tilde{\mu}^o}, \omega = \frac{\tilde{\omega} \tilde{a}^2}{\tilde{\mu}^o \tilde{U}}$$

where  $\tilde{U}$  is the characteristic velocity. The linear filtration velocity  $\tilde{v}_f$  is connected to transmembrane pressure gradient  $\tilde{\omega}$  as:

$$\tilde{V}_f \equiv \frac{\tilde{Q}}{\pi \tilde{b}} = -\tilde{L}_{11} \tilde{\omega},$$

where  $\tilde{L}_{11}$  is hydrodynamic permeability of the membrane and its dimensionless value can be found by integrating velocity profiles using the following expressions:  $\tilde{L}_{11} = -\frac{\gamma^2}{\pi\omega} Q$ ,

$$Q = 2\pi \left( \int_R^1 v^i(r)r dr + \int_1^{1/\gamma} v^o(r)r dr \right)$$

where  $Q \equiv \frac{\tilde{Q}}{\theta a^2}$  is dimensionless liquid flow rate through the membrane.

Finally, for porous medium region ( $R \leq r \leq 1$ ), we get

$$\mu^i(r) \frac{d^2 v^{(i)}}{dr^2} + \frac{dv^{(i)}}{dr} \left( \frac{d\mu^{(i)}(r)}{dr} + \frac{\mu^{(i)}(r)}{r} \right) - \frac{v^{(i)}}{r} = \omega.$$

Assume that the dimensionless viscosity of the non-homogeneous porous medium varies radially as

- (i) Model 1: Exponential law,  $\mu^i(r) = \exp(\alpha(1-r))$ ,  $\alpha > 0$
- (ii) Model 2: Power law,  $\mu^i(r) = r^{-\alpha}$ .

For outside of porous region ( $1 \leq r \leq \frac{1}{\gamma}$ ), we get:

$$\frac{d^2 v^{(o)}}{dr^2} + \frac{1}{r} \frac{dv^{(o)}}{dr} = \omega.$$

*Boundary conditions (in dimensionless form)*

At the boundary between the solid cylinder and its porous shell, the condition of non-slip is set:

$$v^i = 0, \quad r = R.$$

At the liquid-porous interface we will use Ochoa-Tapia conditions [3, 4] – continuity of velocity and jump of shear stresses:  $v^o = v^i$ ,  $\frac{dv^i}{dr} - \frac{dv^o}{dr} = \frac{\beta}{\sqrt{k}} v^o$ ,  $r = 1$ , where  $\beta$  is dimensionless coefficient, which is responsible for the momentum transfer from porous medium to pure liquid ( $\beta > 0$ ) and contra versa ( $\beta < 0$ ). If  $\beta = 0$  we have usual conditions of the flow continuity. For the flow along the cylinders, all four cell conditions (Happel, Kuwabara, Kvashnin and Mehta-Morse/Cunningham) have a simple form:  $\frac{dv^o}{dr} = 0$ ,  $r = \frac{1}{\gamma}$ .

We propose two numerical methods based on variation iteration method [2] and solve the BVPs defined above and compare results for velocity profiles and hydrodynamic permeability of a membrane, regarded as a swarm of partly porous cylindrical particles placed into liquid shells, for two cell models. Convergence of both the methods are also proved in this work.

We conclude that it is possible to regulate the hydrodynamic permeability of a membrane by forming special thin layers on a porous surface of its constituent fibers due to chemical or physical modification that can change the boundary conditions from sticking through partial slippage to superhydrophobic slippage.

## References:

- [1] Filippov, A.N., Koroleva, Y.O. & Verma, A.K. Cell Model of a Fibrous Medium (Membrane). Comparison between Two Different Approaches to Varying Liquid Viscosity. *Membr. Membr. Technol.* 2, 230–243 (2020). <https://doi.org/10.1134/S2517751620040058>
- [2] Singh, Mandeep, Amit Kumar Verma, and Ravi P. Agarwal. On an iterative method for a class of 2 point & 3 point nonlinear sbvps. *Journal of Applied Analysis and Computation* 9, (2019): 1242-1260.
- [3] J. A. Ochoa-Tapia, and S. Whitaker, Momentum transfer at the boundary between a porous medium and a homogeneous fluid—I. Theoretical development, *Int. J. Heat Mass Transf.* 38, 2635 (1995).
- [4] J. A. Ochoa-Tapia, and S. Whitaker, Heat transfer at the boundary between a porous medium and a homogeneous fluid, *Int. J. Heat Mass Transf.* 38, 2647 (1995).

# POSTER SECTION

## PHYSICAL AGING OF PTMSP-BASED THIN-FILM COMPOSITION MEMBRANES LOADED WITH ORGANIC POROUS FILLERS VIA GAS PERMEABILITY TRACKING

Danila Bakhtin\*, Alexander Malakhov, and Alexey Volkov  
*A.V.Topchiev Institute of Petrochemical Synthesis, RAS (TIPS RAS), Moscow, Russia*

**Summary** Long-term (15 months) experimental and model studies of physical aging of thin film composite membranes based on poly(trimethylsilylpropyne) with organic fillers (porous aromatic frameworks) have been carried out. It has been shown that with organic fillers content increase, physical aging slows down. At the same time, CO<sub>2</sub> permeance remains high (> 17000 GPU) and exceeds the literature values reported for thin film composite membranes.

### INTRODUCTION

High free volume glassy polymers, e.g. disubstituted polyacetylenes, polymers with intrinsic microporosity and polynorbornenes are considered as promising materials for gas and liquid membrane separation applications. However, these polymers suffer a problem of accelerated physical aging [1], during which their properties change, namely, the permeability decreases over time, while the selectivity, on the contrary, increases. One of the ways to overcome physical aging involves the use of porous aromatic frameworks (PAFs) [2]. In this work, PAFs and crosslinked elastomer polyethylenimine (PEI) were used to inhibit physical aging of high free volume glassy polymer poly(trimethylsilylpropyne) (PTMSP). The effectiveness of the new approach was demonstrated by 15 month long gas permeance (N<sub>2</sub>, O<sub>2</sub>, CO<sub>2</sub>) monitoring.

### EXPERIMENTAL

A series of composite membranes based on PTMSP as selective layer (0.9 ± 0.1 mμ) and microfiltration membrane MFFK-1 (Vladipor, Russia) as support was obtained by kiss-coating technique. PEI was added in casting solution in concentration of 4 wt.% relative to PTMSP and cross-linked by using poly(ethylene glycol) diglycidyl ether [3]. Lab-made aromatic frameworks PAF-11 (the surface area S<sub>BET</sub> = 514 m<sup>2</sup>/g, average the pore size 4.5 nm) were used as organic porous fillers. Gas permeability monitoring data presented in Table 1

Table 1. Residual fraction of the gas permeance (%) after 15 months

Filler	N <sub>2</sub>	O <sub>2</sub>	CO <sub>2</sub>
-	6.0	8.3	10.6
PEI	16.3	19.8	32.9
PEI + 10% PAF	8.7	11.6	18.4
PEI + 20% PAF	26.5	33.0	42.2
PEI + 30% PAF	26.2	31.9	43.1

### RESULTS

The experimental time-dependent gas permeance through the composite membranes (Figure 1) was approximated using the modified relaxation function. The common relaxation function  $f(t)$  is given by

$$Q(t) = Q_{eq} + [Q(0) - Q_{eq}]f(t) \quad (1)$$

where  $Q(t)$  is the permeance at the time  $t$ ,  $Q(0)$  is the initial permeance and  $Q_{eq}$  is the limited value of  $Q$  at the  $t \rightarrow \infty$ , i.e. it is the metastable equilibrium permeance. The relaxation function changes from 1 at start time to 0 when equilibrium is reached. The value of  $Q_{eq}$  is practically inaccessible (the time of complete relaxation of glasses can take months and years). To solve this problem, the expression (1) can be represented differently by replacing the equilibrium value of  $Q_{eq}$  with the permeance value at a certain (sufficiently long) aging time  $t^*$ :

$$Q(t) = Q(t^*) + [Q(0) - Q(t^*)]F(t, t^*) \quad (2)$$

Here  $F(t, t^*)$  is the new (modified) relaxation function, depending not only on the current time, but also on the given value of  $t^*$ :

\*Corresponding author. E-mail: db2@ips.ac.ru.

$$F(t, t^*) = \frac{f(t) - f(t^*)}{1 - f(t^*)} \quad (3)$$

As  $t^* \rightarrow \infty$  the function  $F(t, t^*)$  is reduced to the  $f(t)$ . The experimental value of the permeance corresponding to the maximum aging time (15 months) was chosen as the  $Q(t^*)$  value. The stretched exponential function, commonly known as the Kohlrausch–Williams–Watts (KWW) function, was used for the relaxation function:

$$f(t) = \exp\left[-(t/\tau)^\beta\right] \quad (4)$$

with the parameters  $\tau$  (the relaxation time) and  $\beta$  ( $0 < \beta \leq 1$ ). By means of this function the modified relaxation function (Eq. (3)) becomes explicit and the raw permeance data  $Q(t)$  can be approximated with Eq. (2). The obtained parameters of the relaxation function are given in the Table 2. The exponent  $\beta$  varies slightly from sample to sample and is in the range 0.51-0.55. The relaxation time increases with the content of organic fillers in the polymer matrix. The residual fraction of the gas permeance increases in the same order (Table 1). This behavior is probably associated with a decrease in the polymer chains mobility, which leads to a slowdown in its physical aging. Note that the presented model approach also allows assessing the "equilibrium" permeability and the time required to achieve it.

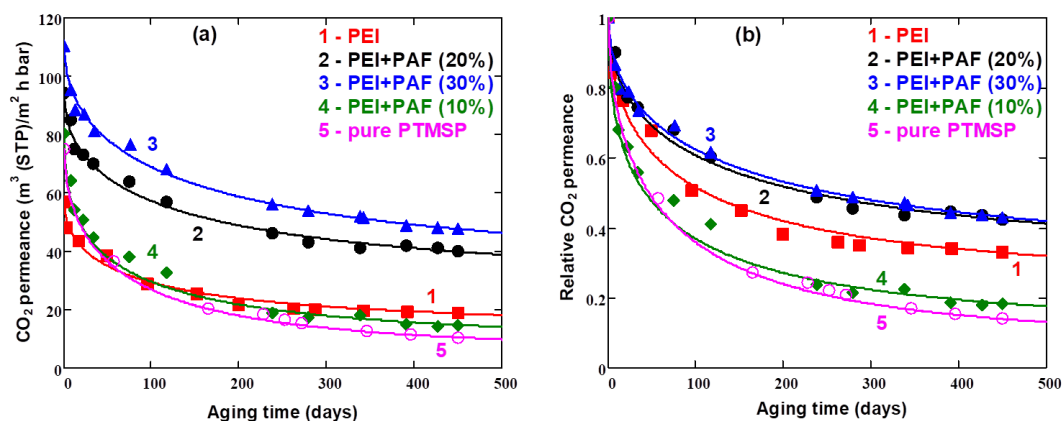


Figure 1. Absolute (a) and relative (b) CO<sub>2</sub> permeability of composite membranes versus time

Table 2. The parameters of the relaxation function for CO<sub>2</sub> permeance (Eq. (1))

Filler	Fitting parameters	
	$\tau$ , days	$\beta$
–	71.6	0.55
PEI	91.0	0.52
PEI+10% PAF	108.0	0.52
PEI+20% PAF	140.7	0.51
PEI+30% PAF	160.0	0.52

## CONCLUSIONS

Via 15 months gas permeance tracking physical aging of membranes based on PTMSP filled with porous aromatic frameworks PAF-11 (up to 30 wt%) and cross-linked PEI (4 wt%) was studied. We obtained that (1), the most permeable membrane, containing cross-linked PEI and 30 wt% of PAF-11, has retained 47.6 m<sup>3</sup>/m<sup>2</sup>·h·bar (~17000 GPU) CO<sub>2</sub> permeance and CO<sub>2</sub>/N<sub>2</sub> selectivity~ 5 by the end of 15 month monitoring; (2) Experimental data of time-dependent permeance was approximated using the stretched exponential function. Evaluated relaxation time reflects polymer chains mobility changes. Thus thin film composite membranes with porous organic fillers investigated are of a great interest as themselves and as fast supports for further selective layer coating.

The work is supported by the Russian Science Foundation (project No. 18-19-00738)

## References

- [1] Low Z.X., Budd P.M., McKeown N.B., Patterson D.A. Gas permeation properties, physical aging, and its mitigation in high free volume glassy polymers. *Chem. Rev.*, 118, 5871-5911, 2018.
- [2] Smith S.J., Hou R., Konstas K., Akram A., Lau C.H., Hill M.R. Control of physical aging in super-glassy polymer mixed matrix membranes. *Acc. Chem. Res.*, 53, 1381-1388, 2020.
- [3] Bazhenov S. D., Borisov I. L., Bakhtin D. S., Rybakova A. N., Khotimskiy V. S., Molchanov S. P., Volkov, V. V. High-permeance crosslinked PTMSP thin-film composite membranes as supports for CO<sub>2</sub> selective layer formation. *Green Ener. Env.*, 1, 235-245, 2016.

## MHD EFFECTS ON MICROPOLAR-NEWTONIAN FLUID FLOW THROUGH A COMPOSITE POROUS CHANNEL

Satya Deo<sup>1</sup> and Deepak Kumar Maurya<sup>\*1,2</sup>

<sup>1</sup>*Department of Mathematics, University of Allahabad, Prayagraj, India*

<sup>2</sup>*Department of Mathematics, Prof. Rajendra Singh (Rajju Bhaiya) Institute of Physical Sciences for Study and Research, V. B. S. Purvanchal University, Jaunpur, India*

**Summary** The present study investigates the flow of a Newtonian fluid, sandwiched between two rectangular porous channels which are filled with micropolar fluid in the presence of uniform magnetic field applied in a direction perpendicular to that of the fluid motion. The governing equations of micropolar fluid are modified by Nowacki's approach. For respective porous channels, expressions for velocity vectors, microrotations, stresses (shear and couple) are obtained analytically. Continuity of velocities, continuities of microrotations and continuity of stresses are used at the porous interfaces; conditions of no slip and no spin are applied at the impervious boundaries of the composite channel. Numerical values of flow rate, wall shear stresses and couple stresses at the porous interfaces are listed in tables for different values of various parameters. Graphs of the flow rate, fluid velocity and Newtonian fluid velocity are plotted and their behaviors are discussed with various values of parameters: micropolar parameter, couple stress parameter, viscosity ratio parameter, Hartmann number, conductivity ratio parameters and permeability parameters.

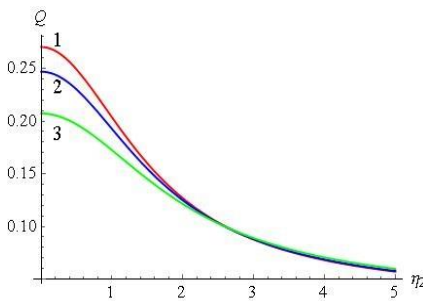


Figure 1. Variation of the flow rate:  
(1)  $H = 0.01$ ; (2)  $H = 0.5$ ; (3)  $H = 1$ .

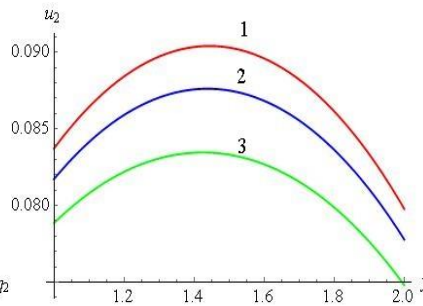


Figure 2. Variation of the fluid velocity:  
(1)  $H = 0.75$ ; (2)  $H = 1$ ; (3)  $H = 1.25$ .

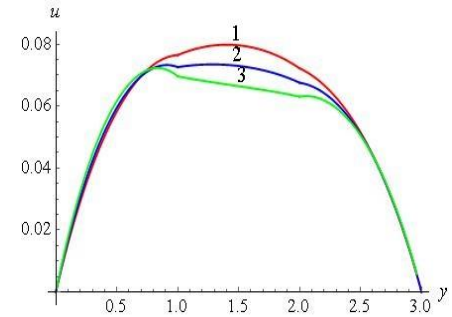


Figure 3. Variation of Newtonian fluid velocity:  
(1)  $H = 0.2$ ; (2)  $H = 0.4$ ; (3)  $H = 0.6$ .

### HIGHLIGHTS

- Effect of magnetic field on the Newtonian fluid flow porous channel, sandwiched between two rectangular porous channels filled with micropolar fluid is investigated.
- The direction of fluid flow is taken along  $x$ -axis and the uniform magnetic field is applied in the direction perpendicular to the direction of the fluid motion. For the corresponding fluid flow regions,
- Analytic expressions of fluid velocities (micropolar and Newtonian), stresses (shear and couple) and flow rate are obtained by applying suitable boundary conditions. Numerical values of the shear wall stresses and couple wall stresses at the porous interfaces are also tabulated.
- The volumetric flow rate, fluid velocity and Newtonian fluid velocity are plotted and discussed for different values of micropolar parameter ( $M$ ), couple stress parameter ( $L$ ), viscosity ratio parameter ( $\phi$ ), Hartmann number ( $H$ ), conductivity ratio parameters ( $\Lambda_1, \Lambda_3$ ), permeability parameters ( $\eta_1, \eta_2, \eta_3$ ).

\*Corresponding author. E-mail: deepak893395@gmail.com.

## CONCLUSIONS

This research work is useful in the filtration of groundwater (contaminated), oil recovery process through reservoir, circulation of blood flow through veins of human body, etc. Investigating the effect of these parameters, following conclusions are made:

- The fluid flow rate through the cross-section of channels, decreases in each cases either  $M$  increases or  $L$  increases or  $\phi$  increases or  $H$  increases or  $\Lambda_1$  increases or  $\Lambda_3$  increases or  $\eta_1$  increases or  $\eta_2$  increases or  $\eta_3$  increases.
- The fluid velocity passing through respective porous channels, decreases in each cases either  $M$  increases or  $L$  increases or  $\phi$  increases or  $H$  increases or  $\Lambda_1$  increases or  $\Lambda_3$  increases or  $\eta_1$  increases or  $\eta_2$  increases or  $\eta_3$  increases. The velocity profile is parabolic in each case.
- The velocity of Newtonian fluid decreases in each cases either  $M$  increases or  $L$  increases or  $\phi$  increases or  $H$  increases or  $\Lambda_1$  increases or  $\Lambda_3$  increases or  $\eta_1$  increases or  $\eta_2$  increases or  $\eta_3$  increases. The profile of Newtonian fluid velocity is parabolic for parameters  $M, L, \phi, H, \Lambda_3, \eta_2$ .

## References

- [1] Lukaszewicz, G. *Micropolar Fluids: Theory and Applications*. Springer, New York 1999.
- [2] Eringen, A.C. Theory of micropolar fluids. *J. Math. Mech.* 16, 1-18, 1966.
- [3] Stokes, V.K. *Theories of fluids with microstructure*. Springer, New York 1984.
- [4] Khanukaeva D.Yu., Filippov, A.N. Isothermal Flows of micropolar liquids: formulation of problems and analytical solutions. *Colloid J.* 80, 14-36, 2018.
- [5] Nowacki, W. *Theory of micropolar elasticity*. Springer, New York 1970.
- [6] Khanukaeva, D.Yu., Filippov, A.N., Yadav, P.K., Tiwari, A. Creeping flow of micropolar fluid parallel to the axis of cylindrical cells with porous layer. *Eur. J. Mech. B Fluids* 76, 73-80, 2019.
- [7] Chandris, M., Jamet, D. Boundary conditions at a planar fluid-porous interface for a Poiseuille flow. *Int. J. Heat Mass Transfer* 49, 2137-2150, 2006.
- [8] Deo, S, Maurya, D.K. Generalized stream function solution of the Brinkman equation in the cylindrical polar coordinates. *Spec. Top. Rev. Porous Med.* 10, 421-428, 2019.
- [9] Deo S, Maurya, D.K., Filippov, A.N. Influence of magnetic field on micropolar fluid flow in a cylindrical tube enclosing an impermeable core coated with porous layer. *Colloid J.* (Accepted).
- [10] Jaiswal, S, Yadav, P.K. Flow of micropolar-Newtonian fluids through the composite porous layered channel with movable interfaces. *Arab. J. Sci. Engg.* 45, 921-934, 2020.
- [11] Nield, D.A., Bejan, A. *Convection in porous media*. Springer, New York 2006.
- [12] Srinivasacharya, D., Murthy, J.V.R., Venugopal, D. Unsteady Stokes flow of micropolar fluid between two parallel porous plates. *Int. J. Engg. Sci.* 39, 1557-1563, 2001.
- [13] Yadav, P.K., Jaiswal, S, Sharma, B.D. Mathematical model of micropolar fluid in two-phase immiscible fluid flow through porous channel. *Appl. Math. Mech.* 39, 993-1006, 2018.
- [14] Yadav, P.K., Jaiswal, S., Asim, T., Mishra, R. Influence of a magnetic field on the flow of a micropolar fluid sandwiched between two Newtonian fluid layers through a porous medium. *Eur. Phys. J. Plus* 133, 2018, DOI 10.1140/epjp/i2018-12071-5.
- [15] Yadav, P.K., Tiwari, A., Deo, S., Yadav, M.K., Filippov, A., Vasin, S., Sherysheva, E. Hydrodynamic permeability of biporous membrane. *Colloid J.* 75, 473-482, 2013.
- [16] Yadav, P.K., Jaiswal, S. Influence of an inclined magnetic field on the Poiseuille flow of immiscible micropolar-Newtonian fluids in the porous medium. *Can. J. Phy.* 96, 1016-1028, 2018.
- [17] Umavathi, J.C., Chamkha, A.J., Sridhar, K.S.R. Generalized plain Couette flow and heat transfer in a composite channel. *Trans. Porous Med.* 85, 157-169, 2010.
- [18] Srinivasacharya, D., Shiferaw, M. Hydromagnetic effects on the flow of a micropolar fluid in a diverging channel. *Z. Angew. Math. Mech.* 89, 123-131, 2009.

## MATHEMATICAL MODELLING OF THE EFFECT OF PULSED ELECTRIC FIELD ON THE SPECIFIC PERMSELECTIVITY

Andrey Gorobchenko, Semyon Mareev, and Victor Nikonenko\*  
Membrane Institute, Kuban State University, Krasnodar, Russia

**Summary** The enhancement of membrane permselectivity for specific ions by the application of pulsed electric fields (PEF) is modelled using the Nernst-Planck-Poisson equations. The application of PEF allows an increase in the transport number of the preferably transported ion at a given current density. It is shown that this effect is due to mitigation of the concentration polarization.

### INTRODUCTION

One of the problems accounted in separation/removal of certain kind of ions using electro dialysis (ED) is that the membrane permselectivity for specific ions decreases with increasing current density [1, 2]. The reason is that under an applied electric current, the concentration of the preferably transferred counterion (1) decreases at the membrane surface, while the concentration of the retained counterion (2) increases (or decreases to a lesser extent). The resulting concentration gradients provide the diffusion, which tend to decrease the flux of counterion 1 and increase the flux of counterion 2. When the current density reaches its limiting value,  $i_{lim}$ , the partial current densities of a competing ion,  $i_{k\ lim}$ , do not depend on the membrane properties [1]:

$$i_{k\ lim} = \frac{F}{\delta} D_k z_k c_k^0 \left( 1 + \left| \frac{z_k}{z_3} \right| \right), \quad k=1, 2 \quad (1)$$

where  $F$  is the Faraday constant;  $\delta$  is the diffusion layer thickness;  $D_k$ ,  $c_k$  and  $z_k$  are the diffusion coefficient, concentration, and charge number of ion  $k$ , respectively; subscript 3 refers to the coion, which is common for both counterions.

However, experiment shows that the use of PEF mode in electro dialysis allows essentially improve the performance of the process. Namely, during the electro dialysis of the milk whey in PEF mode, the following effects were reported [3]: the reduction of the water splitting, the increase in mass transfer rate and current efficiency, the enhancement of specific permselectivity towards the bivalent cations ( $Ca^{2+}$  and  $Mg^{2+}$ ) and the mitigation of fouling. In this paper, we propose a mathematical model, which describes the effect of the PEF on the specific permselectivity.

### FORMULATION OF THE MODEL

The model is based on the non-stationary 1D Nernst-Planck and Poisson equations written for three different ions (two counterions and one co-ion) in the membrane and two diffusion layers; the material balance equation is also applied:

$$J_k = -D_k \left( \left( 1 + \frac{\gamma_k}{c_k} \frac{\partial \gamma_k}{\partial c_k} \right) \frac{\partial c_k}{\partial x} + z_k c_k \frac{\partial \varphi}{\partial x} \right), \quad (2)$$

$$\varepsilon \varepsilon_0 \frac{\partial E}{\partial x} = F \left( \sum_{k=1}^3 z_k J_k + z_m \bar{Q} \right), \quad (3)$$

$$\frac{\partial c_k}{\partial t} = -\text{div} J_k, \quad (4)$$

where  $J_k$ , and  $\gamma_k$  are the flux density and activity coefficient of ion  $k$  ( $k=1, 2, 3$ ), parameters  $D_k$  and  $\gamma_k$  take different values in the solution and membrane;  $\bar{Q}$  is the exchange capacity of the membrane ( $\bar{Q}$  is zero in solution).

Electrical current density in the system is described by Eq. (5):

$$i = F \sum_k z_k J_k. \quad (5)$$

At the membrane solution interfaces, the continuity of concentrations and electric potential are assumed. An electric current density,  $i$ , is set as a known function of time;  $i$  is a constant in the usual continuous current mode; in the PEF mode, it takes a given value during a pulse lapse and is zero during a pause lapse (Figure 1a). Condition (6) is used at the boundary enriched solution/bulk solution:

$$\frac{\partial \varphi(x=d+\delta^II)}{\partial x} = \frac{RT}{F} \left( \frac{i}{F} + \sum_{k=1}^3 z_k D_k \frac{\partial c_k}{\partial x} \right) \frac{1}{\sum_{k=1,2,3} z_k^2 D_k c_k} \quad (6)$$

### RESULTS

The calculations are made for the case of a 0.01 N NaCl+0.01 N CaCl<sub>2</sub> mixed solution and a conventional sulfo cation-exchange membranes (such as MK-40, Ralex or CMX). Calcium is preferably transported through such membranes due

\*Corresponding author. E-mail: v\_nikonenko@mail.ru.

to the high selectivity of its sorption in comparison with sodium. With increasing DC current density, the permselectivity towards calcium decreases (Figure 2a).

As the calculation shows, at  $i=0.6 i_{lim}$ , the  $T_{Ca} : T_{Na}$  ratio in DC mode is 0.52:0.48, while in PEF mode (duty cycle=0.5, frequency  $f=0.5$  Hz) this ratio is essentially higher: 0.66:0.34. The PEF effect is due to partial restoration of concentrations during a pause. The restoration occurs near the surface, a little change in concentration produces an important decrease in resistance,  $R$ . As a consequence, after a pause, the profiles are closer to those, which occur at a lower DC current density, which explains a higher permselectivity. An important feature is that the  $Na^+$  flux is negative during the pause lapse, while the  $Ca^{2+}$  flux remains positive (Figure 2b). This explains the increase in permselectivity attained in the PEF mode. However, when comparing the values of permselectivity coefficient in the DC and PEF modes in conditions that the average over the period current density  $i_{av}$  is the same and equal to  $0.3 i_{lim}$  (i.e. when  $i_{PEF}=0.6 i_{lim}$  and  $i_{DC}=0.3 i_{lim}$  with duty cycle=0.5), we find the same  $T_{Ca} : T_{Na}$  ratio equal to 0.66:0.34.

The obtained results show that the observed in experiment effect of PEF on the electro dialysis performance is more complicated than the developed model assumes. Most likely, in PEF mode there is a decrease in the water splitting. This leads to increasing current efficiency, hence, in PEF mode, a higher useful current is applied to ion transfer, which explains the positive effect on the specific permselectivity.

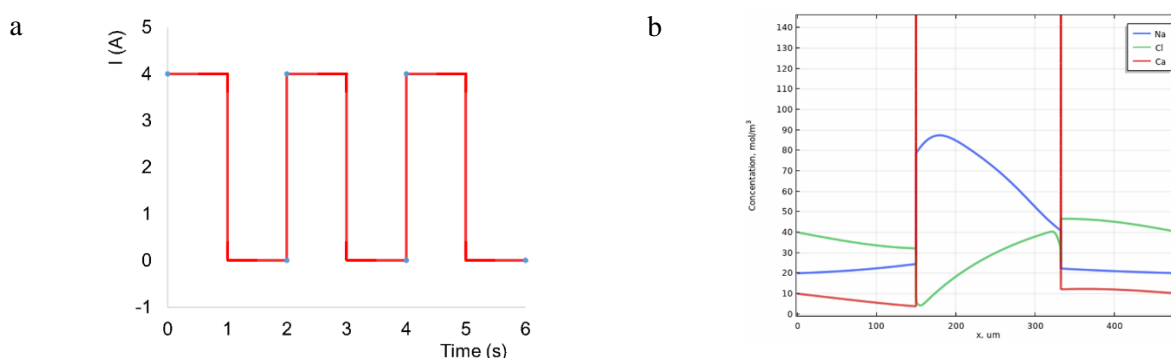


Figure 1. (a) Time dependence of the current density, and (b) concentration profiles occurred in the membrane system at the end of a pause (beginning of a pulse), the moment is shown with a blue dot on (a);  $i/i_{lim}=0.6$ ,  $f=0.5$  Hz.

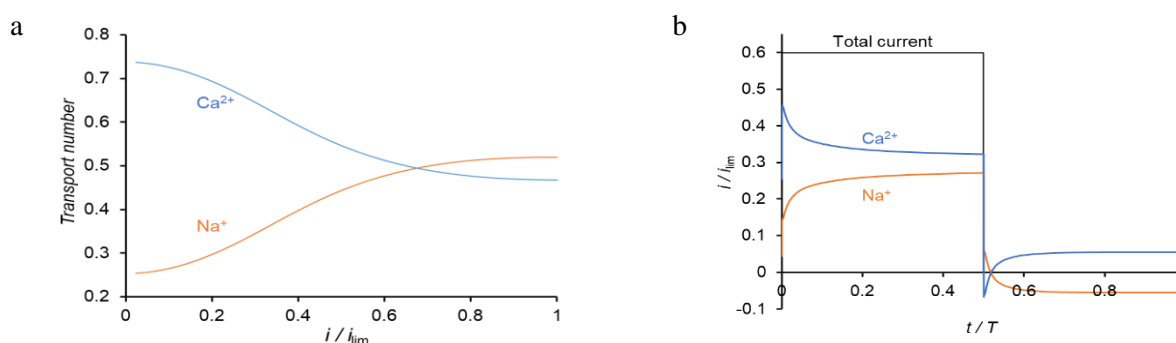


Figure 2. (a) Effective transport numbers of  $Na^+$  and  $Ca^{2+}$  in MK-40 vs. the  $i/i_{lim}$  ratio in the constant DC (solid lines) and PEF (dashed lines) modes. (b) Partial current densities of  $Na^+$  and  $Ca^{2+}$  and the total current density vs. time in PEF mode at  $i/i_{lim}=0.6$ ;  $T$  is the PEF period,  $f=0.5$  Hz.

## CONCLUSIONS

The membrane specific permselectivity can be improved in the PEF mode, if the same current is used in DC mode and during the pulse in PEF mode. However, no effect was found, if the values of permselectivity are compared at the same average current. The mechanism of enhancement of specific permselectivity in PEF mode is more complicated than the model assumes.

The work is supported by the RFBR, project #19-48-230023.

## References

- [1] Nikonenko V.V., Zabolotskii V.I., Gnusin N.P., *Sov. Electrochemistry* 16, 472-479, 1980.
- [2] Rubinstein I., *J. Chem. Soc. Faraday Trans.* 86, 1857-1861, 1990.
- [3] Lemay N., Mikhaylin S., Mareev S., Pismenskaya N., Nikonenko V., Bazinet L., *J. Membr. Sci.*, 603, 117878, 2020.

## MEMBRANE HYDRODYNAMIC PERMEABILITY: APPROXIMATION FOR THE MICROPOLAR FILTRATE

Daria Khanukaeva\*, Anatoly Filippov

*Department of Higher Mathematics, Gubkin Russian State University of Oil and Gas, Moscow, Russia*

**Summary** The hydrodynamic permeability of globular-structured membranes is considered in a micropolar flow. Known numerical results obtained in the framework of the cell model technique are approximated and presented in a simple explicit analytical form. A solid-liquid, a porous-liquid and a solid-porous-liquid cell are considered. The dependences of the hydrodynamic permeability on the cell structure and liquid characteristics are taken into account.

### MICROPOLAR FLUIDS AS FILTRATES

Membrane science and technologies are developing both in an experimental direction and theoretical part. Various modifications of membrane material represent the major trend in experiments aimed at the improvement of membrane characteristics. Along with the adequate description of the membrane microstructure, it is also important to use the corresponding model of the filtrating fluid. Classical hydrodynamics treats liquid as a conglomerate of material points and works fine at macroscales. Flows in membranes represent microscale problems as the flow domains are confined regions formed by the membrane microstructure. The flows in such domains are subjected to the influence of the boundaries and sufficiently involve filtrate interaction with the membrane material. Thus, taking into account the microstructure of the filtrate is a perspective sophistication of the liquid model which may sufficiently improve the models of filtration in membranes. The simplest model of liquid with microstructure is the micropolar liquid introduced by the Cosserat brothers. The mathematical apparatus of micropolar media was developed by Eringen [1].

The elements composing the micropolar liquid perform translational motion with velocity  $\mathbf{v}$  and independent rotational motion with angular velocity  $\boldsymbol{\omega}$ . The stress and couple stress tensors are non-symmetric as well as the deformation rate tensor and the curvature-twist rate tensor. The coefficients in the linear constitutive equations relating them are called the viscosity coefficients of the micropolar liquid. They appear in the governing equations of the micropolar liquid flow which include the continuity equation, the momentum equation and the moment of momentum equation. Flows in membranes are slow enough for the steady Stokes approximation to be valid. In the absence of body forces and body moments, the system of governing equations looks as follows:

$$\begin{aligned}\nabla \cdot \mathbf{v} &= 0, \\ (\mu + \kappa)\Delta \mathbf{v} + 2\kappa \nabla \times \boldsymbol{\omega} &= \nabla P, \\ (\alpha + \delta - \zeta)\nabla \nabla \cdot \boldsymbol{\omega} + (\delta + \zeta)\Delta \boldsymbol{\omega} + 2\kappa \nabla \times \mathbf{v} - 4\kappa \boldsymbol{\omega} &= \mathbf{0},\end{aligned}$$

where  $P$  is the pressure, and  $\mu, \kappa, \alpha, \delta, \zeta$  are the viscosity coefficients of the micropolar medium.

If the problem geometry possesses symmetry, coefficient  $\alpha$  is excluded from the moment of momentum equation, and the system can be solved analytically. Moreover, all the viscosity coefficients can be collected within two non-dimensional parameters, namely, the coupling number,  $N^2 = \kappa / (\mu + \kappa)$  and the scale parameter,  $L^2 = (\delta + \zeta) / (4\mu b^2)$ .

The former demonstrates the ratio of rotational viscosity  $\kappa$  to the sum of dynamic  $\mu$  and rotational viscosities, i.e. the measure of the flow retardation due to the rotation of liquid elements. The latter may be interpreted as the ratio of the problem microscale (structure particle size) to the problem macroscale (cell core size),  $b$ .

### HYDRODYNAMIC PERMEABILITY OF A GLOBULAR-STRUCTURED MEMBRANE

The cell model technique [2] is one of the well-developed and verified theoretical tools for filtration modeling. By the original principle, the porous structure is replaced by a set of cells – solid particles covered by liquid shells. The ratio of the solid core size,  $b$  to the outer cell size,  $c$  is associated with the membrane porosity,  $\gamma$ , i.e. a relative volume of liquid in a cell. Globular-structured membranes are represented by spherical or spheroidal cells, so, their porosity is evaluated as  $\gamma = (c^3 - b^3) / c^3 = 1 - (b/c)^3$ . The flow problem is considered in a single cell. The boundary conditions at the outer cell surface simulate various types of cell interaction.

The formulation of the boundary value problem (BVP) may vary, and the analytical solution can be obtained in any case. Hydrodynamic permeability of the membrane,  $L_{11}$  is further calculated on the basis of these solutions. It is defined as the ratio of the flow rate and the applied pressure gradient. Analytical expressions for hydrodynamic permeability are known for many types of cell structure, including the cells with porous and composite core. Originally, the theory was developed for viscous flows [3]. Recently it was extended to micropolar liquid flows with various types of boundary conditions at the interphase surfaces [4].

The major difficulty lies in the representation of the calculation results. Even for viscous flows they are so cumbersome that can be reported only via graphs. Thus, both the comparison of these results with experimental data and the exploitation

---

\*Corresponding author. E-mail: khanuk@yandex.ru.

of them in the applications are almost impossible. The present work is devoted to the presentation of the membrane hydrodynamic permeability as the approximate formula suitable for engineering applications.

### APPROXIMATING FORMULAE

The approximations of hydrodynamic permeability  $L_{11}app(\gamma)$  were found in [5] for a viscous filtrate in the form

$$L_{11}app(\gamma) = \frac{\gamma^x}{45(1-\gamma)^y},$$

where the values of  $x$  and  $y$  depend on the type of the considered BVP.

The solution of the flow problem for a micropolar filtrate depends on two more parameters:  $N$  and  $L$ . Therefore, the approximating formula for  $L_{11}^{polar} app$  must depend on  $\gamma$ ,  $N$  and  $L$ . It is sought in the multiplicative form  $L_{11}^{polar} app(\gamma, N, L) = L_{11}app(\gamma) \cdot L_{11}appII(N, L)$ . Analyzing the theoretical expression for  $L_{11}^{polar}$  we guess the form of  $L_{11}appII(N, L)$ . Using the least squares method, we finally obtain

$$L_{11}^{polar} app(\gamma, N, L) = L_{11}app(\gamma) \left( \frac{1}{L_{11}app(\gamma) e^{t-z\gamma} L^{1.5} + 1} + (1-N^2) \left( 1 - \frac{1}{L_{11}app(\gamma) e^{t-z\gamma} L^{1.5} + 1} \right) \right), \quad (1)$$

where the values of  $t$  and  $z$  depend on the type of BVP used. An example of curves plotted using formula (1) is shown in Figure together with the corresponding exact theoretical curves for a set of parameter  $L$  characteristic values and in the whole range of parameter  $N$  variation. One can see a very good agreement between approximate and exact curves. Analogous approximations are obtained for the other statements of BVP and more complicated flow domains: porous-liquid and composite solid-porous liquid cells.

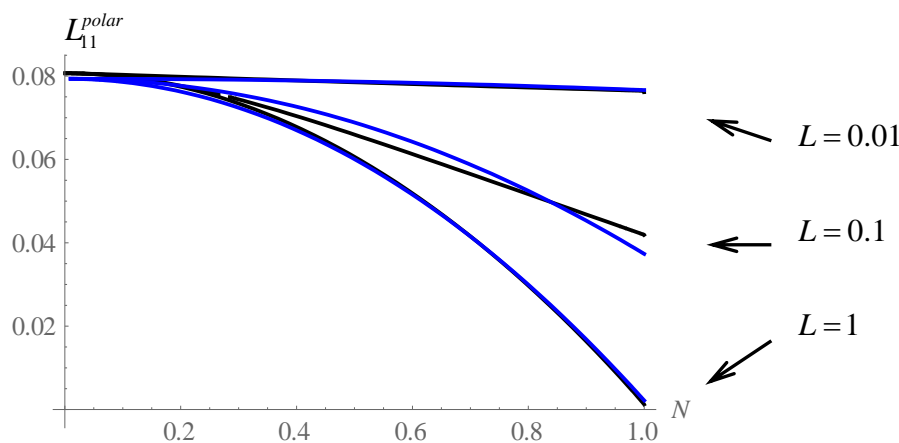


Figure 1. The graphs of  $L_{11}^{polar}(\gamma, N, L)$  versus  $N$  plotted using the theoretical results of [4] (black lines) and formula (1) (blue lines) for various values of  $L$  and  $\gamma = 0.8$

### CONCLUSION

In this work, the approximations of the hydrodynamic permeability for globular-structured membranes are obtained for a micropolar filtrate. They are presented as concisely and simply as possible. All the expressions are given in an explicit form which includes only elementary mathematical functions. No special software is required for their application. This makes the obtained results ready for engineering calculations.

The work is financially supported by RFBR (grant No 20-08-00661).

### References

- [4] Eringen, A.C.: Simple microfluids. *Int. J. Engng. Sci.* 2, 205-217, 1964.
- [5] Happel J., Brenner H. Low Reynolds number hydrodynamics. Martinus Nijhoff Publishers, The Hague 1983.
- [6] Vasin S.I., Filippov A.N., Starov V.M. Hydrodynamic permeability of membranes built up by porous shells: cell models. *Adv. Coll. Interface Sci.* 139, 83-96, 2008.
- [7] Khanukaeva D. Yu.: Filtration of micropolar liquid through a membrane composed of spherical cells with porous layer. *Theoretical and Computational Fluid Dynamics.* 34(3), 215-229, 2020.
- [8] Khanukaeva D.Yu.: Approximation of the hydrodynamic permeability for globular-structured membranes. *Mechanics of Materials.* 148, 103528, 2020.

## POLARIZATION BEHAVIOR OF PERFLUORINATED MEMBRANES MODIFIED WITH POLYANILINE

Natalia Kononenko\*, Natalia Loza, Marina Andreeva

Department of Physical Chemistry, Kuban State University, Krasnodar, Russia

**Summary** The current-voltage curves of anisotropic composites based on MF-4SK membrane and polyaniline was studied. The asymmetry of the parameters of the current-voltage curves was estimated. The pseudolimiting current appearing due to the formation of a bipolar internal boundary was revealed.

### INTRODUCTION

Composites based on MF-4SK membrane and polyaniline with anisotropic structure and asymmetric transport properties are most promising for use in various devices and electrochemical processes. The preparation of these materials under the conditions of an external electric field is faster than in a concentration field and allows to use the reduce concentration of the polymerizing solutions. The aim of this work was to examine the polarization behavior of surface-modified composites based on the MF-4SK membrane and polyaniline (PANI).

### EXPERIMENTAL

The synthesis of the MF-4SK/PANI samples was carried out at direct current density 300 A/m<sup>2</sup>. A 0.01 M aniline solution in 0.05 M HCl was fed into the cell chamber on the anode side and a 0.002 M potassium bichromate solution in 0.05 M HCl was introduced on the cathode side. A polyaniline layer formed on the membrane surface on the cathode side. The current-voltage curves (CVCs) were measured in the same cell in which the composites were prepared. The cell consisted of two electrode chambers with platinum polarizing electrodes and two near-membrane chambers. Direct current was applied at a specified scan rate to the polarizing electrodes using an Autolab pgstat302n potentiostat/galvanostat. The change in the potential difference on the membrane was recorded using Luggin–Haber capillaries connected with the membrane and the silver/silver chloride electrodes. The silver chloride electrodes were connected to the potentiostat/galvanostat, from which the signal was fed to a computer, which allowed real-time recording of the experimental  $\Delta E$  value. The parameters of CVCs were determined by the tangent method using numerical differentiation in the Microsoft Excel program.

### RESULTS

According to the data presented in Figure 1a, depending on the orientation of the modifying polyaniline layer to the counterion flow the CVCs are asymmetric. If the counterion flow meets the polyaniline layer, the limiting current and the conductivity of the electromembrane system (EMS) decrease, while the potentials of the start of the overlimiting state increase compared with that for the original membrane. A similar form of polarization curves was observed for the anisotropic composites obtained by sequential diffusion of polymerizing solutions across the membrane into water [1, 2].

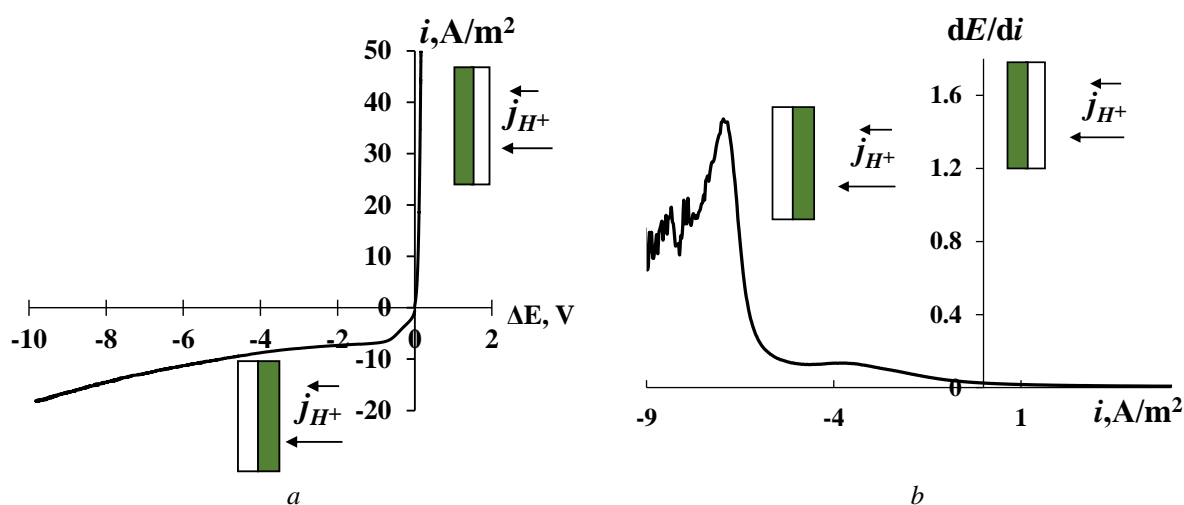


Figure 1. Integrated (a) and differential (b) CVCs of the MF4SK/PANI composites in 0.05 M HCl

\*Corresponding author. E-mail: kononenk@chem.kubsu.ru

We assumed that the reason of asymmetry of CVCs is the presence of two layers formed in accordance with the asymmetric conditions of synthesis in the modified sample. Polyaniline having anion-exchange properties [3] is mainly localized in the surface layer of the sulfocationite membrane. The formation of an internal bipolar boundary between the cation- and anion-exchange layers in a perfluorinated membrane can lead to catalytic dissociation of water. When the membrane is oriented toward the counterion flow by its polyaniline layer, the counterions cease to participate in current transport because they are partially neutralized by hydroxyl ions generated on the bipolar boundary, which should lead to the appearance of a quasilimiting state in the EMS. This is confirmed by a detailed analysis of the region of small displacements of the potential from equilibrium (from 0 to 100 mV) on the CVC. The effect of the appearance of the quasilimiting state and of the second inflection on the CVC at low potentials (Figure 1b) is directly related to the emergence of a PANI layer on the membrane surface. The appearance of “fast ions” in the system due to the catalytic dissociation of water was confirmed by analyzing the frequency impedance spectrum.

The evaluation of the conductivity of the EMS from the slope of the ohmic region of CVCs showed that the asymmetry of this parameter is observed regardless of the measurement mode of the polarization curve, the orientation of the anisotropic membrane playing the determining role. The EMS conductivity is lower when the modified side of the membrane is directed toward the counterion flow. The different conductivities of the membrane system can be explained by different concentration profiles formed in this bilayer membrane. Thus, the diode effect or the effect of switching the EMC conductivity was revealed for anisotropic composite membranes prepared in an external electric field.

## CONCLUSIONS

Composite membranes based on MF-4SK and polyaniline with an anisotropic structure and asymmetric current-voltage curves can be obtained under the conditions of an external electric field. An analysis of various regions of the CVC of the composite membranes shows the asymmetry of the CVC parameters. Also, the pseudolimiting current appears due to the formation of an internal bipolar boundary. Based on the analysis of the polarization behavior of the samples, we can determine their effective applications in various electrochemical devices. Materials with asymmetry of the current-voltage curve and high density of the limiting current are promising for use in electrodialysis because, as is known, modification of perfluorinated membranes with polyaniline increases their selectivity and reduces the diffusion and electroosmotic permeability. Anisotropic composite membranes with a diode-like effect may be used as membrane switches or relays.

This work was supported by the Russian Foundation for Basic Research, project No 18-08-00771.

## References

- [1] Tan S., Belanger D. Characterization and transport properties of Nafion/Polyaniline composite membranes. *J. Phys. Chem.* 109, 23480-23490, 2005.
- [2] Berezina N.P., Kononenko N.A., Sytcheva A.A.-R., Loza N.V., Shkirskaya S.A., Hegman N., Pungor A. Perfluorinated Nanocomposite Membranes Modified by Polyaniline: Electrotransport Phenomena and Morphology. *Electrochimica Acta.* 54, 2342-2352, 2009.
- [3] Wang, J. Anion exchange nature of emeraldine base (EB) polyaniline (PAn) and a revisit of the EB formula. *Synth. Met.* 132, 49-52, 2002.

## ON A MICROPOLAR FLUID FILTRATION PROBLEM THROUGH AN AXIALLY SYMMETRIC CELL

Yulia Koroleva\* and Daria Khanukaeva

*Department of Higher Mathematics, Gubkin Russian State University of Oil and Gas, Moscow, Russia*

**Summary** We study a model problem on the filtration of micropolar fluid in the framework of a cell model technique. A porous medium is presented as an assemblage of axially symmetric cells of an arbitrarily geometry. Each cell consists of a solid core, porous layer and liquid shell. The flow problem is solved in a single cell, the influence of the neighbouring cells is taken into account via Cunningham's-type boundary condition. We derive apriori estimates for flow characteristics which show the behaviour of the velocity filed. The boundedness of velocity filed is justified by the derived estimates.

### STATEMENT OF THE PROBLEM AND THE MAIN RESULTS

One can extend the study of the micropolar fluid filtration to a cell of arbitrary shape with axial symmetry. This property of the cell geometry plays a key role in the formulation of the field equations in the form allowing for their integration. Denote by  $(\mathbf{v}_i, \boldsymbol{\omega}_i, p_i)$  the unknown dimensionless linear velocity, angular velocity and pressure of flow passing through the domain  $\Omega_i, i=1,2$  (see Figure 1). Introduce dimensionless parameters

$$N^2 = \frac{\kappa}{\mu + \kappa}, \quad L^2 = \frac{\delta + \zeta}{4\mu d_{\Omega_2}^2}, \quad \sigma = \frac{d_{\Omega_2}}{\sqrt{k}},$$

where  $k$  is the permeability of the porous medium,  $\delta, \zeta, \mu, \kappa$  are viscosity constants,  $d_{\Omega_2}$  is the diameter of the domain  $\Omega_2$ . The parameter  $N^2$  demonstrates the fraction of rotational viscosity in the sum of rotational and translational viscosities,  $L^2$  represents the relation between the micro scale of the problem and its macro scale, the parameter  $\sigma$  represents the ratio of the macro scale of the cell to the micro scale of the porous layer.

The governing system of equations for the filtration of the micropolar fluid in porous media reads as follows ([1]):

$$\begin{aligned} \nabla \cdot \mathbf{v}_i &= 0, & \text{in } \Omega_i, i=1,2 \\ \varepsilon \left( \frac{1}{N^2} - 1 \right) \nabla p_1 &= \frac{1}{N^2} \Delta \mathbf{v}_1 + 2 \operatorname{curl} \boldsymbol{\omega}_1 - \frac{\varepsilon \sigma^2}{N^2} \mathbf{v}_1, & \text{in } \Omega_1 \\ \varepsilon \left( \frac{1}{N^2} - 1 \right) \nabla p_2 &= \frac{1}{N^2} \Delta \mathbf{v}_2 + 2 \operatorname{curl} \boldsymbol{\omega}_2, & \text{in } \Omega_2 \\ L^2 \Delta \boldsymbol{\omega}_i + \frac{N^2}{2(1-N^2)} \operatorname{curl} \mathbf{v}_i - \frac{N^2}{2(1-N^2)} \boldsymbol{\omega}_i &= \mathbf{0}, & \text{in } \Omega_i, i=1,2 \end{aligned}$$

Here  $\varepsilon$  is the porosity of the porous medium. We assume the following boundary conditions:

$$\mathbf{v}_1|_{\Gamma_1} = \mathbf{0}, \quad \boldsymbol{\omega}_1|_{\Gamma_1} = \mathbf{0}, \quad \mathbf{v}_2|_{\Gamma_2} = \mathbf{v}_1|_{\Gamma_1}, \quad \boldsymbol{\omega}_2|_{\Gamma_2} = \boldsymbol{\omega}_1|_{\Gamma_1}, \quad \mathbf{v}_2|_{\Gamma_3} = \bar{\mathbf{U}}, \quad \boldsymbol{\omega}_2|_{\Gamma_3} = \mathbf{0}.$$

The velocity  $\bar{\mathbf{U}}$  of the incoming flow coincides with linear velocity at the outer boundary of the cell.

The solution to our problem is treated in the weak sense. We prove its uniqueness and derive some apriori estimates for the behaviour of flow. The main result is the following theorem.

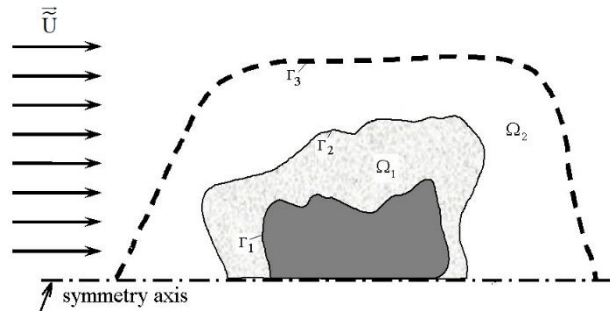


Figure 1. The geometry of a porous cell.

\*Corresponding author. E-mail: koroleva.y@gubkin.ru.

**Theorem**

The weak solution to the given problem is unique. The norms of linear and angular velocities are uniformly bounded and satisfy to the estimates:

$$\begin{aligned} \|\mathbf{v}_1\|_{L_2}^2 &< 0.5\varepsilon^{-1}\sigma^{-2} + \varepsilon^{-1}\sigma^{-2} \max(2N^2, 4L^2(1-N^2)) \left( \|\boldsymbol{\omega}_1\|_{H^1}^2 + \|\boldsymbol{\omega}_2\|_{H^1}^2 \right) \\ \|\mathbf{v}_2\|_{L_2}^2 &< \left( \frac{1+0.5d_{\Omega_1}^2}{1-0.5d_{\Omega_1}^2} \right) (0.5 + \max(2N^2, 4L^2(1-N^2))) \left( \|\boldsymbol{\omega}_1\|_{H^1}^2 + \|\boldsymbol{\omega}_2\|_{H^1}^2 \right) + 1 \\ \|\boldsymbol{\omega}_1\|_{H^1}^2 + \|\boldsymbol{\omega}_2\|_{H^1}^2 &\leq \max \left\{ \frac{N^2}{2L^2(1-N^2)}, 2 \right\} \left( \|\mathbf{v}_1\|_{H^1}^2 + \|\mathbf{v}_2\|_{H^1}^2 \right) \\ \|\mathbf{v}_1\|_{H^1}^2 + \|\mathbf{v}_2\|_{H^1}^2 &< \frac{1}{C}, \end{aligned}$$

where the constant  $C$  depends both on viscosity parameters and diameter of the porous cell.

$$C = \begin{cases} 2 - d_{\Omega_1}^2 + 16L^2N^2 - 16L^2, & \text{if } \frac{N^2}{L^2(1-N^2)} < 2, \\ 2 - d_{\Omega_1}^2 - 16N^2, & \text{if } 2 \leq \frac{N^2}{L^2(1-N^2)} < 4, \\ 2 - d_{\Omega_1}^2 - \frac{2N^4}{L^2(1-N^2)}, & \text{if } \frac{N^2}{L^2(1-N^2)} \geq 4. \end{cases}$$

**CONCLUSIONS**

The obtained inequalities allow making easy estimates of linear and angular velocities at micro scale in filtration flows of micropolar fluids. Moreover, with the help of the derived estimates we have shown the boundedness of weakly defined velocity fields. The presence of the characteristic scale  $d_{\Omega_2}^2$  of the problem in the estimates is one more exhibition of the absence of the similarity property for the micropolar fluid. This fact is of crucial importance for flows in micro domains, where anormal growth of viscosity is usually observed when Newtonian liquid is used for the modeling. Besides, the characteristic scale of the problem presents in each estimate and solution, as it enters parameter  $L$ , which substantially defines the flow pattern. Evaluating coefficients in estimates for the angular velocities one can see that these coefficients do not depend on the liquid dynamic viscosity  $\mu$ . They are defined by the ratio of the rotational  $\kappa$  and angular  $\delta + \zeta$  viscosities as well as by the characteristic scale of the flow domain. This observation demonstrates a very high importance of the liquid microstructure consideration, because the characteristics of the liquid microstructure influence the flow independently of its common for classical hydrodynamics parameter  $\mu$ .

The exact analytical formulae solving our problem for the case of spherical particle are given in [2].

The work is supported by RFBR (project 19-08-00058 A)

**References**

- [1] Hamdan M.H., Kamel, M.T., *Spec.Top.. Rev. Porous Med.* 2(2), 145-155, 2011.
- [2] Khanukaeva, D.Yu., Filtration of micropolar liquid through a membrane composed of spherical cells with porous layer. *Theoretical and Computational Fluid Dynamics.* 34(3), 215-229, 2020.

## MATHEMATICAL MODELING OF THE AUTOWAVE PROCESS IN A THIN SURFACE LAYER

Anna Kovalenko<sup>\*1</sup>, Natalia Kandaurova<sup>2</sup>, Vladimir Chekanov<sup>3</sup>

<sup>1</sup>*Department of Intelligent Information Systems, Kuban State University, Krasnodar, Russia*

<sup>2</sup>*Department of Information Technology, MIREA-Russian Technological University, Stavropol, Russia*

<sup>3</sup>*Department of Information Systems and Technologies, North-Caucasus Federal University, Stavropol, Russia*

**Summary** Research in the field of interfacial and near-surface phenomena for media with unique characteristics is of unremitting interest for scientists. A liquid dispersed nanostructured system (magnetic fluid or ferrofluid) has unique electrical and electro- and magneto-optical properties, which are of scientific interest from the point of view of studying the interaction of dispersed particles with external fields and with each other. For decades, autowaves have been the object of close attention of physicists, chemists, and biologists. A wide variety of different types of self-organization have been discovered and investigated in various nonlinear diffusion systems. Autowaves in the near-surface layer of a ferrofluid (magnetic fluid) are a unique phenomenon. The scientific novelty of the work lies in the development of a mathematical model of an autowave process experimentally observed in a thin layer of a nanostructured liquid, obtaining a solution in the environment for modeling physical processes COMSOL Multiphysics 5.2, comparing the results of computer simulation with a full-scale experiment.

Basic assumptions for the inference of a one-dimensional model. Let us denote  $C_i, j_i, R_i, i=1, \dots, 6$ , where  $C_1, j_1$  are the concentration and flux of impurity ions A+,  $C_2, j_2$  are the concentration and flux of impurity ions B-,  $C_3, j_3$  are the concentration and flux of ions of positively charged particles of the magnetic fluid M+,  $C_4, j_4$  are the concentration and flux of ions of negatively charged particles of the magnetic fluid M-,  $C_5, j_5$  are the concentration and ion flux of positive induced ions X+,  $C_6, j_6$  are concentration and flux of ions of negative induced ions X-,  $\varphi$  is potential of the electric field,  $R_i$  is homogeneous chemical reactions (dissociation and association).

Then the equations of the general model of one-dimensional transport will be described by the system of equations:

$$\frac{\partial C_i}{\partial t} = -\frac{\partial j_i}{\partial x} + R_i, \quad i=1, \dots, 6 \quad (1)$$

$$j_i = -\frac{F}{RT_0} z_i D_i C_i \frac{d\varphi}{dx} - D_i \frac{dC_i}{dx}, \quad i=1, \dots, 6 \quad (2)$$

$$\frac{d^2 \varphi}{dx^2} = -\frac{F}{\varepsilon_r} \sum_{i=1}^6 z_i C_i \quad (3)$$

In Figure 1a the initial state of concentrations  $C_3(0, x)$  and  $C_4(0, x)$  is presented. We assume that the initially neutral particles of the magnetic fluid are distributed rather densely by  $x=0$  and  $x=H$ . Further, at the initial moment of time  $t=0$ s. They are all fully charged. Near  $x=0$  - positive,  $x=H$  - negative. Then the positively charged particles of the magnetic fluid begin to move to  $x=H$ , and the negatively charged magnetic particles to  $x=0$  (Figure 1b).

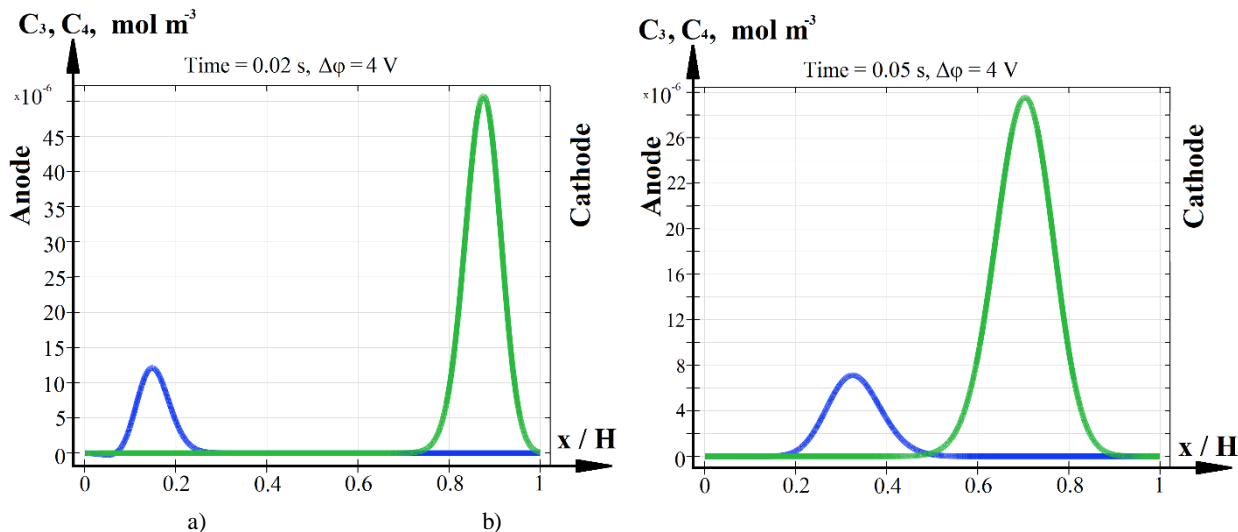


Figure 1. Initial state of C3 and C4 concentrations at time a)  $t=0.02$ c, b)  $t=0.05$ c.

<sup>\*</sup>Corresponding author. E-mail: savanna-05@mail.ru.

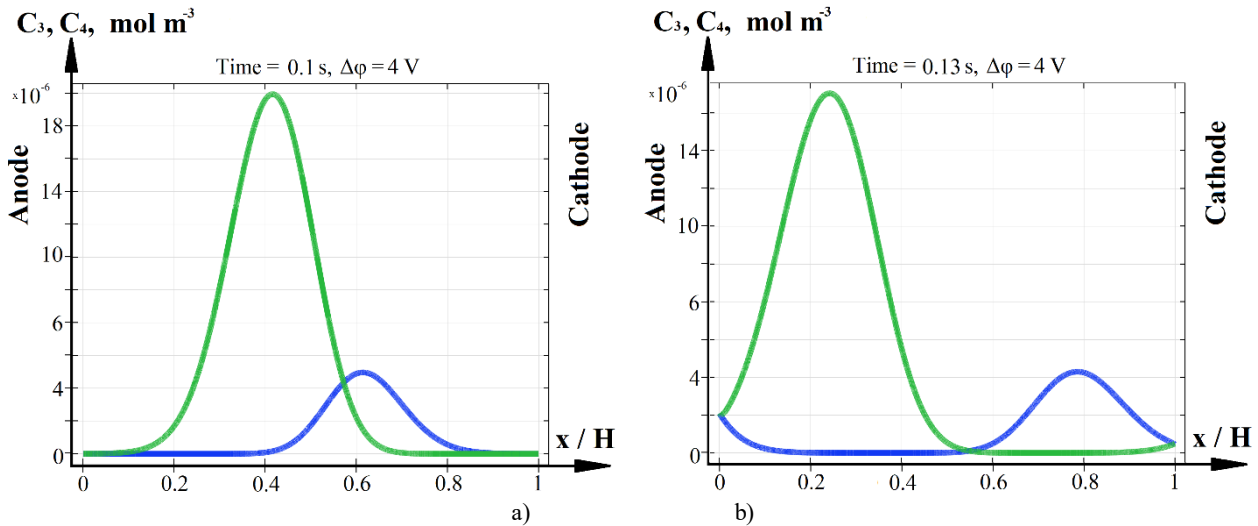


Figure 2. The state of the C3 and C4 concentrations at the time a)  $t = 0.1$  s, b)  $t = 0.13$  s.

Two concentration waves move towards each other Figure 1b and Figure 2a. Initially they are different in amplitude, but then they will become equal in amplitude.

The green wave (C4) is negatively charged magnetic particles that go to a positively charged electrode (anode), while the blue wave (C3) is positively charged magnetic particles that go to a negatively charged electrode (cathode). After the waves reach the corresponding electrodes, they are recharged, i.e. first they become neutral, and then acquire the signs of the corresponding electrodes. For example, there was a zero number of negatively charged particles near the anode, then there were a lot of them, i.e. those negatively charged particles that came to the anode receive a positive charge and go to the cathode. Similarly, positively charged particles arriving at the cathode receive a negative charge and begin to move towards the anode. Then the cycle is repeated.

Thus, the particles move from one electrode to another and back (Figure 2b). Recharging takes place at the electrodes.

The time of one wave in the numerical experiment varies from 0.05 to 0.12 seconds, consistent with the experiment.

In the study, the potential jump is 4V.

Further directions of research are associated with the explanation of the mechanism of "charge exchange", the introduction of the concept of "injected" ions. By adding impurity ions. Generalization. Dissociation and recombination. Moving on to 2D and 3D models.

The scientific novelty of this study is the mathematical and computer 1D modeling of a complex and ambiguous process of recharging of magnetic particles at the electrodes, which fully corresponds to the physical process observed in experiments. The predictive value of this model is the real diffusion coefficients and concentration values for positively and negatively charged magnetic particles.

## CONTRAST STRUCTURES OF SPACE CHARGE IN ELECTROMEMBRANE SYSTEMS

Anna Kovalenko<sup>1</sup>, Machamet Urtenov\*<sup>2</sup>

<sup>1</sup>Department of Intelligent Information Systems, Kuban State University, Krasnodar, Russia

<sup>2</sup>Department of Applied Mathematics, Kuban State University, Krasnodar, Russia

**Summary** For the first time, the possibility of a complex structure of the space charge region in membrane systems, specifically, in the desalination channel of an electro dialysis apparatus formed by anion-exchange (AEM) and cation-exchange (CEM) membranes, is shown, namely, the possibility of the appearance of contrastive space charge structures in the form of internal double electric layers, as well as «round» structures analogous to ball lightning in the atmosphere.

It was assumed that the space charge in membrane systems distributed near ion-exchange membranes is negative for AEM and positive for CEM in the articles [1,2]. It was shown that the space charge leads to the appearance and development of electroconvective vortices, which is the main cause of overlimiting transport in electromembrane systems (EMS) in the articles [3-5]. However, numerical analysis of the boundary value problem of the mathematical model [4] for «distant» overlimiting currents shows a much more complex structure of the space charge region (SCR) in the desalination channel. Namely, the emergence and development of various local structures of the space charge with a short life span is shown.

### «CONTRASTING» STRUCTURES OF THE SPACE CHARGE

In processes, studied by differential equations with small parameters for higher derivatives, internal boundary layers appear under certain conditions [6]. They are called contrasting structures. With natural normalization in the dimensionless system of equations of the model [4], a small parameter occurs for the highest derivative in the Poisson equation.

The occurrence of internal boundary layers under overlimiting regimes was shown in the article [7]. Based on these considerations, the regions of space charge that arise below that differ from the SCR and are adjacent to ion-exchange membranes will be called «contrasting» structures.

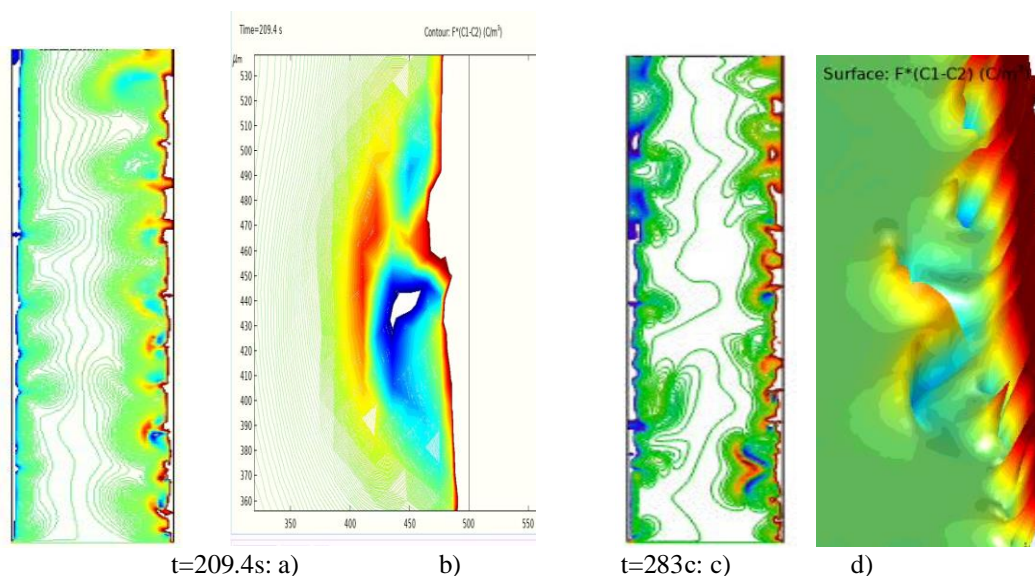


Figure 1. "Contrasting" structures of the space charge at different times: a) and b) - general view of the level lines, C) and d) - increase in the studied "contrasting" structures.

Figure 1a) and Figure 1b) show some contrasting structures of the double electric layer type that occur, in contrast to border-layer SCR, inside the desalination channel.

### «ROUND» STRUCTURES

It follows from the calculations that in some cases small «pieces» break off from the SCR at the membranes and begin to drift independently downstream of the solution, slightly changing their shape, and then disappear connecting with the SCR at the membrane (Figure 2). These properties are similar to ball lightning in the atmosphere.

\*Corresponding author. E-mail: urtenovmax@mail.ru.

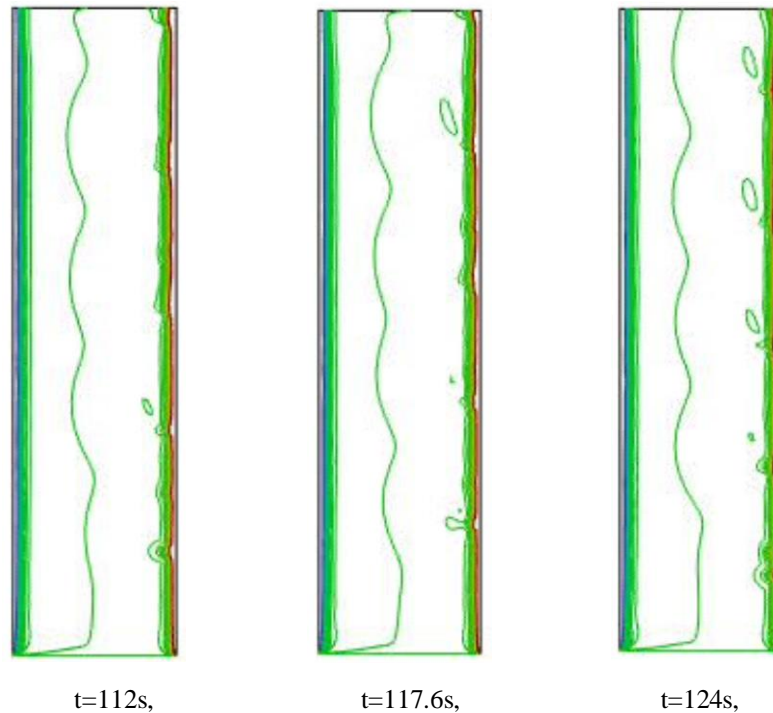


Figure 2. "Round" structures at the different times.

This work was supported by the Russian Foundation for Basic Research, project No. 20-58-12018 NNIO\_a: The influence of electroconvection, water dissociation, and geometry of spacers on electro dialysis desalination in intensive current regimes.

## References

- [1] Rubinshtein, I.; Zaltzman, B.; Prez, J.; Linder C. Experimental verification of the electroosmotic mechanism for the formation of overlimiting current in a system with a cation-exchange electro dialysis membrane. *Electrochemistry*. 38, No 8, 956-967, 2002.
- [2] Nikonenko, V.V.; Zabolotsky, V.I.; Gnusin, N.P. Electric transfer of ions through a diffusive layer with disturbed electroneutrality. *Electrochemistry*. 25, No. 3, 301-306, 1989.
- [3] Rubinstein I., Zaltzman B. *Physical Review E* 62, 2238, 2000.
- [4] Urtenov M.K., Uzdenova A.M., Kovalenko A.V., Nikonenko V.V., Pismenskaya N.D., Vasil'eva V.I., Sistas P., Pourcelly G. Basic mathematical model of overlimiting transfer enhanced by electroconvection in flow-through electro dialysis membrane cells. *J. Memb. Sci.* 447, 190, 2013.
- [5] Kwak R., Guan G., Peng W.K., Han J. Microscale electro dialysis: concentration profiling and vortex visualization. *Desalination*. 308, 138, 2012.
- [6] Vasil'eva A. B., Butuzov V. F., Nefedov N. N. Kontrastnye struktury v singularno vozmushennykh zadachah. *Fundament. i prikl. matem.* [Contrast structures in singularly perturbed problems. Foundation. and appl. math..] 4:3, 799–851, 1998.
- [7] Urtenov, M.; Chubyr, N.; Gudza, V. Reasons for the Formation and Properties of Soliton-Like Charge Waves in Membrane Systems When Using Overlimiting Current Modes. *Membranes*, 10, 189, 2020.

## FEATURES OF THE EFFECT OF WATER SPLITTING ON ELECTROCONVECTION

Anna Kovalenko<sup>\*1</sup>, Makhamet Urtenov<sup>2</sup>, Alexander Pismenskiy<sup>2</sup> and Elizaveta Evdochenko<sup>3</sup>

<sup>1</sup>Department of Intelligent Information Systems, Kuban State University, Krasnodar, Russia

<sup>2</sup>Department of Applied Mathematics, Kuban State University, Krasnodar, Russia

<sup>3</sup>Chemical Process Engineering AVT.CVT, RWTH Aachen University, Aachen, Germany

**Summary** Taking into account the effect of the splitting (dissociation) reaction of water molecules is important for understanding the transport processes in electromembrane systems [1-3]. Some authors believe that the emergence of new charges H<sup>+</sup> and OH<sup>-</sup> can reduce or destroy the space charge that is the basis of other transport mechanisms, such as electroconvection. We have created a mathematical model of transport in electromembrane systems, taking into account three types of ions (Na<sup>+</sup>, Cl<sup>-</sup>, OH<sup>-</sup>) and conducted computer modeling and research of this model [4-10]. In addition, an estimate of the effect of water splitting (dissociation) on the occurrence and development of electroconvective vortices in the cation-exchange membrane was calculated. At the same time, we did not take into account the recombination of hydrogen and hydroxyl ions. Thus, we considered the most unfavorable situation for the development of electroconvection, since hydroxyl ions maximally weaken the space charge at the cation-exchange membrane.

Current-voltage characteristics (I - V characteristic or CVC) shown in Figure 1, which we calculated using models [1,2], taking into account the splitting of water (i.e. 3 types of ions: Na<sup>+</sup>, Cl<sup>-</sup>, OH<sup>-</sup>) and excluding the splitting of water (2 type of ions: Na<sup>+</sup>, Cl<sup>-</sup>). In these models, the average solution velocity, the initial concentration of the solution and hydroxyl are the same. Note that the rate of splitting (dissociation) of water molecules is considered to be maximum and is determined by specifying the flow of hydroxyl ions in the boundary conditions.

The results obtained in this case show (Figure 1, Figure 2):

1. Strong influence of taking into account hydroxyl ions on the transport of salt ions. Figure 1 shows the sloped part of the I - V characteristic, which rapidly begins to increase after the transition to the overlimiting current mode until the appearance of electroconvection, which begins with a potential jump from about 0.2 V and continues to about 1.6 V.
2. About the emergence and development of electroconvective vortices, which begin much later or, which is the same, with much higher potential jumps.

The main conclusion is (Table 1) that the reaction of splitting (dissociation) of water molecules does not lead to the complete suppression of electroconvection, which still remains the main mechanism of overlimiting transfer in overlimiting current regimes.

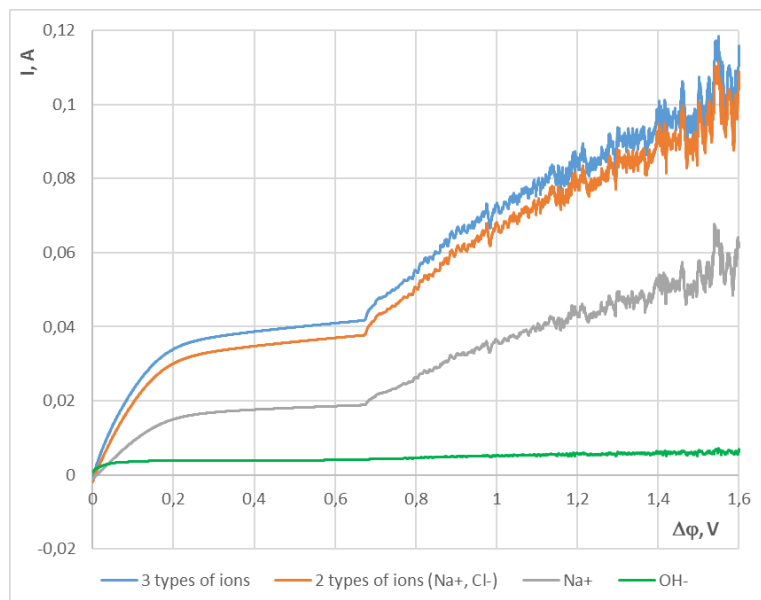


Figure 1. The combination of current-voltage characteristics (CVC) with water splitting (3 types of ions: account of ions of salt and hydroxyl) and without split water (2 types of ions), as well as partial CVC

\*Corresponding author. E-mail: savanna-05@mail.ru.

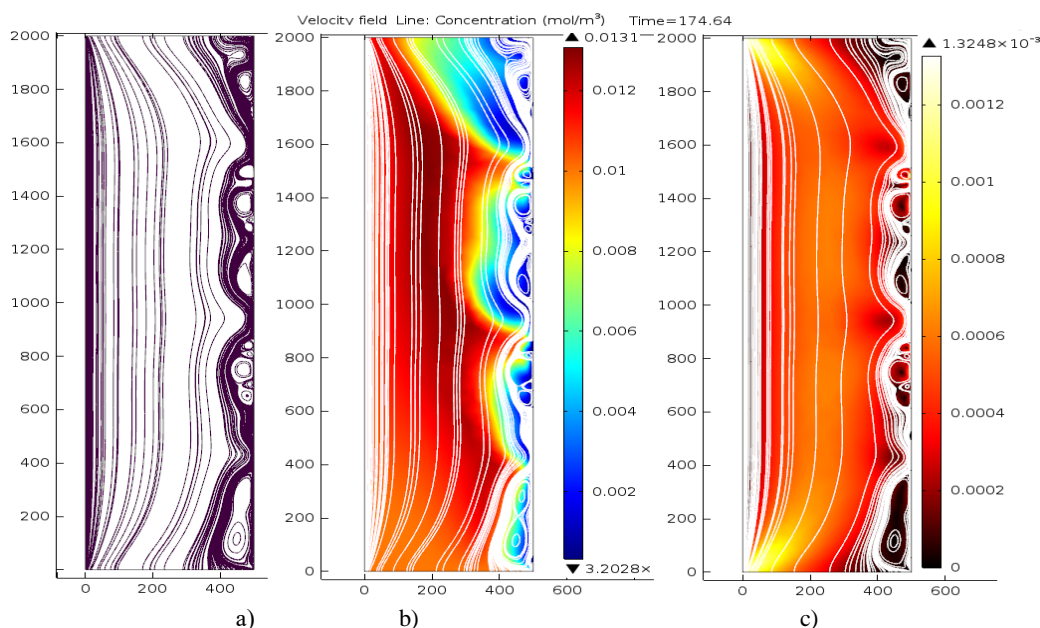


Figure 2. Solution streamlines and concentration (Na<sup>+</sup>): a) streamlines; b) streamlines and ions concentration surface (highlighted) c) streamlines and the velocity rate surface (highlighted)

Table 1. Dependence of the critical potential drop ( $\Delta\phi_{cr}$ ) from the OH<sup>-</sup> flux ( $j_{3m}$ ) defined on CEM/solution interface

$j_{3m}$ , mol/(m <sup>2</sup> s)	0	$10^{-7}$	$5 \times 10^{-7}$	$10^{-6}$	$5 \times 10^{-6}$
$\Delta\phi_{cr}$ , V	0,66	0,68	0,81	0,96	1,11

The reported study was funded by RFBR and DFG according to the research project № 20-58-12018.

## References

- [1] Urtenov M.K., Uzdenova A.M., Kovalenko A.V., Nikonenko V.V., Pismenskaya N.D., Vasil'eva V.I., Sistas P., Pourcelly G. Basic mathematical model of overlimiting transfer enhanced by electroconvection in flow-through electro dialysis membrane cells. *Journal of Membrane Science*. 447, 190-202, 2013.
- [2] Nikonenko V.V., Kovalenko A.V., Urtenov M.K., Pismenskaya N.D., Han J., Sistas P., Pourcelly G. Desalination at overlimiting currents: State-of-the-art and perspectives. *Desalination*. 342, 85–106, 2014.
- [3] Nikonenko V.V., Pismenskaya N.D., Urtenov M.K., Uzdenova A.M., Kovalenko A.V., Mareev S.A., Pourcelly G. Effect of electroconvection and its use in intensifying the mass transfer in electro dialysis (Review). *Russian Journal of Electrochemistry*. 53(10), 1122-1144, 2017.
- [4] Apel P. Yu., Bobreshova O. V., Volkov A. V., Volkov V. V., Nikonenko V. V., Stenina I. A., Filippov A. N., Yampolskii Yu. P., Yaroslavl'tsev A. B. Prospects of Membrane Science Development. *Membranes and Membrane Technologies*. 1, 45–63, 2019.
- [5] Belova E., Lopatkova G., Pismenskaya N., Nikonenko V., Larchet C. Role of water splitting in development of electroconvection in ion-exchange membrane systems. *Desalination*. 199, 59–61, 2006.
- [6] Zyryanova S., Mareev S., Gil V., Korzhova E., Pismenskaya N., Sarapulova V., Rybalkina O., Boyko E., Larchet C., Dammak L., Nikonenko V., How Electrical Heterogeneity Parameters of Ion-Exchange Membrane Surface Affect the Mass Transfer and Water Splitting Rate in Electro dialysis. *Int. J. Mol. Sci*. 21, 973-996, 2020.
- [7] Nikonenko V., Urtenov M., Mareev S., Pourcelly G., Mathematical Modeling of the Effect of Water Splitting on Ion Transfer in the Depleted Diffusion Layer Near an Ion-Exchange Membrane, *Membranes*. 10, 22-45, 2020.
- [8] Mareev S.A., Evdochenko E., Wessling M., Kozaderova O.A., Niftaliev S.I., Pismenskaya N.D., Nikonenko V. V., A comprehensive mathematical model of water splitting in bipolar membranes: Impact of the spatial distribution of fixed charges and catalyst at bipolar junction, *J. Memb. Sci*. 603, 118010, 2020.
- [9] Simons R., Khanarian G. Water dissociation in bipolar membranes: Experiments and theory. *J. Membr. Biol.* 38, 11–30, 1978.
- [10] Gнусin N.P. Overlimiting electrodiffusion transport in the diffusion layer as a function of rate constants of dissociation and recombination of water: A numerical calculation. *Russ. J. Electrochem.* 38, 839–845, 2002.

## SOFTWARE COMPLEX FOR ANALYZING THE CURRENT-VOLTAGE CHARACTERISTICS OF ELECTROMEMBRANE SYSTEMS

Anna Kovalenko<sup>1</sup>, Mahamet Urtenov<sup>\*2</sup> and Inna Shkorkina<sup>2</sup>

<sup>1</sup>Department of Intelligent Information Systems, Kuban State University, Krasnodar, Russia

<sup>2</sup>Department of Applied Mathematics, Kuban State University, Krasnodar, Russia

**Summary** We have developed a software package of "Deep learning for CVC 1.0", which contains databases and knowledge bases of theoretical and experimental current-voltage characteristics (CVC) using the method of deep machine learning (Deep learning). The developed software package allows you to simulate mass transfer in the electromembrane systems (EMS), which has a single interface with a built-in reference system, analysis and synthesis of theoretical and experimental current-voltage characteristics.

The current-voltage characteristic (CVC) is the most important integral characteristic of transport processes in electromembrane systems. The study of experimental CVC [1] shows a complex, non-stationary and unstable behavior of the CVC. However, a theoretical study of the CVC has not yet been conducted. This is due to the fact that on the one hand, it takes a lot of time to calculate one CVC and therefore costs hundreds of thousands of dollars. On the other hand, it is necessary to use methods that adequately reflect the non-stationary and unstable behaviour of the CVC over time. For the first time, we managed to solve these problems in a complex using a specially created artificial intelligence system.

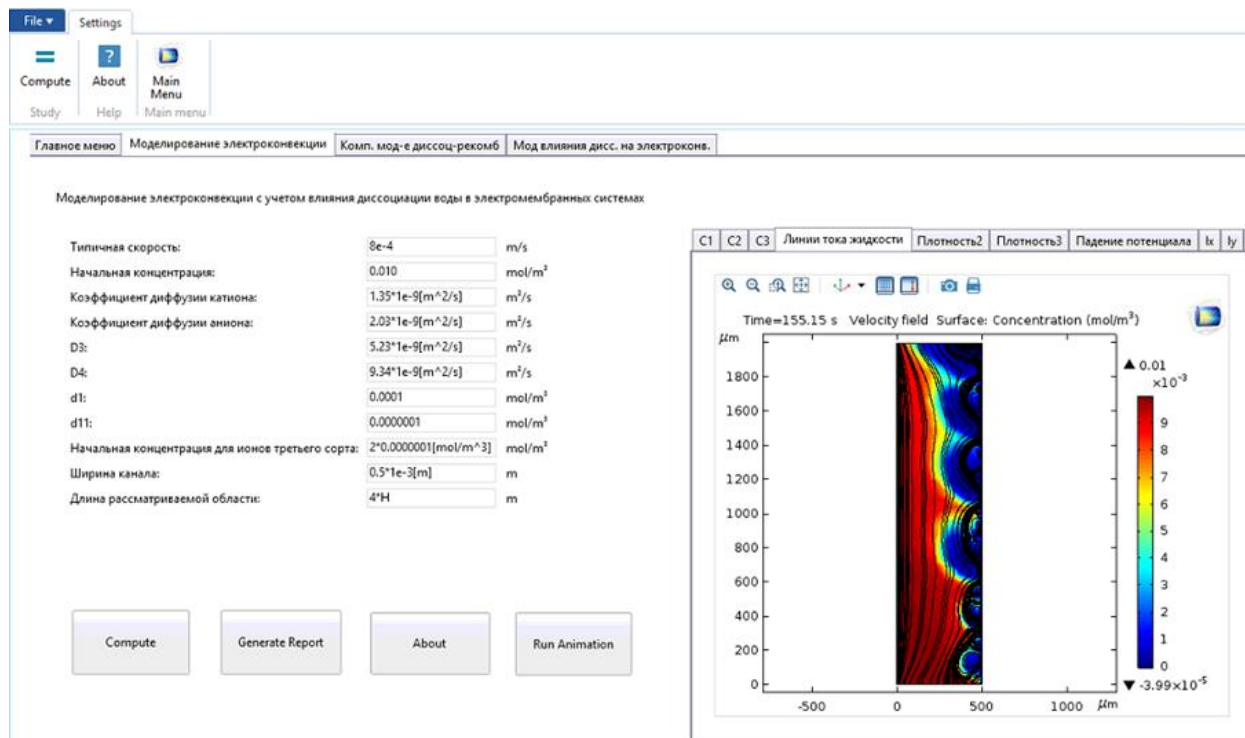


Figure 1. Window of the created application with the "electroconvection Simulation" tab open».

Software complex "Deep learning for CVC 0.1" (see Figure 1), contain databases and knowledge base theoretical and experimental current-voltage characteristics for deep machine learning allows you to highlight specific areas of the graphs of CVC. For example, a parcel beginning of electroconvection [2, 3] at cation-exchange membrane (CEM), the beginning of electroconvective from the anion-exchange membrane (AEM), the phase of the beginning of the interaction electroconvective vortices at the CEM and AEM and others. In these areas, the software package allows you to perform Fourier and Wavelet analyses, identify the trend, subtract the CVC trend from the data, calculate the oscillation amplitude, determine the main and accompanying oscillation frequencies, use the results to record the "restored" CVC and compare it with the real one, find the dependence of the CVC on the parameters of the problem with the approximation condition. In addition, the created software package allows you to calculate the critical values of currents, Hurst indicators for each section of the CVC and Lyapunov indicators, associated frequencies, oscillation amplitudes, and tilt angles of CVC in different sections on graphs of CVC.

\*Corresponding author. E-mail: [urtenovmax@mail.ru](mailto:urtenovmax@mail.ru).

The work is supported by the RFBR in the framework of the scientific project 19-08-00252 A " Theoretical and experimental study of current-voltage characteristics of electromembrane systems».

### References

- [1] Nikonenko, V.V., Mareev, S.A., Pis'menskaya, N.D. et al. Effect of electroconvection and its use in intensifying the mass transfer in electrodialysis (Review). *Russ J Electrochem.* 53, 1122–1144, 2017.
- [2] Nikonenko V.V., Kovalenko A.V., Urtenov M.K., Pismenskaya N.D., Han J., Sistas P., Pourcelly G. Desalination at overlimiting currents: state-of-the-art and perspectives. *Desalination.* 342, 85-106, 2014.
- [3] Urtenov M.K., Uzdenova A.M., Kovalenko A.V., Nikonenko V.V., Pismenskaya N.D., Vasil'eva V.I., Sistas P., Pourcelly G. Basic mathematical model of overlimiting transfer enhanced by electroconvection in flow-through electrodialysis membrane cells. *Journal of Membrane Science.* 447, 190-202, 2013.

## ON THE PECULIARITIES OF SIMULATED FLOWS IN SPHERICAL CELLS

Leonid Ostrer, Daria Khanukaeva\*

*Department of Higher Mathematics, Gubkin Russian State University of Oil and Gas, Moscow, Russia*

**Summary** The solution of the flow problem in the framework of the cell model is analysed. A universal property of the solution which consists in the formation of standing waves is demonstrated, analysed and interpreted.

### THE SIMPLE CELL MODEL

The hydrodynamic aspects of filtration flows in membranes representing porous structures are successfully modeled in the framework of the Happel-Brenner cell model technique [1]. By the idea of this method, a porous medium is replaced with a conglomerate of particles, each being encapsulated in a hypothetical cell. The interaction of particles with each other and with the flow is accounted for with the help of the appropriate boundary conditions on the cell surface.

We consider the classical simple cell consisting of a solid spherical core and a concentric liquid layer. The non-dimensional units are introduced in such a way that the solid core has unity radius and the outer liquid surface has a non-dimensional radius  $m$  ( $m > 1$ ). The direction of uniform flow velocity vector  $\mathbf{U}$  corresponds to  $\theta = 0$  of the spherical coordinate system  $(r, \theta, \varphi)$  ( $0 \leq \theta \leq \pi$ ,  $0 \leq \varphi < 2\pi$ ). Filtration velocity  $\mathbf{v}(r, \theta)$  related to the magnitude of  $\mathbf{U}$  is small enough to use the Stokes approach in the following form of the governing equations:

$$\begin{aligned}\nabla \cdot \mathbf{v} &= 0, \\ \mu \Delta \mathbf{v} &= \nabla P,\end{aligned}$$

where  $P$  is the pressure, and  $\mu$  is the dynamic viscosity coefficient of the filtrate.

Due to the symmetry of the flow, one can find the solution of this system using the method of the separation of variables and present it in the form  $\mathbf{v}(r, \theta) = \{u(r) \cos \theta; v(r) \sin \theta; 0\}$ ,  $P(r, \theta) = p(r) \cos \theta$ .

The classical statement of the boundary value problem (BVP) for the considered system of equations includes the no-slip conditions on the solid surface:  $u(1) = 0$ ,  $v(1) = 0$ , the continuity condition for the velocity normal component at the outer cell surface  $u(m) = 1$ , and one of the alternative conditions at  $r = m$ . In fact, all of the mentioned alternative conditions deal with the value of  $v(m)$  in this or that manner. The solutions of various BVPs are known for different types of cells. In the present study, we focus on general properties of these solutions and consider them using a simple solid-liquid cell.

### THE REMARKS ON STANDING WAVES IN A SPHERICAL CELL

It was proved in [2] the existence of two spheres (of radius  $r_0$  and  $r_1$ ) in the liquid layer of the cell, such that the value of the tangential velocity component  $v(r_0)$  does not depend on the boundary value of  $v(m)$ , and  $v(r_1)$  does not depend on the value of  $v(1)$ . At the same time, the normal velocity  $u(r)$  does not possess such properties (see Figure 1 and Figure 2).

#### *Meridian waves*

When  $\theta$  varies from 0 to  $2\pi$  the components of the velocity vector  $\mathbf{v}(r, \theta) = \{u(r) \cos \theta; v(r) \sin \theta; 0\}$  draw, correspondingly, sinusoidal waves  $v_r(r, \theta) = u(r) \cos \theta$ ,  $v_\theta(r, \theta) = v(r) \sin \theta$  on any meridian circle  $r = \text{const}$ ,  $\varphi = \text{const}$ . The phase shift between these waves is  $\pi/2$ . If the boundary conditions change, for example, occasionally or as a result of an external flow disturbance the amplitudes of these waves,  $u(r)$  and  $v(r)$  vary in time. The waves begin "to breathe", and two classical standing waves appear. The nodes of these waves are located in points  $\theta = \pm\pi/2$  for  $v_r(r, \theta)$  and in points  $\theta = 0; \pi$  for  $v_\theta(r, \theta)$ . On a sphere  $r = \text{const}$ ,  $0 \leq \varphi < 2\pi$ , one obtains two annulus standing waves in the velocity space. The amplitudes of these waves,  $u(r)$  and  $v(r)$  depend on the sphere radius.

The geometric interpretation of meridian waves in velocity space can be the following. The coordinates of velocity vector  $\mathbf{v}(r, \theta)$  satisfy the equation  $\frac{v_r^2}{u^2(r)} + \frac{v_\theta^2}{v^2(r)} = 1$ . It means that for any fixed  $r$  and  $\varphi$  the variation of  $\theta$  from 0 to  $2\pi$

results in the following motion of the end of velocity vector: it moves in ellipse which rolls on meridian circle. So, one obtains a generalized epicycloid as the hodograph. The perturbations of the boundary conditions lead to the variation of the ellipse semi-axes. The epicycloid "breathes" and forms a standing wave. A standing annulus wave can be seen on any sphere in the liquid layer of the cell, its amplitude being dependent on the sphere radius.

---

\*Corresponding author. E-mail: khanuk@yandex.ru.

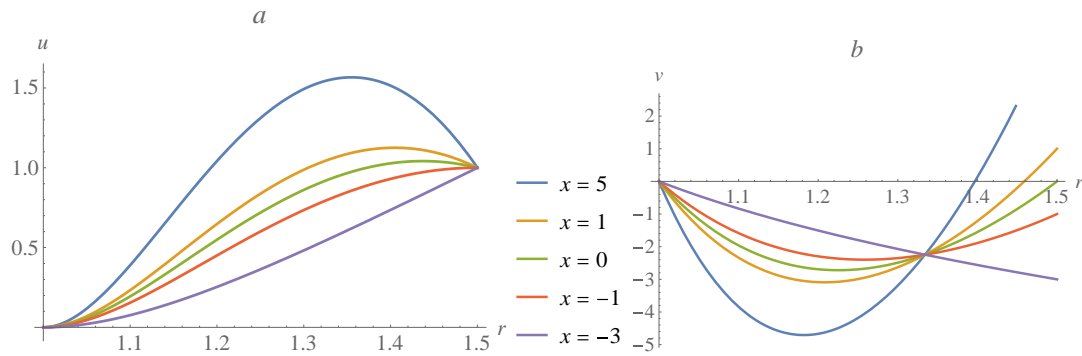


Figure 1. (a) Radial velocity component,  $u(r)$ ; (b) tangential velocity component,  $v(r)$  for BVPs differed by condition  $v(m) = x$ ,  $m = 1.5$

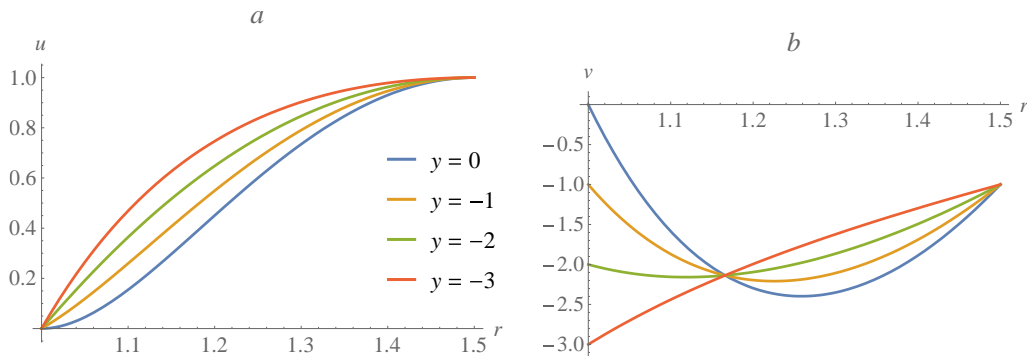


Figure 2. (a) Radial velocity component,  $u(r)$ ; (b) tangential velocity component,  $v(r)$  for BVPs differed by condition  $v(1) = y$ ,  $m = 1.5$

**Radial waves**

The properties of  $v(r)$  demonstrated in Figures 1 and 2 are interesting to consider under the varying external conditions in the flow. The expression for  $v(r)$  is the sum of terms each of which is defined by its boundary condition  $u(1), v(1), u(m), v(m)$ . In order to evaluate the contribution of boundary condition  $v(m) = x$ , we set  $u(1) = u(m) = v(1) = 0$ . If  $v(m)$  varies in time under the action of external conditions a classical standing wave of tangential velocity appears in any section  $\theta = \text{const}, \varphi = \text{const}$ . The nodes of this radial wave lie in circles  $r = 1; r = r_0$ . For non-zero values of  $u(1), u(m), v(1)$  this wave superposes with the corresponding solutions shown in Figure 1. The spatial behavior of the tangential velocity component  $v_\theta(r, \theta)$  for any  $\varphi$  is a “breathing” annulus wave. An analogous peculiarity of the distribution of  $v(r)$  is observed when boundary condition  $v(1)$  varies in time. The nodes of the resulting wave appear in points  $r = r_1; r = m$  as it follows from Figure 2.

**CONCLUSION**

The universal properties of the solution obtained in the framework of the cell model for filtration flows are found and interpreted in this work. The standing waves of the flow velocity component have invariant nodes and amplitudes depending on the boundary conditions. This universal property can be used in modelling of non-stationary flows, despite it was obtained for a stationary solution.

**References**

[1] Happel J., Brenner H. Low Reynolds number hydrodynamics. Martinus Nijhoff Publishers, The Hague 1983.  
 [2] Khanukaeva D.Yu., Ostrer L.A. On the boundary conditions in the Stokesian flows. *Theoretical and Computational Fluid Dynamics* DOI 10.1007/s00162-020-00552-w.

## PRODUCTION OF CHEAP PHOSPHORUS-AMMONIUM FERTILIZERS USING ELECTRODIALYSIS. PROBLEMS AND SOLUTIONS

Natalia Pismenskaya<sup>\*1</sup>, Olesya Rybalkina<sup>1</sup>, Kseniia Tsygurina<sup>1</sup>, Ekaterina Melnikova<sup>1</sup>, Mikhail Sharafan<sup>1</sup>, Sergey Mikhaylin<sup>2</sup>, Laurent Bazinet<sup>2</sup>

<sup>1</sup>Membrane Institute, Kuban State University, Krasnodar, Russia

<sup>2</sup>Institute of Nutrition and Functional Foods (INAF), Dairy Research Center (STELA), Laboratory of Food Processing and Electro-Membrane Processes (LTAPEM), Food Science Department, Université Laval, Québec, QC, Canada

**Summary** Mathematical modelling helps to identify the mechanisms of transfer of ampholytes (anions of phosphoric acid, ammonium cations, etc.), the electric charge of which depends on the  $\phi$  of the medium, and also to interpret experimental data that differ significantly from those known for strong electrolytes.

### THEORETICAL AND EXPERIMENTAL RESULTS

The rapid degradation of ecosystems requires the development of “green” technologies to prevent the release of harmful substances into the environment and to extract valuable components. Such technologies for producing cheap phosphorus-ammonium fertilizers from livestock and municipal wastes were proposed as combinations of biochemical and membrane methods. Amongst them, electrodialysis (ED) allows changing the pH value of the processed media without reagents and thereby controls the electric charge of the target components. The main ED problems are high energy consumption and fouling.

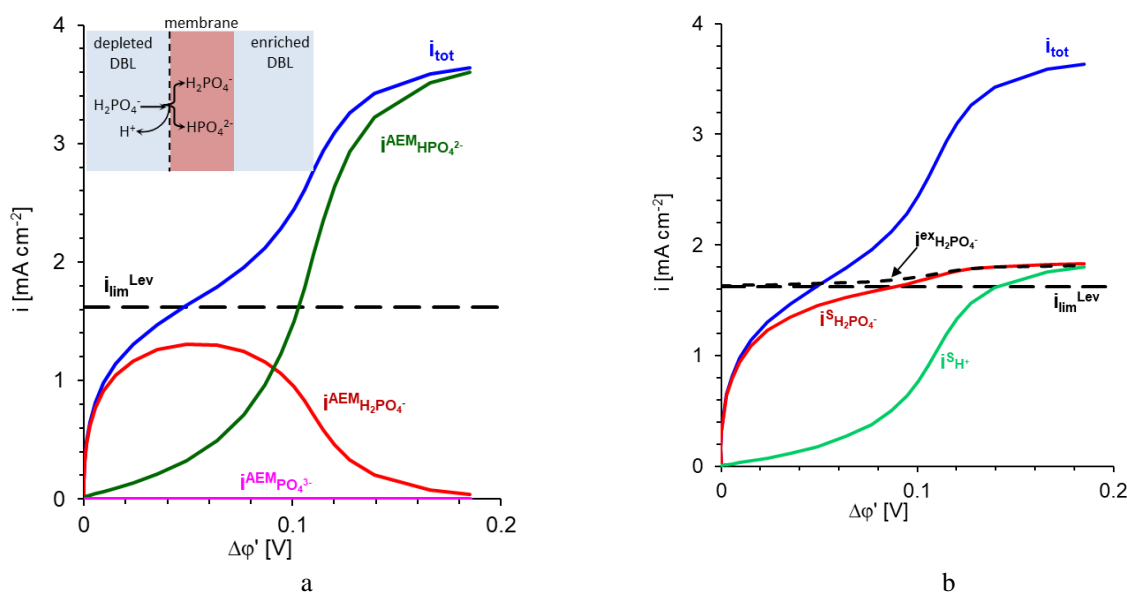


Figure 1. Theoretical total current density ( $i_{tot}$ ) and partial currents of the  $H_2PO_4^-$  ( $i_{H_2PO_4^-}^{AEM}$ ) and  $HPO_4^{2-}$  ( $i_{HPO_4^{2-}}^{AEM}$ ) ions in an AMX membrane (a) as well as the partial currents of  $H_2PO_4^-$  ( $i_{H_2PO_4^-}^s$ ) and  $H^+$  ( $i_{H^+}^s$ ) ions in the depleted solution at the membrane surface (b) as functions of the corrected potential drop. Solid lines are calculated using model [1]. Dashed lines show the limiting current  $i_{lim}^{Lev}$  calculated using the Leveque equation, [2], and the exaltation current,  $i_{H_2PO_4^-}^{ex}$  [3]. “I” and “II” show the first and second inclined plateaus, respectively.

Using mathematical modelling and different experimental techniques, we investigated the mechanisms of mass transfer of ammonium cations and phosphoric acid anions in electrodialysis. It has been established that the specificity of the transport of these molecules (ampholytes) in comparison with strong electrolytes lies in the fact that they enter into proton-transfer reactions with water and with each other. The products of these reactions are protons and hydroxyl ions that are excluded from the anion-exchange (AEM) and cation-exchange (CEM) membranes as co-ions. As a result, the pH of the internal solution is 2-4 units higher (in AEMs) or lower (in CEMs) in comparison with the external solution. Hence, concentration polarization caused by the application of an electric field increases the pH difference between the internal and external membrane solutions. These phenomena become a “trigger” for a chain of phenomena reducing the ED performances: increase in the “parasitic” generation of protons and hydroxyl ions at the membrane/solution boundaries (Figure 1), enhance the unwanted diffusion of ammonium cations through AEM, which causes an increase in the flux of

\*Corresponding author. E-mail: n\_pismen@mail.ru

doubly charged anions of orthophosphoric acid at a given value of the reduced potential drop (Figure 2), suppression of electroconvection, and others.

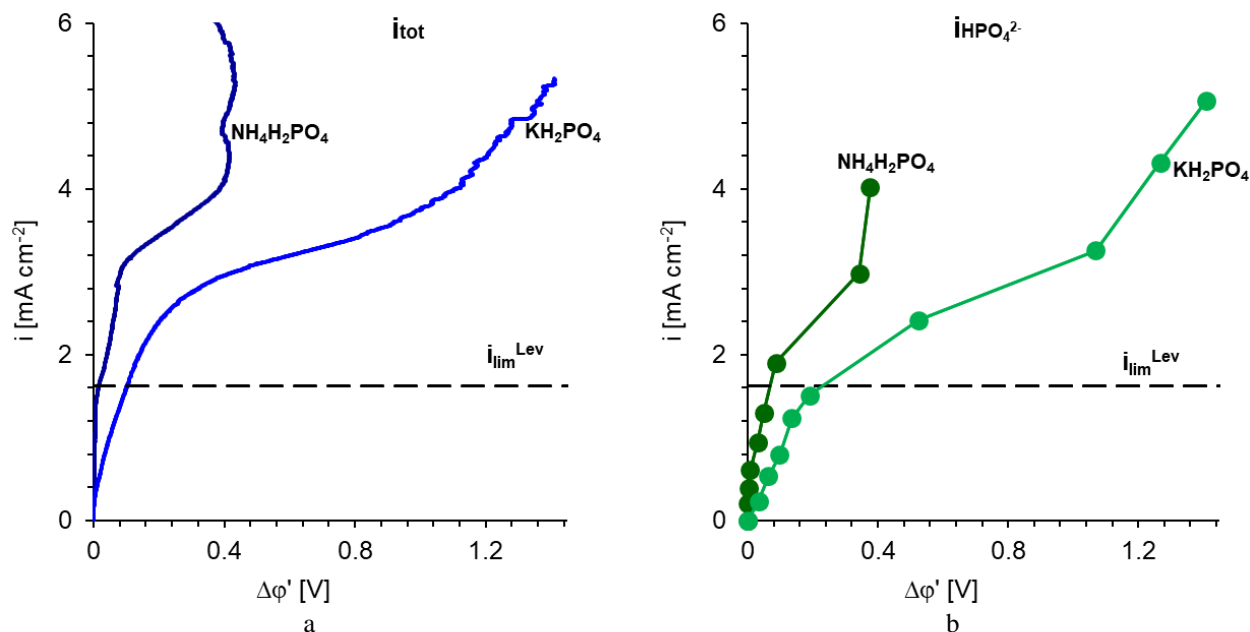


Figure 2. Experimental total current densities (a) and partial currents of  $\text{HPO}_4^{2-}$  ions (b) in the AMX membrane as functions of the corrected potential drop. Data were obtained in 0.02 eq / L solutions of  $\text{KH}_2\text{PO}_4$  and  $\text{NH}_4\text{H}_2\text{PO}_4$ .

## CONCLUSIONS

Understanding the origin of these phenomena allows optimization of current regimes, in particular, the application of pulsed electric fields to increase current efficiency, mass transfer and reduce fouling during ED extraction of ammonium cations and phosphates from liquid media.

We thank the Kuban Scientific Foundation grant MFI-20.1/128 (Natalia Pismenskaya) and NSERC grant SD RGPIN-2018-04128 (Laurent Bazinet) for financial support.

## References

- [1] Belashova E.D., Pismenskaya N.D., Nikonenko V.V., Sizat P., Pourcelly G. Current-voltage characteristic of anion-exchange membrane in monosodium phosphate solution. Modelling and experiment. *J. Membr. Sci.* 542, 177–185, 2017.
- [2] Newman J.S. *Electrochemical Systems*, New York, Prentice Hall, Englewood Cliffs 1973.
- [3] Melnikova E.D., Pismenskaya N.D., Bazinet L., Mikhaylin S., Nikonenko V.V. Effect of ampholyte nature on current-voltage characteristic of anion-exchange membrane. *Electrochim. Acta* 285, 185–191, 2018.

## RECOVERY MTBE FROM WATER USING HIGH SELECTIVE POLYALKYLMETHYLSILOXANE COMPOSITE MEMBRANES BY PERVAPORATION

Ivan Podtynnikov\*, Evgenia Grushevenko, Ilya Borisov, Olga Scharova  
A.V. Topchiev Institute of Petrochemical Synthesis RAS, Moscow, Russia

**Summary** For the first time, the effect of the side-chain in polyalkylmethylsiloxane towards pervaporative removal of MTBE from water was studied. Enhancement of separation factor during the pervaporation of 1 wt.% MTBE solution in water through the dense film (40–50  $\mu\text{m}$ ) can be achieved by substitution of a methyl group (separation factor 111) for heptyl (161), octyl (169) or decyl (180) one in polyalkylmethylsiloxane. Composite membrane with the selective layer ( $\sim 8 \mu\text{m}$ ) made of polydecylmethylsiloxane on top of microfiltration support demonstrated separation factor (SF) of 310, which was 72% greater than for the dense film (180). A high SF together with an overall flux of  $0.82 \text{ kg}\cdot\text{m}^{-2}\cdot\text{h}^{-1}$  allowed this composite membrane to outperform the commercial composite membranes. The feed flow velocity should be gradually increased from  $5 \text{ cm}\cdot\text{s}^{-1}$  for an initial solution (1 wt.% of MTBE in water) to  $13 \text{ cm}\cdot\text{s}^{-1}$  for a depleted solution (0.2 wt.% of MTBE in water) to overcome the concentration polarization phenomena in case of composite membrane M10/MFFK ( $T_{\text{exp}} = 50 \text{ }^\circ\text{C}$ ).

Methyl tert-butyl ether (MTBE) is widely used antiknock additive in fuel. From over hand MTBE is the second most frequently detected compound in coastal and groundwater [1].

A promising method for water treatment is membrane separation, in particular, the pervaporation process. The advantages of this method include the absence of reagents, continuous and mild conditions of the separation process [2]. The most common material for hydrophobic pervaporation is polydimethylsiloxane (PDMS). It has the highest permeability among siloxane rubbers, but its selectivity for organic components is not sufficient due to high water fluxes. The promising way to increase selectivity is the introduction of hydrophobic substituents into the main and side-chain of the polymer [3].

However, the use of membranes with increased selectivity and permeability for the separation of MTBE from dilute solutions is inevitably accompanied by an increase in the negative contribution of the “concentration polarization” effect [4].

In this work we concentrate on a systematic study of the influence of the length of the side groups in substituted polymethylsiloxane on pervaporation properties of membranes obtained on their basis and investigate the effect on concentration polarization. The objects of investigation are dense membranes based on polymethylsiloxanes with different hydrocarbon substituents in the side chain:  $\text{C}_1$  – M1,  $\text{C}_7$  – M7,  $\text{C}_8$  – M8,  $\text{C}_{10}$  – M10; and composite membrane M10/MFFK. Pervaporation experiments were carried out in a vacuum mode. The detailed description of the pervaporation experiments can be found elsewhere [5]. Results of pervaporation experiments are presented in figure 1A.

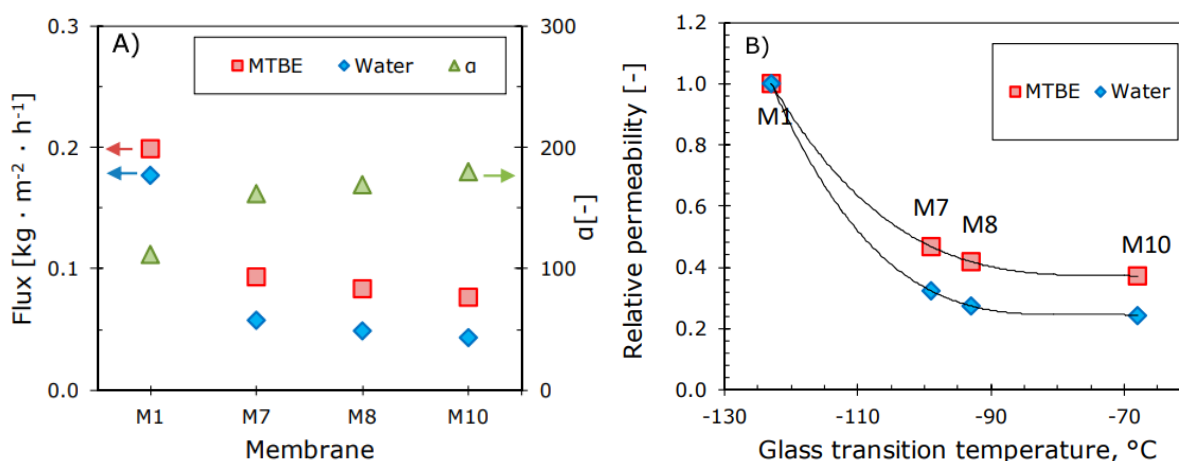


Figure 1. A) The dependences of the partial fluxes of MTBE and water and the MTBE/water separation factor on the side - chain length for the studied polyalkylmethylsiloxane membranes. The membranes thickness was 50 microns.  $T = 30 \text{ }^\circ\text{C}$ , 1% wt. MTBE in water. B) The dependences of the relative permeabilities of MTBE and water in polyalkylmethylsiloxanes on their glass transition temperature (relative to the corresponding values for M1).

It is evident that with an increase in the length of the side-chain substituent, the partial fluxes of the components decrease, while the separation factor increases from  $\sim 110$  to 180 for M10. To explain these phenomena, Figure 1B shows the dependences of the reduced pervaporation parameters (relative to the corresponding values for M1 membrane) on the glass transition temperature of the investigated polymers. Membrane permeability reduces several times with an increase in the glass transition temperature of the polymer. The MTBE permeability coefficient in going from M1 to M10 gradually decreases by 62%, while in water it decreases by 76%. This leads to a gain in the selectivity of the polymer, due to an increase in its hydrophobicity. The M10/MFFK composite membrane has high values of permeate flux ( $0.82 \text{ kg m}^{-2} \text{ h}^{-1}$ ) and separation factor (310) that exceed the characteristics of dense M10 membrane. This increase in selectivity can be

\*Corresponding author. E-mail: podtynnikov@ips.ac.ru

caused by the partial intrusion of the polymer of the selective layer into the upper layer of the porous support resulted in its restricted swelling.

On this composite membrane, experiments were carried out to study the effect of concentration polarization phenomena, results are presented in figure 2.

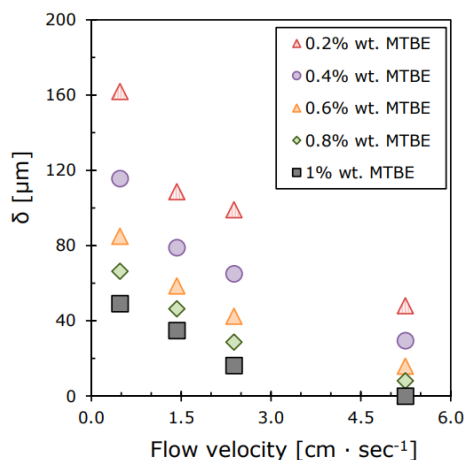


Figure 2. The dependences of the boundary layer thickness on the feed flow velocity at various MTBE concentrations.

In Figure 2 it can be seen that the boundary layer thickness drops sharply when the feed flow velocity rises from 0.5 to 2.0  $\text{cm}\cdot\text{s}^{-1}$ . This indicates a change in the hydrodynamic regime in the membrane module. The boundary layer thickness approaches zero at the feed flow velocity of 5.2  $\text{cm}\cdot\text{s}^{-1}$  and MTBE concentration 1.0 wt%. This indicates the absence of diffusion difficulties in the liquid phase. However, at lower MTBE concentrations in the solution, the role of concentration polarization is significant for the separation process. It has been shown that this problem for the given concentration range of MTBE can be solved by increasing the flow velocity. For example, extrapolating the value of boundary layer thickness to 0 for a 0.2 wt% MTBE solution indicates the disappearance of the diffusion hindrances at the feed flow velocity of 13  $\text{cm}\cdot\text{s}^{-1}$ . This method allows optimization of the hydrodynamic regime of pervaporation in order to achieve maximum separation selectivity at minimum cost for the feed solution pumping. It is essential to ensure the required removal rate in one pass and to reduce the cost of the pumping equipment.

## CONCLUSIONS

The effect of the length of a hydrocarbon side-chain on the transport properties of polyalkylsiloxanes in the pervaporation of MTBE-water solutions has been investigated for the first time. It was shown that the increase in the length of the alkyl side-chain from C1 up to C10 allowed to increase MTBE/water separation factor from 111 (PDMS) to 180 (PDecMS) during the pervaporation of 1 wt% MTBE solution in water through the dense film (40–50  $\mu\text{m}$ ). It is interesting to notice that the composite membrane with the selective layer made of polydecylmethylsiloxane ( $\sim 8 \mu\text{m}$ ) on top of a microfiltration support (MFFK membrane) demonstrated an MTBE/water separation factor of 310, which was 72% greater than for the dense film (180). Such a dramatic increase in the separation performance can be attributed to partial penetration of silicone material into the porous structure of the support layer resulted in its restricted swelling. It has been shown that problem of concentration polarization phenomena for the given concentration range of MTBE can be solved by increasing the flow rate.

This research was funded by the Russian Science Foundation, grant number 17-79-20296.

## References

- [1] Levchuk, I., Bhatnagar, A., Sillanpaa, M. Overview of technologies for removal of methyl tert-butyl ether (MTBE) from water. *Sci. Total Environ.* 476, 415–433, 2014.
- [2] Liu, G., Wei, W., Jin, W. Pervaporation membranes for biobutanol production. *ACS Sustain. Chem. Eng.* 2, 546–560, 2014.
- [3] Grushevenko, E.A., Podtynnikov, I.A., Golubev, G.S., Volkov, V.V., Borisov, I.L. Polyheptylmethylsiloxane - A novel material for removal of oxygenates from water by pervaporation. *Pet. Chem.* 58, 941–948, 2018.
- [4] Borisov, I.L., Kujawska, A., Knozowska, K., Volkov, V.V., Kujawski, W. Influence of feed flow rate, temperature and feed concentration on concentration polarization effects during separation of water-methyl acetate solutions with high permeable hydrophobic pervaporation PDMS membrane. *J. Membr. Sci.* 564, 1–9, 2018.
- [5] Borisov, I., Podtynnikov, I., Grushevenko, E., Scharova, O., Anokhina, T., Makaev, S., Volkov, A.; Volkov, V. High Selective Composite Polyalkylmethylsiloxane Membranes for Pervaporative Removal of MTBE from Water: Effect of Polymer Side-chain. *Polymers.* 12(6), 1213, 2020.

## MEAN RESIDUAL LIFE AND ANALYSIS RELIABILITY INVESTIGATION OF ELECTRICAL SUBMERSIBLE PUMPS

Vladimir Rusev<sup>1</sup>, Aleksandr Skorikov<sup>\*1</sup>, and Emil Magafurov<sup>2</sup>

<sup>1</sup>*Department of Higher Mathematics, Gubkin University, Moscow, Russia*

<sup>2</sup>*Department of Field Development and Operation, Gubkin University, Moscow, Russia*

**Summary** In the paper it is suggested that the two - parameter Gnedenko-Weibull distribution of the object failures determines the working life model of the object. The mean residual time was assumed as a reasonable measure of reliability. For the Gnedenko-Weibull model, new representations of the mean residual are obtained. The considered examples of processing real operational data of pumps failures allow predicting the residual operating time of submersible equipment at the operational stage and can be effectively used to assess the resource parameters of the equipment.

Mean residual life (MRL)  $\mu(t) = M(T - t | T > t)$  refers to one of the oldest topics of statistical analysis, namely biometric functions. The beginning of research on this topic was the work of Edmond Halley [1], in which life tables were given and the concept of the average life expectancy was introduced for the first time. It is noted that mean residual life sums up the entire distribution of the remaining resource of time  $t$ , and the very popular in the reliability theory *failure rate* refers only to the risk of immediate failure at time moment  $t$ . It should be noted, however, that they are mathematically equivalent, since knowing one of them, you can determine the other.

The paper uses studies of the average residual operating time for the two - parameter Gnedenko-Weibull distribution [2,3]. In particular, an analytical representation  $\mu(t)$  via incomplete gamma functions  $\gamma(a, x)$ ,  $\Gamma(a, x)$  and the hypergeometric function of Kummer  ${}_1F_1(a; b; x)$  were presented. Calculations performed using the Wolfram Mathematica package for representations by means of  $\gamma(a, x)$ ,  ${}_1F_1(a; b; x)$  give an oscillation of values  $\mu(t)$ ; for representations  $\mu(t)$  through  $\Gamma(a, x)$  there is no oscillation of values (Figure 1).

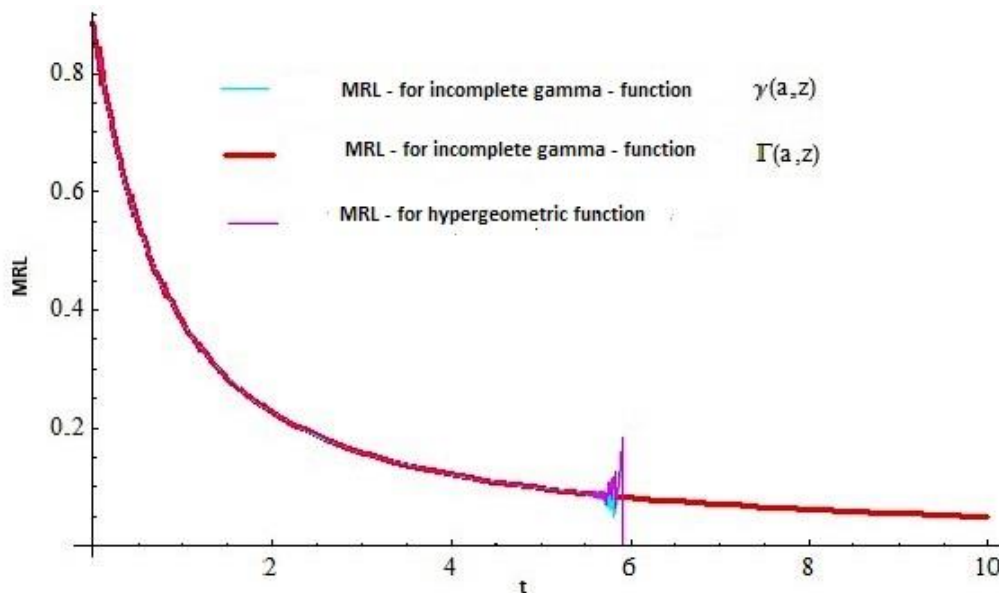


Figure 1. Weibull – Gnedenko MRL comparison for shape factor  $\beta = 2$

Obtained formulas for the average residual operating time for the Gnedenko-Weibull model and empirical mean residual operating time allow predicting the remaining operating time of submersible equipment at the operational stage and can be used to quite effectively assess the resource characteristics of equipment in order to optimize the functioning of the studied objects (Figure 2).

---

\*Corresponding author. E-mail: [skorikov.a@gubkin.ru](mailto:skorikov.a@gubkin.ru)

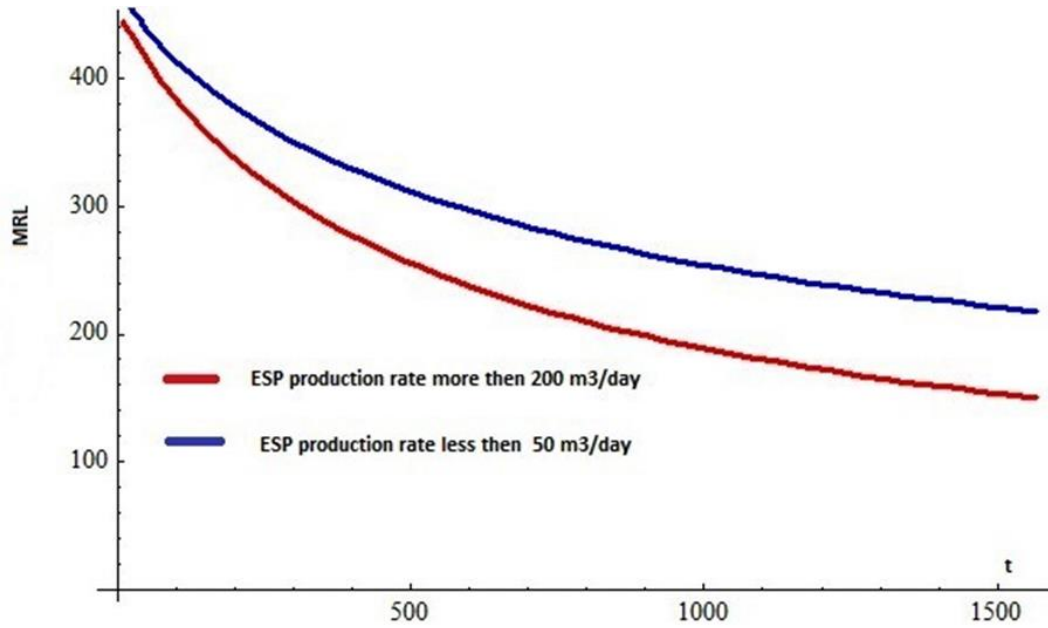


Figure 2. Weibull – Gnedenko MRL comparison between two ESP systems of different production rate

As an application of suggested MRL representations a new method for calculating the reliability of submersible pumps, based on the use of the average residual operating time, was proposed in [3].

### References

- [1] Halley, E. An Estimate of the Degrees of the Mortality of Mankind, Drawn from Curious Tables of the Births and Funerals at the City of Breslaw; With an Attempt to Ascertain the Price of Annuities upon Lives Phil. Trans. Royal Society of London, 1693. Vol.17, №7, p. 596-610.
- [2] Nassar, M.M., Eissa, F.H. On the Exponentiated Weibull Distribution. *Communications in Statistics - Theory and Methods*. 2003. Vol. 32, №7, p. 1317-1336.
- [3] Dengaev, A.V., Rusev, V.N., Skorikov, A.V. Mean residual life (MRL) of Gnedenko-Weibull distribution. Estimates of residual life time of submersible pump equipment *Proceedings of the Gubkin University*, 2020. №1/298, p.25 - 37.

## DEVELOPMENT OF ELECTROCONVECTION AT THE SURFACE OF AN ANION-EXCHANGE MEMBRANE IN CHLORIDE AND PHOSPHATE-CONTAINING SOLUTIONS

Olesya Rybalkina\*, Ilya Moroz, Natalia Pismenskaya  
Membrane Institute, Kuban State University, Krasnodar, Russia

**Summary** Differences were found in the formation of electroconvective vortex structures in the case of electro dialysis desalting of NaCl and NaH<sub>2</sub>PO<sub>4</sub> solutions. To understand the features of the development of electroconvection in membrane systems with ampholyte-containing solutions (NaH<sub>2</sub>PO<sub>4</sub>), it is necessary to develop a mathematical model that takes into account the participation of ampholytes in protolysis reactions inside the ion-exchange membrane, at the membrane / solution interface, and in adjacent diffusion layers.

### EXPERIMENTAL RESULTS

The total and partial current densities of anions in an anion-exchange AMX membrane, as well as visualization of electroconvective vortex structures at the AMX surface were made according to the methods described in [1]. The studies were carried out in underlimiting and overlimiting current modes. The limiting current  $i_{lim}^{Lev}$  is calculated using the Leveque equation [2].

It was found that the phosphorus total flux is limited by the H<sub>2</sub>PO<sub>4</sub><sup>-</sup> transport from the feed solution to the membrane surface, which is close to  $i_{lim}^{Lev}$ . A slight excess of the phosphorus flux over  $i_{lim}^{Lev}$  is observed, which is due to electroconvection and exaltation effects. However, our estimations show: the exaltation effect is too small to provide the experimentally observed H<sub>2</sub>PO<sub>4</sub><sup>-</sup> ions flux in the diffusion layer near the membrane surface. Thus, the main cause of the flux growth is electroconvection, which significantly increases the mass transfer in membrane systems with dilute solutions of strong electrolytes. Our experiments show that in the systems under study, in the case of NaCl solution, the first large vortex structures (about 150 μm in size) are visualized at the outlet of the channel under study, when  $i / i_{lim}^{Lev} = 1$  (Figure 1,2). The dimensions of the vortices increase and electroconvective structures gradually fill the entire space at the receiving surface of the membrane under study with growth current density (Figure 2). In the case of NaCl, the linear dimensions of individual clusters of electroconvective vortexes reach 230 μm at  $i / i_{lim}^{Lev} = 3$ .

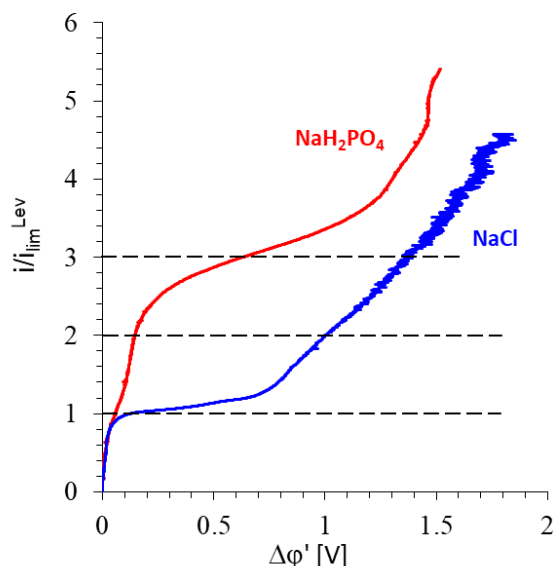


Figure 1. Current-voltage characteristics of an AMX membrane in 0.02 M NaCl and NaH<sub>2</sub>PO<sub>4</sub> solutions.

In the case of NaH<sub>2</sub>PO<sub>4</sub> solution, a dark zone forms at the surface of the anion exchange membrane, which is an indicator of a very low concentration of salt ions at  $i / i_{lim}^{Lev} = 1$  (Figure 2). However, any vortex structures are not visualized in this zone. Small perturbations of the near-surface solution become noticeable only when the theoretical limiting current is exceeded twice. Clusters of electroconvective vortices are recorded only at  $i / i_{lim}^{Lev} \geq 3$ . Moreover, these clusters are "attached" to a certain point of the membrane surface, while in the case of NaCl, they actively move along this surface in the direction of movement of the liquid pumped through the channel under study. The reason for reducing electroconvection in the case of NaH<sub>2</sub>PO<sub>4</sub> solution, apparently, is the high rate of H<sup>+</sup> ions generation at the same value of the  $i / i_{lim}^{Lev}$  ratio. Getting into the space charge region at the depleted membrane surface, protons cause a decrease in its

\*Corresponding author. E-mail: olesia93rus@mail.ru

density [3]. In the case of strong electrolyte solutions (NaCl), the water splitting occurs after reaching a certain threshold concentration of salt ions near the membrane surface. After overcoming this threshold, which is reached at a certain value of the potential drop, the  $H^+$  and  $OH^-$  ions are generated as a result of water splitting. This reaction is carried out with the participation of fixed groups at the membrane / solution interface [4,5]. In the case of  $NaH_2PO_4$  solution, the generation of  $H^+$  ions occurs in the non-threshold mode as a result of deprotonation of a part of  $H_2PO_4^-$  ions when they enter the membrane bulk. This process takes place as soon as an external electric field is applied to the membrane.

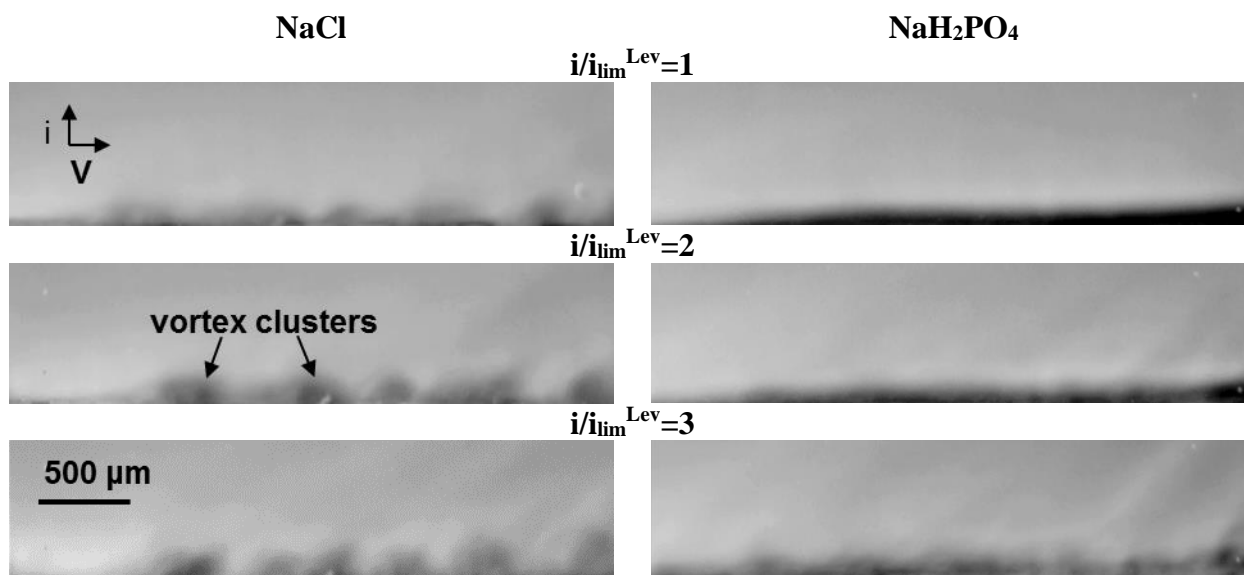


Figure 2. Visualization of electroconvective vortex structures at the surface of the AMX membrane in 0.02 M NaCl and  $NaH_2PO_4$  solutions, pumped through a channel formed by two anion-exchange membranes. The membrane under study is at the bottom. The linear flow velocity of the solution is  $V = 0.07$  mm/s.

## CONCLUSIONS

At present, electroconvection has been studied in detail theoretically only in relation to strong electrolytes (see for example review [6]). We show that in membrane systems with ampholyte-containing solutions (e.g.  $NaH_2PO_4$ ), the dissociation of ampholyte anions when entering the membrane essentially affects electroconvection. The  $H^+$  ions released during the dissociation bear the charge sign opposite to that of the extended space charge region (SCR). This reduces the charge density of the SCR, and as a consequence, the intensity of electroconvection. For better understanding of the features of the electroconvection phenomenon in such systems, proper mathematical modelling is needed.

The reported study was funded by Russian Foundation of Basic Research, project number 20-38-90054.

## References

- [1] Melnikova E.D., Pismenskaya N.D., Bazinet L., Mikhaylin S., Nikonenko V.V. Effect of ampholyte nature on current-voltage characteristic of anion-exchange membrane. *Electrochim. Acta*, 285, 185–191, 2018.
- [2] Newman J.S. *Electrochemical Systems*, New York, Prentice Hall, Englewood Cliffs 1973.
- [3] Mishchuk N.A. Concentration polarization of interface and non-linear electrokinetic phenomena. *Adv. Colloid. Interface Sci*, 160, 16–39, 2010.
- [4] Simons R. Strong electric field effects on proton transfer between membrane-bound amines and water. *Nature*, 280, 824–826, 1979.
- [5] Zabolotskii V.I., Shel'deshov N.V., Gnusin N.P. Dissociation of water molecules in systems with ion-exchange membranes. *Russ. Chem. Rev.*, 57, 801–80, 1988.
- [6] Nikonenko V.V., Mareev S.A., Pis'menskaya N.D., Uzdenova A.M., Kovalenko A.V., Urtenov M.K., Pourcelly, G. Effect of electroconvection and its use in intensifying the mass transfer in electrodialysis (Review), *Russ. J. Electrochem.*, 53 (10), 1122-1144, 2017.

## MODIFICATION OF ION-EXCHANGE MEMBRANES TO INCREASE THE SELECTIVITY OF COUNTERION TRANSFER

Veronika Sarapulova, Natalia Pismenskaya\*, Victor Nikonenko  
Membrane Institute, Kuban State University, Krasnodar, Russia

**Summary** One of the reasons for the decrease in the counterion permselectivity of ion-exchange membranes is the presence of extended micropores, which are localized at the boundaries of ion-exchange material and the filaments of the reinforcing fabric. This defect is amplified if the reinforcing filaments are protruded to the surface. In this case, the selectivity of the membranes can be increased by coating the surface with a dense ion-exchange film. The microheterogeneous model [1] was applied for tracking the membrane structural-kinetic parameters, which control the membrane permselectivity.

### SELECTIVITY OF ANION EXCHANGE MEMBRANES

The homogeneous CJMA-3, CJMA-6 and CJMA-7 anion exchange membranes (AEMs) are manufactured by Hefei Chemjoy Polymer Materials Co. Ltd. (Hefei, China). Their ion-exchange matrix contains polyvinylidene fluoride functionalized with quaternary ammonium groups. Side chains of the matrix are selfcrosslinking with aromatic crosslinking agents. These membranes are produced by the casting method and after are reinforced with polyester net by hot rolling (Figure 1). The values  $f_2$  and also the exchange capacity of the gel phase of swelling membranes ( $\bar{Q}$ ) were found from the concentration dependences of the conductivity of membranes in NaCl solutions (Figure 2a) using the microheterogeneous model [1].

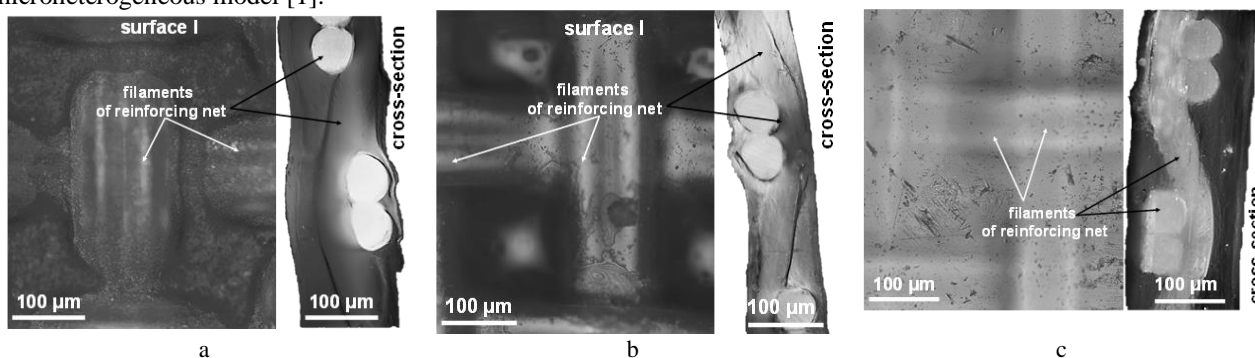


Figure 1. Optical images of surfaces and cross-sections of CJMA-3 (a), CJMA-6 (b) and CJMA-7 (c) membranes, the thickness of which is equal to:  $150 \pm 5$  (CJMA-3),  $120 \pm 3$  (CJMA-6) and  $175 \pm 10$  (CJMA-7)  $\mu\text{m}$

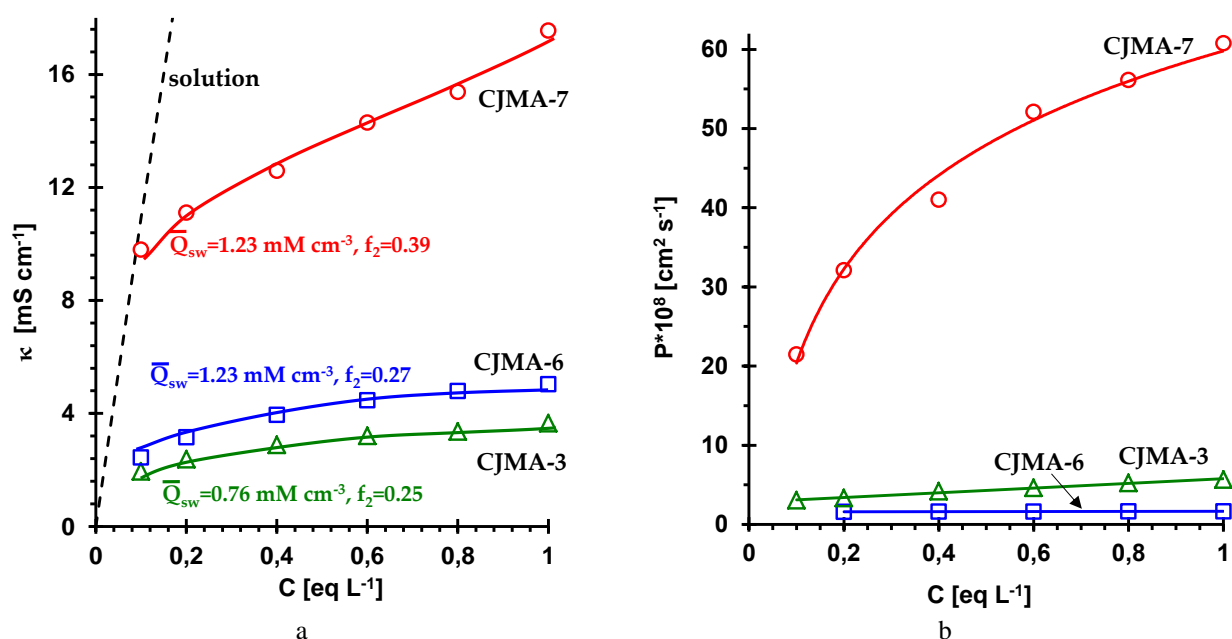


Figure 2. Concentration dependences of electrical conductivity (a) and integral coefficient of diffusion permeability (b) of studied membranes in NaCl solutions.

\*Corresponding author. E-mail: n\_pismen@mail.ru

Reinforcing net is displaced to one of the surfaces of the studied membranes (Figure 1). Apparently, not too rigid cross-linking of side chains, as well as extended macropores that are formed at the interface of the reinforcing net / ion-exchange material, are the reason for high values of the volume fraction of the intergel space ( $f_2$ ) of studied membranes, which do not exceed 0.1 for most known homogeneous AEMs that have another matrix. As predicted by the microheterogeneous model [1], the behavior of CJMA-3 and CJMA-6 membranes, which have similar  $f_2$ , is controlled by the values of the ion exchange capacity of the gel phase. An almost twofold excess of the ion exchange capacity CJMA-6 in comparison with CJMA-3 provides it a higher electrical conductivity (Figure 2a), lower diffusion permeability (Figure 2b) and the highest true transfer numbers of counterions (selectivity) (Figure 3). Very high  $f_2$  values of CJMA-7 predetermine a sharp increase in electrical conductivity (Figure 2a) and diffusion permeability (Figure 2b), as well as a sharp decrease in the true transfer numbers (Figure 3) of the membrane with an increase in solution concentration.

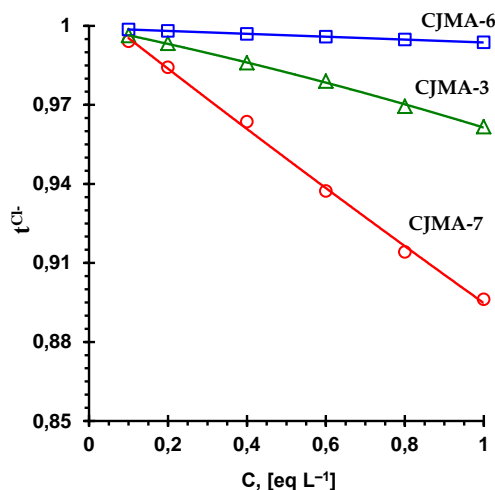


Figure 3. Concentration dependences of counterion transport numbers ( $t^{Cl-}$ ) of studied membranes in NaCl solutions.

### INCREASE IN CJMA-7 SELECTIVITY BY SURFACE MODIFICATION

An analysis of optical images allows us to conclude that some of the filaments of the reinforcing net protrude to the surface, facilitating the access of the external solution into the membrane. This defect, which is one of the reasons for the decrease in CJMA-7 selectivity, can be easily eliminated by covering the membrane surface with a highly crosslinked ion-exchange film. For example, in the case of using a fluoropolymer-based modifier, the density of the film increases with the temperature at which the sample is held. The higher the temperature, the more noticeably the diffusion permeability of the modified sample reduces and the co-ion transport number decreases (Table.1). The application of the microheterogeneous membrane to the non-modified and modified CJMA-7 membrane has shown that the main parameter, which was changed after the modification, was the volume fraction of the intergel spaces  $f_2$ . The effective value of this parameter decreased from 0.39 to 0.25. The value of this parameter in the modifying film was 0.12 and 0.06, when applying 25 °C and 80 °C, respectively.

Table.1. Influence of the temperature at which the modified sample CJMA-7 is kept on the diffusion permeability ( $P$ ) and the co-ion transport number ( $t^{Na+}$ ) in the membrane

Temperature, °C	$100*(P_{CJMA-7} - P_{CJMA-7M}) / P_{CJMA-7}$ , %	$100*(t^{Na+}_{CJMA-7} - t^{Na+}_{CJMA-7M}) / t^{Na+}_{CJMA-7}$ , %
25	64	11
80	72	40

### CONCLUSIONS

One of the reasons for the decrease in the selectivity of ion-exchange membranes is extended micropores, which are localized at the boundaries of ion-exchange material / the reinforcing net. This defect is amplified if the reinforcing filaments are protruded to the surface. In this case, the selectivity of the membranes can be increased by coating the surface with a dense ion-exchange film.

The work is supported by Russian Foundation of Basic Research, project number 20-08-00933.

### References

- [1] Zabolotsky V.I., Nikonenko V.V. Effect of structural membrane inhomogeneity on transport properties. *J. Membr. Sci.* 79, 181–198, 1993.

## INFLUENCE OF POLYANILINE ON WATER TRANSPORT IN PERFLUORINATED ION EXCHANGE MEMBRANES

Svetlana Shkirskaia\*, Natalia Kononenko

*Physical Chemistry Department, Kuban State University, Krasnodar, Russia*

It is well known that the concentration process by electro dialysis is influenced by a variety of technological and physicochemical factors. Physicochemical factors include properties of the membranes forming the membrane packet. It is established that the dominant influence on salt solution concentration have the electroosmotic and osmotic flux while the diffusion component of the salt flux has a negligibly small influence. One of the promising methods for increasing of work of the electro dialyzer–concentrator is the development of a new type of membrane. Such membranes must be characterized by low osmotic and electroosmotic permeability for decreasing the volume of water entering the concentration chambers.

Therefore, the purpose of this work is to evaluate changes osmotic and electroosmotic flux in MF-4SK membrane and composite with polyaniline (PANI) based on it in NaCl solutions. The osmotic and electroosmotic fluxes coincide and as a result total water flux directs to concentration chamber during the electro dialysis process. This makes it possible to calculate the contribution of electroosmotic and osmotic mechanisms to the total water transport. It was established that the total water flux through cation-exchange membrane MF-4SK in NaCl solution while maintaining a constant concentration difference of 10 times (Figure 1a) does not change with increasing absolute values of concentrations (from 1/0.1 till 3/0.3). However, it was found that the contribution of osmotic and electroosmotic fluxes in the total water transport changed. It was shown that increasing concentration of salt solution leads to decrease of the electroosmotic flux contribution. This is due to a decrease of the water amount in the hydration shell of the Na<sup>+</sup>-ion with increasing concentration. It was found that the modified membrane MF-4SK/PANI reduces the total water flux by 3 times. It should be noted that the contribution of osmotic water flux is reduced more significantly – 5-6 times compared to the original membrane, while the electroosmotic transfer is reduced only 1.5 times (Figure 1b). This is due to the barrier effect of the polyaniline layer to the water transport through the composite membrane, as a result only water of close hydration is transported [1].

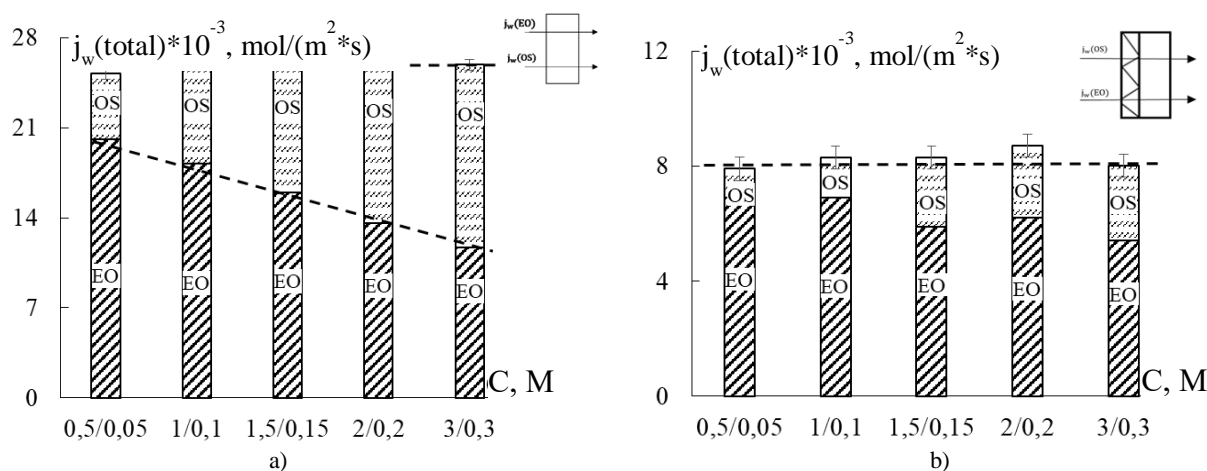


Figure 1. The total water flux through MF-4SK (a) and MF-4SK/PANI (b) membranes in NaCl solutions: OS and EO - the contribution of osmotic and electroosmotic mechanism of water transport correspondently.

### CONCLUSIONS

Thus, the contributions of electroosmotic and osmotic fluxes to the total water transport through individual membranes were first time experimentally determined. The decrease of osmotic flux through MF-4SK/PANI membrane is related to a reduce of the membrane water content, therefore the transport of free water through modified membrane essential decrease. The obtained experimental results will be used to verify various model approaches to the theoretical description of the ion and water transfer phenomena.

The work is supported by the Russian Foundation for Basic Research (project № 19-08-00925-a).

### References

- [1] Berezina N.P., Shkirskaia S.A., Kolechko M.V., Popova O.V., Senchikhin I.N., Roldugin V.I. Barrier effects of polyaniline layer in surface modified MF-4SK/Polyaniline membranes. *Russ. J. Electrochem.* 47, 995-1005, 2011.

\*Corresponding author. E-mail: shkirskaia@mail.ru

## DEPENDENCE OF CURRENT-VOLTAGE CHARACTERISTIC OF NON-STATIONARY TRANSPORT OF 1:1 SALT IONS IN A CROSS-SECTION OF DESALINATION CHANNEL ON A POTENTIAL DIFFERENCE SWEEP RATE

Inna Shkorkina<sup>1</sup>, Natalia Chubyr<sup>2</sup>, Vitaly Gudza<sup>1</sup> and Makhmet Urtenov<sup>\*1</sup>

<sup>1</sup>Department of Applied Mathematics, Kuban State University, Krasnodar, Russia

<sup>2</sup>Department of Applied Mathematics, Kuban State Technological University, Krasnodar, Russia

**Summary** An effect of a potential difference sweep rate on the current-voltage characteristic (CVC) of non-stationary 1:1 salt ion transport in the cross-section of the desalination channel is studied, taking into account the dissociation/recombination reaction of water molecules. The fundamental regularities of changes in a CVC are determined. It is shown that for small values of the sweep rate, the CVC has a classical form. This is due to the fact that at such values, a quasi-stationary mode occurs, characterized by an approximate equality of electromigration and diffusion currents. At "large" values of the sweep rate, the electromigration current initially increases, while the diffusion current practically does not change, resulting in a surge in the CVC. In the future, the electromigration current begins to decrease, and the diffusion current begins to grow, and a quasi-stationary mode is gradually established.

The CVC is one of the fundamental characteristics of the transfer process in membrane systems, which, moreover, is quite easy to determine experimentally [1]. For theoretical calculation of the CVC, it is necessary to use a mathematical model of the transfer process and a formula for calculating the CVC. The mathematical model used in this paper is described below. An integral average that is stable with respect to rounding errors is used as a formula for calculating the CVC.

### MATHEMATICAL MODEL

Non-stationary transfer of salt ions for 1:1 electrolyte in the cross section of the desalination channel, taking into account the spatial charge and the dissociation/recombination reaction, is described by a system of equations [2]:

$$\frac{\partial C_i}{\partial t} = -\frac{\partial j_i}{\partial x} + R_i \quad (1), \quad j_i = -z_i \frac{F}{RT} D_i C_i \frac{\partial \varphi}{\partial x} - D_i \frac{\partial C_i}{\partial x}, \quad i = 1, \dots, 4 \quad (2),$$

$$\frac{\partial^2 \varphi}{\partial x^2} = -\frac{F}{\varepsilon_r} \sum_{i=1}^4 z_i C_i \quad (3), \quad R_1 = R_2 = 0, \quad R_3 = R_4 = k_r (k_w - C_3 C_4) \quad (4), \quad I_c = F \sum_{i=1}^4 z_i j_i \quad (5).$$

Here (1) – material balance equations, (2) – Nernst-Planck equations for the flows of potassium ( $K^+$ ,  $i = 1$ ), chlorine ( $Cl^-$ ,  $i = 2$ ), hydrogen ( $H^+$ ,  $i = 3$ ) and hydroxyl ( $OH^-$ ,  $i = 4$ ),  $z_i$  – corresponding charge numbers, (3) – Poisson equation for the electric field potential, (4) – formulas describing the dissociation/recombination reaction of water molecules [3], (5) – current flow equation, which means that the current flowing through the cross-section of the desalination channel is determined by the flow of ions,  $\varepsilon_a$  – permittivity of the solution,  $F$  – Faraday number,  $R$  – universal gas constant,  $\varphi$  – potential,  $C_i$ ,  $j_i$ ,  $D_i$  – concentration, flow, diffusion coefficient of the  $i$ -th ion,  $I_c$  is the current density determined by the ion flow.

Let  $x = 0$  – correspond to the conditional interface «Anion-exchange membrane (AEM)/solution», and  $x = H$  – to the conditional interface «solution/cation-exchange membrane (CEM)». In the future, the ideal selectivity of ion-exchange membranes is assumed. Boundary conditions are set at points  $x = 0$  and  $x = H$ , where  $H$  is the cross-section width of the desalination channel. The values of ion concentrations passing through the membranes at these points are determined by the exchange capacities of the corresponding ion-exchange membranes. Theoretically, the exchange capacity of the membrane changes with time, but for a small period of time, this change can be ignored.

We assume that a potential difference  $\varphi_d(t)$  is set on the membrane, which increases linearly with time at a certain rate  $d$ . The current density flowing through the system,  $I_c(t)$  is a response to a given potential difference. Thus, the boundary conditions have the form:

$$\left( -\frac{F}{RT} C_1 D_1 \frac{\partial \varphi}{\partial x} - D_1 \frac{\partial C_1}{\partial x} \right) \Big|_{x=0} = 0, \quad C_2(t, 0) = C_{2a}, \quad \left( -\frac{F}{RT} C_3 D_3 \frac{\partial \varphi}{\partial x} - D_3 \frac{\partial C_3}{\partial x} \right) \Big|_{x=0} = j_{3a}, \quad \frac{\partial C_4(t, 0)}{\partial x} = 0,$$

$$C_1(t, H) = C_{1k}, \quad \left( \frac{F}{RT} C_2 D_2 \frac{\partial \varphi}{\partial x} - D_2 \frac{\partial C_2}{\partial x} \right) \Big|_{x=H} = 0, \quad \frac{\partial C_3(t, H)}{\partial x} = 0, \quad \left( \frac{F}{RT} C_4 D_4 \frac{\partial \varphi}{\partial x} - D_4 \frac{\partial C_4}{\partial x} \right) \Big|_{x=H} = j_{4k},$$

$$\varphi(t, 0) = \Delta_r \varphi = d \cdot t, \quad \varphi(t, H) = 0.$$

In the future, the non-catalytic dissociation/recombination reaction of water molecules is considered [4]. It is assumed that there is no injection of hydrogen and hydroxyl ions from the membrane surface:  $j_{3a} = j_{4k} = 0$ .

The initial conditions have the form:  $C_1(0, x) = C_2(0, x) = C_{10}(x) = C_{20}(x)$ ,  $C_3(0, x) = C_4(0, x) = 0$ ,  $\varphi(0, x) = 0$ .

\*Corresponding author. E-mail: [urtenovmax@mail.ru](mailto:urtenovmax@mail.ru).

## RESULTS

The numerical solution is obtained by the finite element method for a binary electrolyte solution  $KCl$ . Determine the

average current density [5]: 
$$I_{av}(t) = \frac{1}{H} \int_0^H I_c(t, x) dx$$

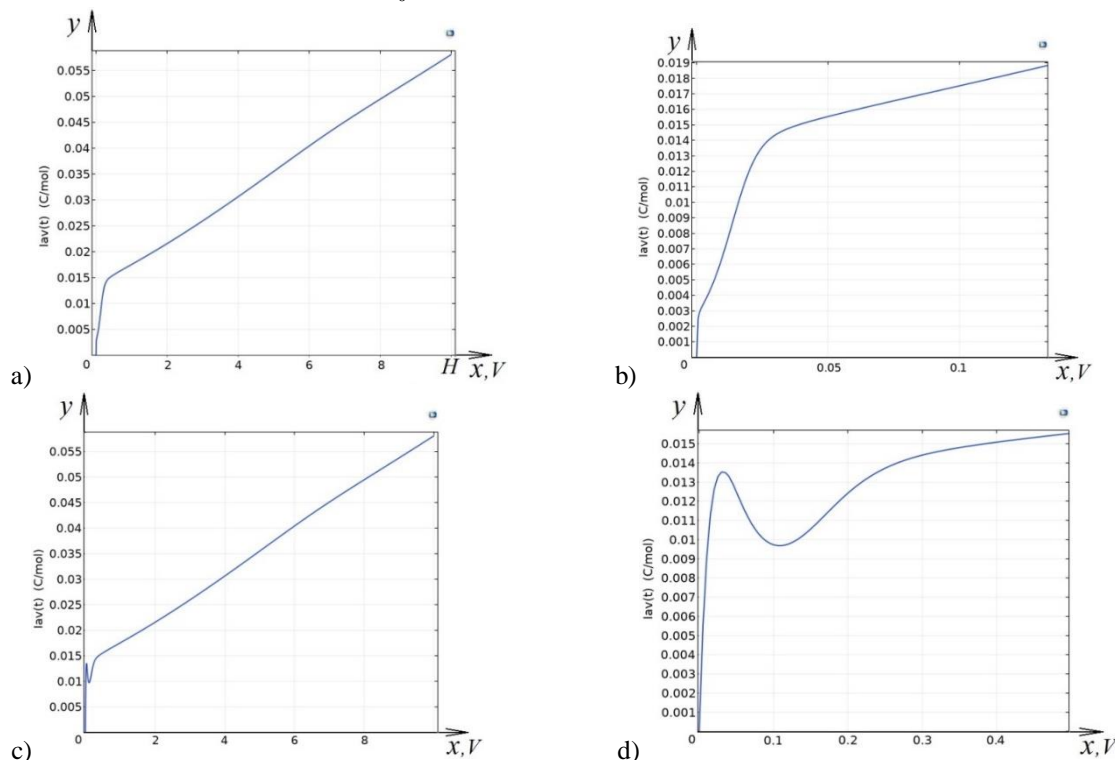


Figure 1. Graphs of the average current density calculated by the formula (6) for the solution  $KCl$ : a), c) general view, b), d) increase near zero. a), b) for  $d = 0.00001 \text{ V/s}$ ; C), d) – for  $d = 0.0001 \text{ V/s}$

Figures 1a), b) shows that when the sweep rate  $d = 10^{-5} \text{ V/s}$  CVC has a classic view, while  $d = 10^{-4} \text{ V/s}$  from figures 1c), d) shows that at the beginning when a potential difference of from  $0 \text{ V}$  and to about  $0.1 \text{ V}$  a «surge» of CVC. As calculations show, at first the transfer current is determined almost exclusively by salt ions. The local maximum in Figure 1d is that electromigration current grows in the beginning, and the diffusion does not change, then migration begins to decrease, as diffusion increases and gradually they become about the same. Further, the contribution of the current to the hydrogen and hydroxyl ions gradually increases, and therefore the CVC also increases almost linearly.

## CONCLUSIONS

The CVC of non-stationary 1:1 salt ion transport in the cross-section of the desalination channel is studied, taking into account the dissociation/recombination reaction of water molecules and the effect of the potential difference sweep rate over time on it. The fundamental regularities of changes in the CVC are determined, and the influence of electromigration and diffusion currents on the CVC over time is explained.

The work is supported by the Russian Foundation for Basic Research (project № 19-08-00252 A).

## References

- [1] Belashova E.D., Melnik N.A., Pismenskaya N.D., Shevtsova K.A., Nebavsky A.V., Lebedev, K.A. Overlimiting Mass Transfer Through Cation-Exchange Membranes Modified by Nafion Film and Carbon Nanotubes. *Electrochimica Acta*, 59, 412-423, 2012
- [2] Newman J. Electrochemistry systems. (Russ.: Ehlektrokhimicheskie sistemy), Publ.: Mir 463 p., 1977
- [3] Chubyr N.O., Kovalenko A.V., Urtenov M.Kh. Chislennyye i asimptoticheskie metody analiza perenosa 1:1 ehlektrolita v membrannykh sistemakh [Numerical and asymptotic methods for analyzing 1:1 electrolyte transfer in membrane systems]. Krasnodar, 2018, 106 p.
- [4] Kovalenko A.V. et al. Vliyaniye temperaturnykh ehffektov, svyazannykh s reaktsiei dissotsiatsii/rekombinatsii molekul vody i dzhoul'evym nagrevom rastvora na statsionarnyi perenos ionov soli v diffuzionnom sloe [Influence of temperature effects associated with the reaction of dissociation / recombination of water molecules and Joule heating on the stationary transfer transport in the diffusion layer]. *Ehkolozhicheskii vestnik nauchnykh tsentrov Chernomorskogo ehkonomicheskogo sotrudnichestva*. [Ecological Bulletin of Scientific Centers of the Black Sea Economic Cooperation] No.4, 67-84, 2018.
- [5] Urtenov M.Kh., Kovalenko A.V., Sukhinov A.I., Chubyr N.O., Gudza V.A. Model and numerical experiment for calculating the theoretical current-voltage characteristic in electro-membrane systems. IOP Conference Series: Materials Science and Engineering Collection of materials of the XV International Scientific - Technical Conference. Don State Technical University. 2019. p. 012030.

## A 2D MODEL OF ANODIC OXIDATION OF ORGANIC COMPOUNDS USING POROUS REACTIVE ELECTROCHEMICAL MEMBRANE

Ekaterina Skolotneva<sup>1</sup>, Clement Trelu<sup>2</sup>, Marc Cretin<sup>3</sup> and Semyon Mareev<sup>1</sup>

<sup>1</sup>Physical Chemistry Department, Kuban State University, Krasnodar, Russia

<sup>2</sup>Laboratoire Géomatériaux et Environnement (EA 4508), Université Gustave Eiffel, Paris, France

<sup>3</sup>Institut Européen des Membranes, IEM-UMR 5635, ENSCM, CNRS, Univ. Montpellier, Montpellier, France

**Summary** The effect of geometric parameters of reactive electrochemical membranes used in anodic oxidation of organic compounds on the process efficiency has been investigated by developing a 2D convection-diffusion model based on the Fick-Navier-Stokes equations. There is a good agreement in the calculated and experimental degradation rate of a model pollutant at different permeate fluxes and current densities. We theoretically find that the effectiveness of the process should be improved when decreasing the pore radius or/and increasing the porosity. The model highlights how convection, diffusion and reaction limitations have to be taken into consideration for understanding the effectiveness of the process.

### INTRODUCTION

The anodic oxidation process is based on the removal of contaminants by a combination of direct electron transfer from the pollutant to the anode and the production of large quantities of hydroxyl radicals from water discharge at the surface of an anode material with high oxygen overpotential. The reactive electrochemical membranes (REM) in the flow-through configuration are used in the anodic oxidation processes for improving the fluid dynamics in the electrochemical cell in order to increase the mass transfer rate and to overcome the diffusion limitation problem. Coupling membrane and electro-oxidation processes provide a promising tool to ensure both the removal of targeted molecules and high throughput via the prevention of fouling [1].

The aim of this work is to investigate the effect of geometric parameters of REM on the effectiveness of the process by using a proposed 2D stationary model of transport of diluted species in the electrolysis system with a REM. The model is based on the Fick-Navier-Stokes equations and takes into account the local geometrical and hydrodynamic properties of the system as well as chemical reactions related to the oxidation of organic compounds by hydroxyl radicals. Porosity and pore radius of the REM were considered as two crucial parameters.

### MATERIALS AND METHODS

The system under study is a cross-flow electrolyzer, which utilizes REM as an anode in inside-outside cross-flow filtration mode operated by galvanostatic conditions, that is, the solution is pumped through the REM. The experimental setup was described in detail in a previous study [2]. The feed solution contains an organic compound (paracetamol) with constant initial concentration and supporting electrolyte, the permeate flux is controlled by transmembrane pressure and depends on the operating conditions of the experiment.

### RESULTS AND DISCUSSION

The oxidation efficiency is estimated by the dependence of percentage removal (PR) of the organic compound on the total organic carbon (TOC) flux. There is a good agreement in the calculated and experimental degradation rate of a model pollutant at different permeate fluxes and current densities (Figure 1).

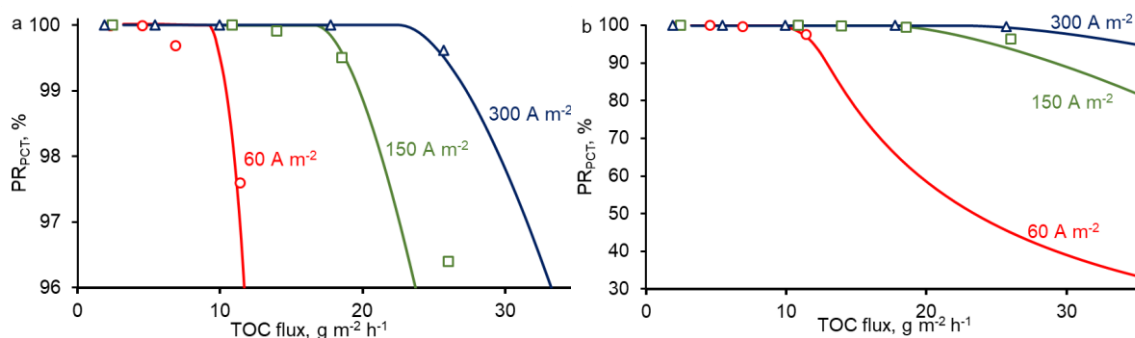


Figure 1. Experimental (dots) and theoretical (lines) dependencies of percentage removal of paracetamol (PR<sub>PCT</sub>) on total organic carbon (TOC) flux at different current densities (mentioned in the figure). (a) is a zoomed version of (b).

In order to investigate the effect of pore radius on the oxidation efficiency, the length of the pore radius ( $R_1$ ) is varied at fixed porosity ( $\epsilon=0,2$ ). As can be seen in Figure 2 (a, b, c), the PR of paracetamol decreases with increasing  $R_1$  at fixed TOC flux. The effect is due to the diffusion limitation of organic compound delivery to the surface of the electrode, where the reactive zone is located. The characteristic time for paracetamol diffusion to the electrode surface decreases with low pore size because

the distance from the center of the pore to the electrode surface is shorter. Thus, at a fixed permeate flux (convection), the probability of a molecule to reach the reaction zone increases with decreasing  $R_1$ .

Similar to the previous case, to investigate the effect of REM porosity on the oxidation efficiency the porosity is varied at a fixed pore radius ( $R_1=0,7 \mu\text{m}$ ). Results predicted from the model indicate that the effectiveness of the process should be improved when increasing the porosity. For a constant pore radius, increasing porosity means that the number of pores over the same surface is increasing. For the same permeate flux, it involves that the water velocity (convection) in each pore is lower, and thus, pollutants have more time to diffuse to the electrode surface. Therefore, increasing the porosity allows the limitation from the diffusion to occur only at higher permeate flux.

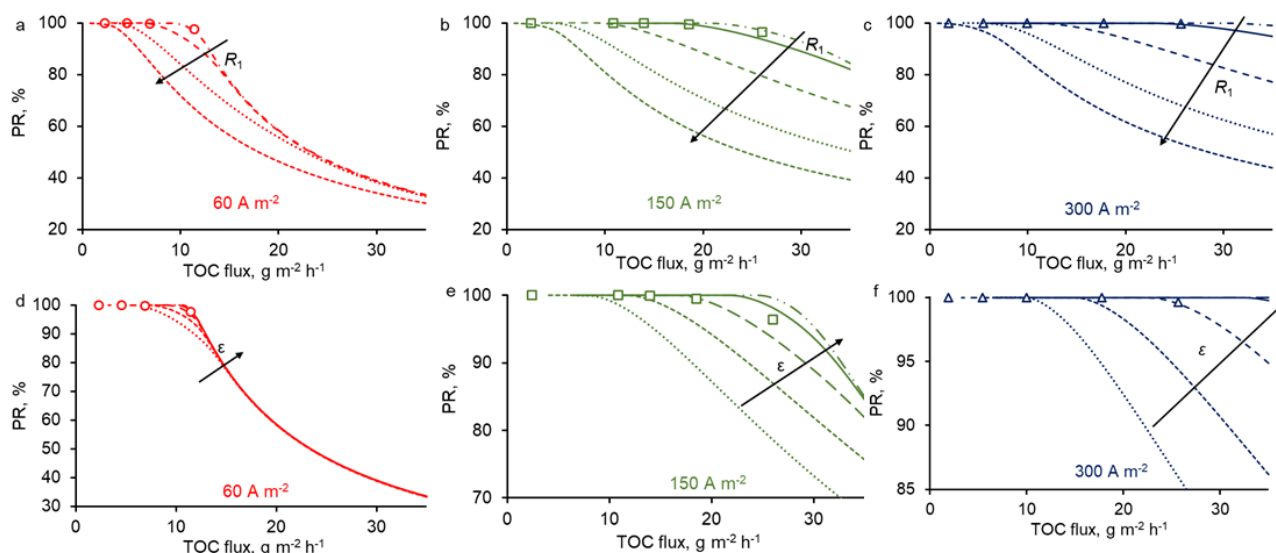


Figure 2. The influence of pore radii on the PR of the PCT at fixed porous fraction  $\varepsilon=0.2$  and  $j = 60$  (a), 150 (b) and 300 (c)  $\text{A}\cdot\text{m}^{-2}$ . The arrow represents an increment of pore radius:  $R_1=0.5, 0.7, 1.5, 3$  and  $5 \mu\text{m}$ . The influence of porosity on the PR at fixed pore size  $R_1=0.7 \mu\text{m}$  and  $j = 60$  (d), 150 (e) and 300 (f)  $\text{A}\cdot\text{m}^{-2}$ . The arrow represents an increment of porosity:  $\varepsilon=0.05, 0.1, 0.2, 0.4, 0.6$ .

## CONCLUSIONS

Porosity and pore radius of the REM significantly affect the removal of the target organic compound: the degradation rate decreases with increasing pore radius or decreasing porosity. These adverse effects are due to the diffusion time of organic compounds to the pore surface that becomes limiting compared to the characteristic time of convection. These theoretical predictions might be useful for the conception of novel REM minimizing mass transport limitations.

The competitive mechanisms relative to the delivery of an organic compound to the reactive zone, where the oxidation reaction occurs, is shown theoretically. Convection, diffusion and reaction limitations have to be taken into consideration to explain the results.

*This research was funded by the Russian Science Foundation, grant number 19-79-00268*

## References

- [1] Trellu, C., Chaplin, B.P., Coetsier, C., Esmilaire, R., Cerneaux, S., Causserand, C., Cretin, M. Electro-oxidation of organic pollutants by reactive electrochemical membranes. *Chemosphere*, 208 (2018) 159–175. doi:10.1016/j.chemosphere.2018.05.026.
- [2] Trellu, C., Coetsier, C., Rouch, J.-C.C., Esmilaire, R., Rivallin, M., Cretin, M., Causserand, C. Mineralization of organic pollutants by anodic oxidation using reactive electrochemical membrane synthesized from carbothermal reduction of  $\text{TiO}_2$ . *Water Res.* 131 (2018) 310–319. doi:10.1016/j.watres.2017.12.070.
- [3] Skolotneva, E.D., Trellu, C., Cretin, M., Mareev S.A. A 2D convection-diffusion model of anodic oxidation of organic compounds mediated by hydroxyl radicals using porous reactive electrochemical membrane. *Membranes*, 2020, 10, 102. doi: 10.3390/membranes10050102

# CHRONOPOTENTIOMETRY AS A NEW METHOD FOR CONTROLLING THE CURRENT-INDUCED TRANSPORT OF COIONS IN AN ION EXCHANGE MEMBRANE

Valentina Titorova, Semen Mareev, Andrey Gorobchenko, Natalia Pismenskaya\*, Victor Nikonenko  
 Membrane Institute, Kuban State University, Krasnodar, Russia

**Summary** Chronopotentiometry using pulses of a constant current of density is a powerful method for characterizing ion-exchange membranes. We found that coion transport greatly affects the shape of chronopotentiogram and propose a new method for the quantitative determination of the transport of coions based on the theoretical analysis of experimental chronopotentiograms.

## 1D NON-STATIONARY MODEL

Counter and coion transport in an ion exchange membrane (IEM) and adjoining diluted and enrichment diffusion layers is described using the Nernst-Planck, Poisson and material balance equations (Figure 1).

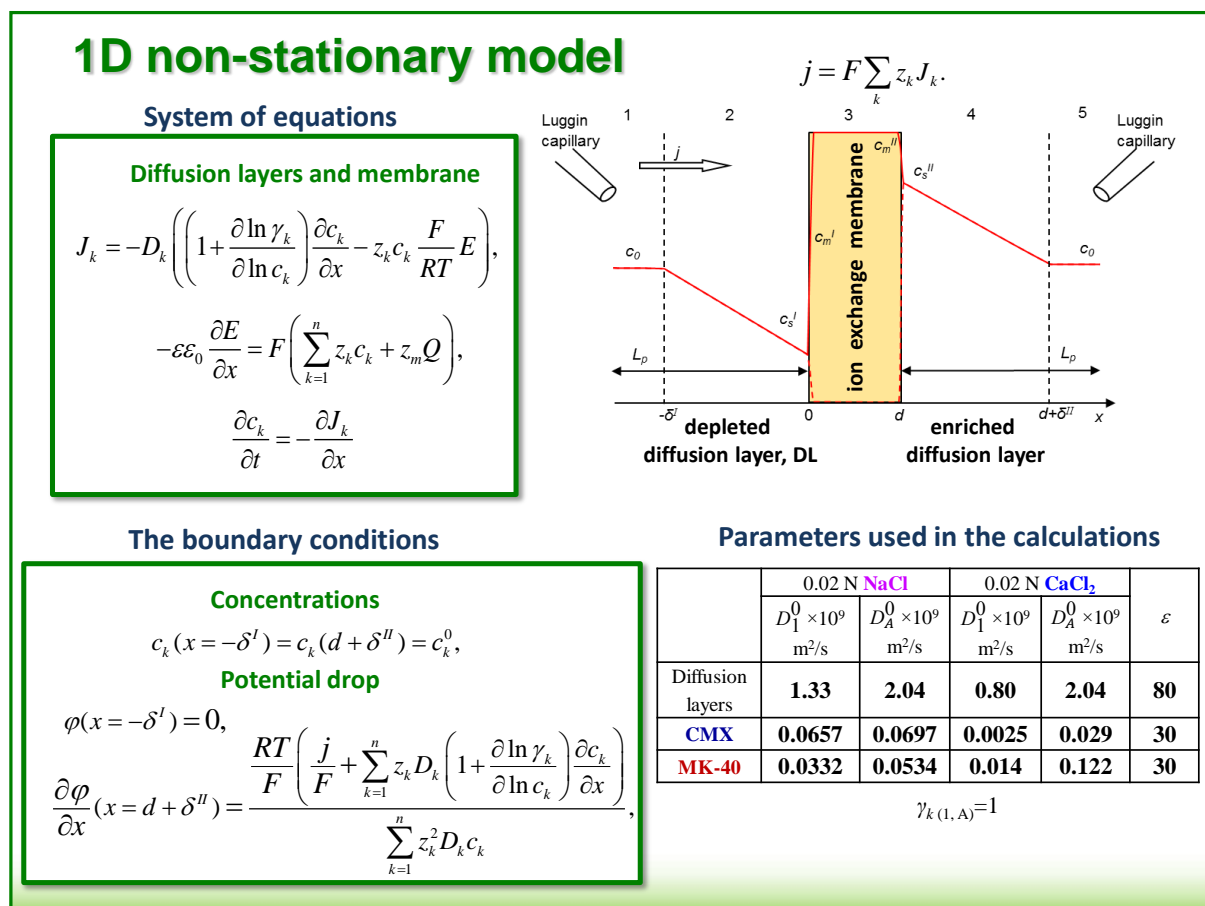


Figure 1. Basic model equations and parameters used in the calculations.

The following assumptions are accepted in this model:

- the membrane is considered as homogeneous;
- the water flux through the membrane, as well as water splitting are not considered;
- the electroconvection is taken into account through the effective diffusion coefficient in the depleted diffusion layer (we assume that the apparent diffusion coefficient of ion k linearly depends on the potential difference across the space charge region in the depleted diffusion layer);
- the gradients of temperature, pressure, and solution density are ignored.

## COMPARISON OF CALCULATION AND EXPERIMENTAL DATA

It is found that the rapid formation of concentration profiles in the diffusion layers adjacent to an IEM, caused by the application of a direct current, is followed by the slow establishment of concentration profiles in the membrane. This

\*Corresponding author. E-mail: n\_pismen@mail.ru

process is accompanied by an increase in the coion flux through the membrane with time. This leads to a mitigation of the membrane concentration polarization and an increase in the limiting current density. In the case of a doubly charged counterion ( $\text{Ca}^{2+}$  and  $\text{Mg}^{2+}$  in the studied cases), an increase in  $j_{\text{lim}}$  leads to a noticeable decrease with time in the resistance of the depleted diffusion layer. As a consequence, the potential difference across the membrane system decreases and a local maximum appears on the chronopotentiogram about 10 seconds after passing the transition time. The height of the maximum increases with growth the current density and the coion transport number in the membrane.

The 1D model gives a quantitative description of this maximum. It is shown that a visible maximum on the ChP occurs when  $\bar{t}_A$  is sufficiently high, about 0.005 or greater. Fitting the calculation to the experimental ChP allows determination of the coion transport number in the membrane,  $\bar{t}_A$ . The value obtained by this method ( $\bar{t}_A=0.0064$  for a CMX membrane in a 0.02 N  $\text{CaCl}_2$  solution) agrees quantitatively with the value found from the CMX conductivity and diffusion permeability.

## CONCLUSIONS

A method for determining the transport numbers of coions and counterions by fitting experimental ChPs and calculated using the developed model curves is developed. The application of the method is much more rapid than the traditional estimation of membrane selectivity from the concentration dependences of IEM diffusion permeability and electrical conductivity. This method seems to be very useful not only for laboratory studies, but also for monitoring the selectivity of membranes in situ in conditions of their use in industrial electro dialysis.

The work is supported by Russian Foundation of Basic Researches, project 18-08-00397a.

# Contents

Victor Starov

<b>CONTRIBUTION OF PROFESSOR ANATOLY FILIPPOV TO MODELLING OF MEMBRANE PROCESSES</b> .....	6
<b>KEYNOTE LECTURES</b> .....	8
Maarten Biesheuvel, Slawomir Porada, Jouke Dykstra <b>THE ORIGIN OF OSMOSIS AND ELECTRO-OSMOSIS</b> .....	8
Vasily Kirsch <b>SIMULATION OF SOLUTE TRANSPORT IN A CROSS-FLOW PAST A ROW OF HOLLOW-FIBER MEMBRANES</b> .....	10
Reinhard Miller, Valentin B. Fainerman, Nenad Mucic, Aliyar Javadi, Libero Liggieri, Francesca Ravera, Giuseppe Loglio, Alexander V. Makievski, Emanuel Schneck <b>STRUCTURE OF SURFACTANT ADSORPTION LAYERS AT THE WATER/ALKANE INTERFACE – COMPETITIVE AND COOPERATIVE EFFECTS</b> .....	12
Victor Nikonenko, Dmitrii Butylskii, Semyon Mareev, Andrey Kislyi, Natalia Pismenskaya, Pavel Apel <b>HIGHLY SELECTIVE SEPARATION OF CATIONS WITH THE SAME CHARGE BY A NEW MEMBRANE METHOD USING SIMULTANEOUSLY APPLIED ELECTRIC AND PRESSURE FIELDS</b> .....	14
Isaak Rubinstein, Boris Zaltzman <b>MECHANISMS OF HYDRODYNAMIC INSTABILITY IN CONCENTRATION POLARIZATION</b> .....	16
Ilya Ryzhkov, Atrur Krom, Mikhail Simunin <b>THEORY OF ION TRANSPORT AND SELECTIVITY IN MEMBRANES WITH ELECTRICALLY CONDUCTIVE SURFACE</b> .....	18
Valery Ugrozov <b>MATHEMATICAL SIMULATION OF GAS TRANSPORT THROUGH COMPOSITE MEMBRANES</b> .....	20
Anna Kovalenko, Matthias Vessling, Victor Nikonenko, Elizaveta Evdochenco, Machamet Urtenov <b>THE PHENOMENON OF SPACE CHARGE BREAKDOWN IN ELECTRO-MEMBRANE SYSTEMS</b> .....	22
<b>ORAL PRESENTATIONS</b> .....	24
Satya Deo, Deepak Kumar Maurya, Anatoly Filippov <b>INFLUENCE OF MAGNETIC FIELD ON HYDRODYNAMIC PERMEABILITY OF BIPOROUS MEMBRANE</b> .....	24
Jouke Dykstra, Maarten Biesheuvel <b>PROTON TRANSPORT ACROSS ANION EXCHANGE MEMBRANES IN ELECTROCHEMICAL SYSTEMS</b> .....	26
Irina Falina, Olga Demina, Victor Zabolotsky <b>CAPILLARY MODEL OF ELECTROOSMOTIC TRANSFER IN ION-EXCHANGE MEMBRANES</b> .....	28
Anna Kovalenko, Makhamet Urtenov <b>ANALYSIS OF THE CURRENT VOLTAGE CURVE OF ELECTROMEMBRANE SYSTEMS</b> .....	30

Semyon Mareev, Victor Nikonenko, Natalia Pismenskaya <b>CHRONOPOTENTIOMETRY OF MONOPOLAR ION-EXCHANGE MEMBRANES: MODELING AND EXPERIMENT</b> .....	33
Maxim Shalygin, Alina Kozlova, Vladimir Teplyakov <b>MODELING OF ALCOHOLS RECOVERY FROM DILUTED WATER SOLUTIONS WITH MEMBRANE VAPOR SEPARATION</b> .....	35
Michele Tedesco <b>UNDERSTANDING THE ROLE OF MEMBRANE THICKNESS IN ELECTRO-MEMBRANE PROCESSES VIA NERNST-PLANCK APPROACH</b> .....	36
Amit Kumar Saini, Satyendra Singh Chauhan, Ashish Tiwari <b>CREEPING FLOW OF VISCOELASTIC FLUID THROUGH A SWARM OF POROUS CYLINDRICAL PARTICLES: BRINKMAN-FORCHHEIMER MODEL</b> .....	38
Anna Trybala, Victor Starov <b>CURRENT PROBLEMS IN KINETICS OF WETTING AND SPREADING</b> .....	40
Asmat Ullah, Victor Starov <b>OSCILLATORY MEMBRANE MICROFILTRATION FOR THE SEPARATION OF CRUDE OIL DROPS FROM PRODUCED WATER</b> .....	41
Aminat Uzdenova <b>MATHEMATICAL MODELING OF ELECTROCONVECTION IN FLOW-THROUGH ELECTRODIALYSIS MEMBRANE CELLS: INFLUENCE OF THE INLET BOUNDARY CONDITION FOR THE ION CONCENTRATION</b> .....	42
Anatoly Filippov, Yulia Koroleva, Amit Verma <b>NUMERICAL STUDY OF STOKES-BRINKMAN SYSTEMS WITH VARYING LIQUID VISCOSITY</b> .....	44
<b>POSTER SECTION</b> .....	46
Danila Bakhtin, Alexander Malakhov, Alexey Volkov <b>PHYSICAL AGING OF PTMSP-BASED THIN-FILM COMPOSITION MEMBRANES LOADED WITH ORGANIC POROUS FILLERS VIA GAS PERMEABILITY TRACKING</b> .....	46
Satya Deo, Deepak Kumar Maurya <b>MHD EFFECTS ON MICROPOLAR-NEWTONIAN FLUID FLOW THROUGH A COMPOSITE POROUS CHANNEL</b> .....	48
Andrey Gorobchenko, Semyon Mareev, Victor Nikonenko <b>MATHEMATICAL MODELLING OF THE EFFECT OF PULSED ELECTRIC FIELD ON THE SPECIFIC PERMSELECTIVITY</b> .....	50
Daria Khanukaeva, Anatoly Filippov <b>MEMBRANE HYDRODYNAMIC PERMEABILITY: APPROXIMATION FOR THE MICROPOLAR FILTRATE</b> .....	52
Natalia Kononenko, Natalia Loza, Marina Andreeva <b>POLARIZATION BEHAVIOR OF PERFLUORINATED MEMBRANES MODIFIED WITH POLYANILINE</b> .....	54
Yulia Koroleva, Daria Khanukaeva <b>ON A MICROPOLAR FLUID FILTRATION PROBLEM THROUGH AN AXIALLY SYMMETRIC CELL</b> .....	56
Anna Kovalenko, Natalia Kandaurova, Vladimir Chekanov <b>MATHEMATICAL MODELING OF THE AUTOWAVE PROCESS IN A THIN SURFACE LAYER</b> .....	58

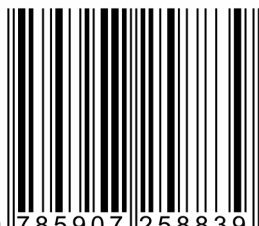
Anna Kovalenko, Machamet Urtenov <b>CONTRAST STRUCTURES OF SPACE CHARGE IN ELECTROMEMBRANE SYSTEMS</b> .....	60
Anna Kovalenko, Makhmet Urtenov, Alexander Pismenskiy, Elizaveta Evdochenko <b>FEATURES OF THE EFFECT OF WATER SPLITTING ON ELECTROCONVECTION</b> .....	62
Anna Kovalenko, Mahamet Urtenov, Inna Shkorkina <b>SOFTWARE COMPLEX FOR ANALYZING THE CURRENT-VOLTAGE CHARACTERISTICS OF ELECTROMEMBRANE SYSTEMS</b> .....	64
Leonid Ostrer, Daria Khanukaeva <b>ON THE PECULIARITIES OF SIMULATED FLOWS IN SPHERICAL CELLS</b> .....	66
Natalia Pismenskaya, Olesya Rybalkina, Kseniia Tsygurina, Ekaterina Melnikova, Mikhail Sharafan, Sergey Mikhaylin, Laurent Bazinet <b>PRODUCTION OF CHEAP PHOSPHORUS-AMMONIUM FERTILIZERS USING ELECTRODIALYSIS. PROBLEMS AND SOLUTIONS</b> .....	68
Ivan Podtynnikov, Evgenia Grushevenko, Ilya Borisov, Olga Scharova <b>RECOVERY MTBE FROM WATER USING HIGH SELECTIVE POLYALKYLMETHYLSILOXANE COMPOSITE MEMBRANES BY PERVAPORATION</b> .....	70
Vladimir Rusev, Aleksandr Skorikov, Emil Magafurov <b>MEAN RESIDUAL LIFE AND ANALYSIS RELIABILITY INVESTIGATION OF ELECTRICAL SUBMERSIBLE PUMPS</b> .....	72
Olesya Rybalkina, Ilya Moroz, Natalia Pismenskaya <b>DEVELOPMENT OF ELECTROCONVECTION AT THE SURFACE OF CHLORIDE AND PHOSPHATE-CONTAINING SOLUTIONS</b> .....	74
Veronika Sarapulova, Natalia Pismenskaya, Victor Nikonenko <b>MODIFICATION OF ION-EXCHANGE MEMBRANES TO INCREASE THE SELECTIVITY OF COUNTERION TRANSFER</b> .....	76
Svetlana Shkirkaya, Natalia Kononenko <b>INFLUENCE OF POLYANILINE ON WATER TRANSPORT IN PERFLUORINATED ION EXCHANGE MEMBRANES</b> .....	78
Inna Shkorkina, Natalia Chubyr, Vitaly Gudza, Makhmet Urtenov <b>DEPENDENCE OF CURRENT-VOLTAGE CHARACTERISTIC OF NON-STATIONARY TRANSPORT OF 1:1 SALT IONS IN A CROSS-SECTION OF DESALINATION CHANNEL ON A POTENTIAL DIFFERENCE SWEEP RATE</b> .....	79
Ekaterina Skolotneva, Clement Trelu, Marc Cretin, Semyon Mareev <b>A 2D MODEL OF ANODIC OXIDATION OF ORGANIC COMPOUNDS USING POROUS REACTIVE ELECTROCHEMICAL MEMBRANE</b> .....	81
Valentina Titorova, Semen Mareev, Andrey Gorobchenko, Natalia Pismenskaya, Victor Nikonenko <b>CHRONOPOTENTIOMETRY AS A NEW METHOD FOR CONTROLLING THE CURRENT-INDUCED TRANSPORT OF COIONS IN AN ION EXCHANGE MEMBRANE</b> .....	83

# **MEMBRANE PROCESS MODELING**

Book of Abstracts

In authors edition

ISBN 978-5-907258-83-9



9 785907 258839